MS THESIS

Fabrication of High-Performance Strain Sensor Using Poly-Acrylamide-Co-AMPS for Human Motion Detection

Submitted By

Kashmala Anwar

192-FET/MSEE/F23

Supervised By:

Dr. Gul Hassan

Department of Electrical and Computer Engineering

Faculty of Engineering and Technology

International Islamic University, Islamabad

2025

Declaration

I certify that the research work titled **"Fabrication of High-Performance Strain Sensor Using Poly-Acrylamide-Co-AMPS for Human Motion Detection"** is my own work and has not been presented elsewhere for assessment. Moreover, the material taken from other sources has also been acknowledged properly.

_____

Kashmala Anwar

Date: _____ **192-FET/MSEE/F23**

In the name of Allah (SWT), the Most Beneficent and the Most Merciful

Dedicated

to

My beloved parents and respected teachers

Acknowledgment

With the blessings of Allah (S.W.T), I humbly offer my gratitude for the guidance and support received during the completion of this research. May peace and blessings be upon the last Prophet Hazrat Muhammad (S.A.W) and his noble companions (R.A), whose sacrifices and devotion to the prosperity of Islam continue to inspire us.

I am truly obliged for the instrumental support provided by my supervisor, Dr. Gul Hassan. Without his invaluable guidance and consistent encouragement, this dissertation would not have been possible. He provided the motivation needed to see this project through to completion, and I am deeply thankful for his contributions.

I would also like to extend my sincere appreciation to the staff members of the Center for Advanced Electronics and Photovoltaic Engineering (CAEPE) for their continual support and cooperation.

_____

Kashmala Anwar

192-FET/MSEE/F23

Abstract

The demand for flexible, biocompatible, and highly sensitive strain sensors has significantly grown due to their potential applications in wearable electronics, human motion detection, soft robotics, and biomedical monitoring. This research presents a comprehensive study on the fabrication of self-healable and stretchable strain sensor based on biocompatible materials using a composite formulation of polymers including Polyvinyl Alcohol (PVA), Acrylamide (AM), and 2-Acrylamido-2-methylpropane sulfonic acid (AMPS) and contributing towards smart cutting-edge technology. The study aims to synthesize and optimize a strain sensor to enhance its performance for real time implementation. The research objectives have been thoroughly achieved through the synthesis, formulation of the device, and optimization done systematically one material at a time for all composites. The performance is evaluated, using metrics including resistance variation versus applied strain, stability cycles, sensitivity, stretchability and self-healing time. The influence of the sensor geometry, which includes width, length, and thickness is also investigated, confirming that the sensor's structural dimensions significantly affect performance. The high-performance fabricated strain sensor resulted in sensitivity with tuned GF of 1.6 and stretchability of 1200% which can detect small and large-scale motions as well. The self-healing capability is shown by its outstanding ability to heal in just 1.7s with stretching after self-healing up to 125%. This inherent ability provides the sensor longer lifetime and a high level of reliability. These experimental results demonstrate a balance between mechanical robustness and electrical responsiveness thus showcasing the effectiveness of the proposed strain sensor in monitoring mechanical deformations and its implementation for real-world human motion detection.

Table of Contents

List of Abbreviations

Acronym	Abbreviation
AI	Artificial Intelligence
AM	Acrylamide
AMPS	2-Acrylamido-2-Methylpropane Sulfonic Acid
AgNWs	Silver Nanowires
APS	Ammonium Persulfate
CNC	Cellulose Nanocrystals
CNFs	Cellulose Nanofibers
CNTs	Carbon Nanotubes
DA	Dopamine
GelMA	Gelatin Methacryloyl
GF	Gauge Factor
GA	Glutaraldehyde
GNs	Graphene Nanosheets
HDPE	High Density Polyethylene
HVAC	Heating, Ventilation, and Air Conditioning
IoT	Internet of Things
Irgacure	2-Hydroxy-4’-(2-hydroxyethoxy)-2-methylpropiophenone
LASER	Light Amplification by Stimulated Emission of Radiation
LDPE	Low Density Polyethylene
LIDAR	Light Detection and Ranging
LiCl	Lithium Chloride
LiF	Lithium Floride
MBA	N,N′-Methylenebisacrylamide
MEMS	Microelectromechanical Systems
MOSFET	Metal Oxide Semiconductor Field Effect Transistor
MPF	Multilayered Polyurethane Fiber
MWCNT	Multiwalled Carbon Nanotubes
NaCl	Sodium Chloride
OGFET	Organic Gate Field Effect Transistor
PANI-NPs	Polyaniline Nanoparticles
PDA	Polydopamine

PDMS	Polydimethyl Siloxane
PEDOT: PSS	Poly(3,4-ethylenedioxythiophene):poly(styrene sulfonate)
PEG	Polyethylene Glycol
PNAGA	N-(2-amino-2-oxoethyl)-2-propenamide (NAGA)
PPA	Polyphosphoric Acid
PTFE	Polytetrafluoroethylene
PU	Polyurethane
PVA	Polyvinyl Alcohol
PVIM	Poly(vinylimidazol)
Py	Pyrrole
RTD	Resistance Temperature Detector
SBMA	Zwitterionic 3-[Dimethyl-[2-(2-methylprop-2-enoyloxy) ethyl] azaniumyl] propane-1-sulfonate
TA	Tannic Acid
TEA	Triethanolamine
TPU	Thermoplastic Polyurethane

List of Figures

List of Table

Chapter 1

Introduction

1.1. Overview

Strain sensors play a key role in diverse fields including soft robotics, structural health monitoring, biomedical devices and wearable electronics. Their ability to detect and convert any type of mechanical deformation into electrical signals makes them indispensable in real-time human motion tracking and various disease diagnostics. The earliest form of strain sensors was limited to conventional strain gauges that were capable of withstanding only small strains (~5%) with less accurate output data. The drawback of these sensors was the inflexibility and rigidness due to the structure and materials with which they are made resulting in limiting their applicability in flexible or stretchable environments and making them unsuitable for daily life wearable applications [1]. The general structure of a conventional strain gauge and a modern flexible strain sensor is shown in Figure 1.1.

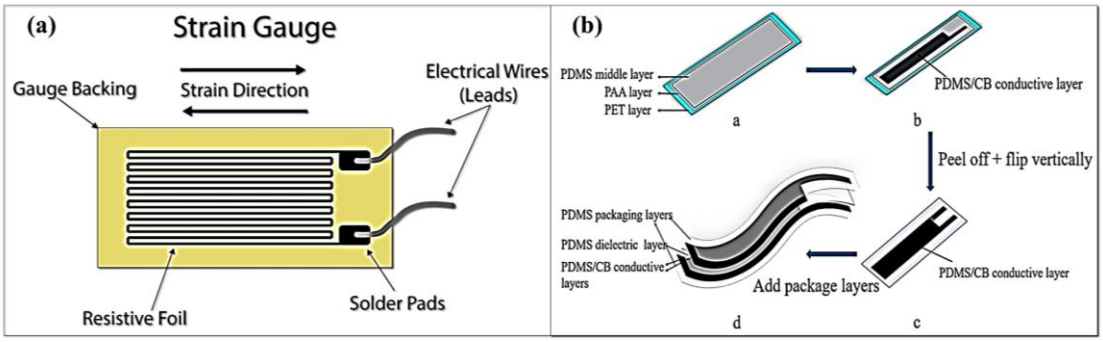

Figure 1.1: (a) Conventional strain gauges **(b)** Flexible strain sensor [2]

Advancements in materials science and nanotechnology have transformed commercial brittle, inflexible strain sensors into soft, precise and robust strain sensors with recent technology focusing on developing flexible strain sensors with enhanced electrical properties, mechanical strength, thermal and optical properties. Compared to conventional sensors, these flexible strain sensors have shown high biocompatibility and real-time implementation with extensive utilization in health-monitoring, movement detection, wearable electronics, robotics, human machine interface devices and moving towards the integration of these flexible devices with machine learning

algorithms enabling systems to make predictive decisions and interpret data in an intelligent way resulting in smarter and autonomous systems [3].

Researchers have now developed sensors using polymer nanocomposites and nanomaterials which created revolution in strain sensing technology with unique properties like excellent electrical conductivity offering tunable sensitivity, durability and stretchability making them ideal for applications in smart systems and biomedical monitoring. Self-healing strain sensors that autonomously repair themselves after damage, cracks, or cuts due to material qualities and bonding cites are being studied. Ionic interactions and dynamic bonding allow polymer-based materials to restore electrical and mechanical characteristics. This invention greatly extends sensor lifespan and reliability in repetitive and harsh environments [4]. Despite advances in flexible sensor design creating a balance between stretchability, sensitivity and mechanical stability remains a challenge. Highly sensitive strain sensors reduce mechanical stability and stretchability due to microcrack propagation and tunnelling. Conversely highly stretchable strain sensors offer reduced sensitivity. In order to overcome this constraint hybrid materials are currently being investigated. Mechanical hysteresis can also create measurement inaccuracies throughout repetitive cycles. Hybrid nanocomposites and improved encapsulation are needed since environmental factors like temperature and humidity impair sensor performance, particularly for hydrogels and specific polymers. These challenges demand the formulation of innovative materials and design strategies to balance electrical and mechanical performance, making stretchable strain sensors a viable long-term deployment choice [5]. The technological advancements of strain sensors over the past decade from skin sensors for touch detection in 2014 to integrated wireless skin sensors in 2024 is highlighted in Figure 1.2.

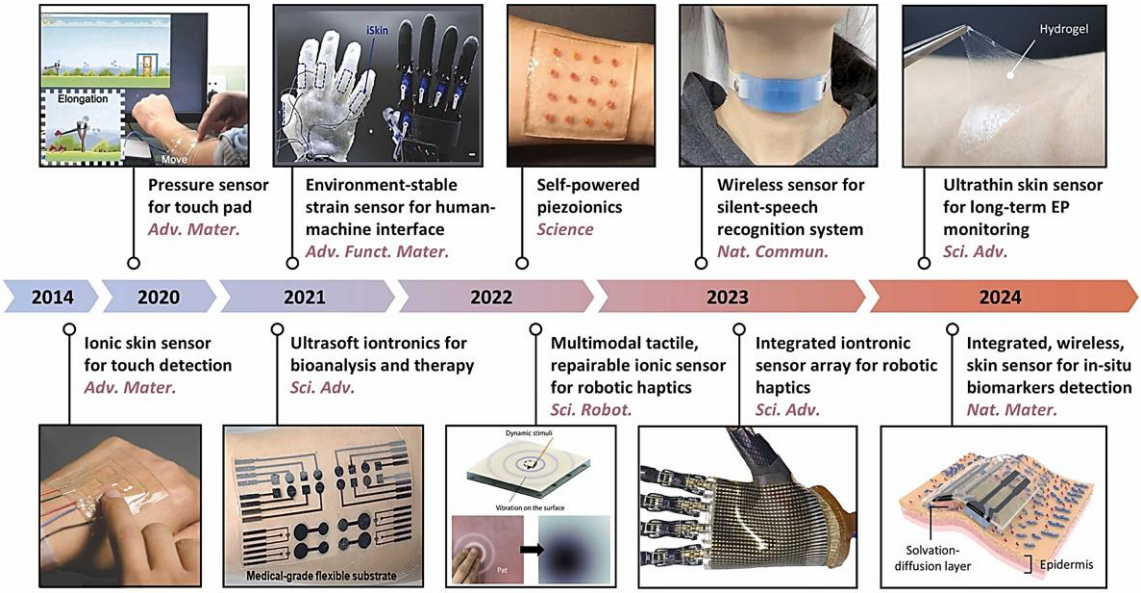

Figure 1.2: Timeline of Key Developments in Flexible and Skin Mountable Strain Sensors (2014-2024) [6]

This research work "Fabrication of High-Performance Strain Sensor Using Poly-Acrylamide-Co-AMPS for Human Motion Detection" optimizes material composition, device parameters, and dimensions (length, width, and thickness) to create a high performance flexible and stretchable strain sensor with real output monitoring. The work also offers biocompatibility with the help of non-toxic and bio-compatible polymers in the synthesis. Compositional tuning establishes a percolation network of ionic conductivity and dimensional optimization while retaining repeatability and healing to maximize strain sensing performance. The proposed sensor's data will be analyzed and evaluated using performance criteria that include resistance variation with strain, cyclic stability, sensitivity, stretchability and self-healing to choose the best device. The sensor's flexibility and stretchability will improve efficiency and durability thus enabling a new generation of smart sensor technologies for health monitoring, robotic control, and smart textiles.

1.2. Hydrogels

Soft hydrogel is a 3D network of hydrophilic polymer with high water content. The material is versatile and eco-friendly, making it suited for many sectors. Chemical or physical cross-linking of hydrophilic polymer chains creates hydrogel's viscoelastic structure. They are used in many common items due to their high-water content and

flexibility. These materials are capable of diffusing water into them, making them soft and elastic [7].

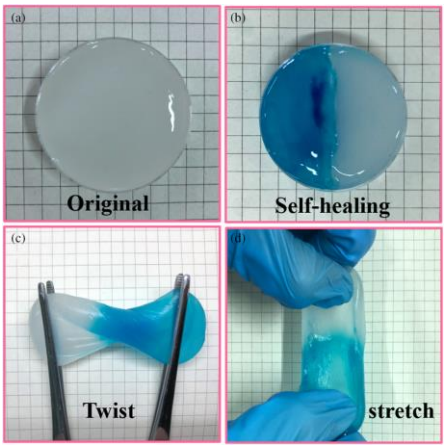

Figure 1.3: Self-Healing and Stretching of Hydrogel based Strain Sensor [8]

Acrylate-based superabsorbent hydrogels are skin-friendly, biocompatible and fluid-absorbent. Their structural similarity to natural tissues makes them ideal for biomedical applications like dressings and wound healing, where they create a moist environment for tissue regeneration and healing. Moisture, pain reduction, and flexibility make them perfect for chronic wounds and motional injuries. Smart hydrogel dressings feature microprocessors, biosensors and wireless systems for continuous tracking and controlled drug delivery. Their porous nature allows prolonged medication administration, and microfluidic applications facilitate diagnostics and organ-on-a-chip technologies [9]. The image representation of a PVA/PEG/Glycerol based composite gel is shown in Figure 1.3.

1.3. Composite Material for Strain Sensors

The composition of strain sensors consists of various materials, each contributing to specific properties essential for real-world applications. The careful selection of these materials is crucial for determining the overall performance of the sensor, including the durability and application range. In this research the formulation of hydrogel includes a base polymer material providing structural support to the device, cross-linking agent, ionic monomers, plasticizers and photo initiators. With the use of these materials the final device of strain sensor is fabricated which possess different characteristics including stretchability, flexibility, conductivity, self-healing ability, and mechanical strength. These parameters can be further optimized and reached up to their best

possible value by taking into consideration the environmental factors, ratios of the materials with respect to each other and dimensions of the sensor. The following section covers the details of each of the materials used and how they affect the hydrogel's characteristics.

1.3.1. Polyvinyl Alcohol (PVA)

Polyvinyl alcohol is a synthetic polymer with strong tensile strength, flexibility and excellent film-forming abilities. PVA initially used as textile coating and sizing has been expanded over time to diverse fields including biomedical engineering, packaging industry and electronic sensors because of the biocompatible, hydrophilic and biodegradable nature. Its high hydrogen bonding make it useful as a polymer matrix in strain sensors to improve mechanical strength, self-healing and flexibility [10]. In the research, the foundation of hydrogel-based strain sensors is a polymer which is highly stretchable and has water-retention capabilities, with polyvinyl alcohol (PVA) being the main material in this formulation. PVA is utilized since it easily dissolves in water, forming a homogeneous dispersion of different materials which may be conductive fillers, polymers or crosslinkers in hydrogel strain sensors [11].

1.3.2. Acrylamide (AM)

Acrylamide is a vinyl monomer known for its excellent solubility, adhesiveness and crosslinking. The amide groups (-$CONH_2$) of this compound provides binding sites for heavy metal ions rendering it useful in biological applications such as drug delivery, wound healing and tissue engineering, laying the foundation for its integration in multifunctional sensing platforms. Its properties have been introduced in PVA based hydrogels as a co-polymer to enhance flexibility and mechanical toughness. Individually existing as solid powdered form, it forms soft and stretchable network upon polymerization which enhances the toughness and elongation of the sensor in which it is incorporated. It also ensures that mechanical stress is efficiently converted to strain and contributes to the sensor strain sensitivity. However, due to its limited conductivity, the inclusion of electrically conductive materials with high mobile ions and free electrons is essential [12].

1.3.3. 2-Acrylamido-2-Methylpropane Sulfonic Acid (AMPS)

AMPS, a derivative of acrylamide, is a reactive, hydrophilic anionic monomer that contains amide (-CONH-) and sulfonic acid (-SO_3H) groups. It has excellent water

retention capabilities, ionic conductivity and good chemical stability. The strong adhesion and high charge density of this monomer made it useful in water treatment, drug delivery systems and high-performance hydrogel synthesis [13]. AMPS has been proved to be a critical element in the development of hydrogel-based strain sensors. Sulfonic acid groups in AMPS improve ionic conductivity, allowing charges to pass efficiently inside the hydrogel matrix. AMPS-based hydrogels stretchability, flexibility and self-healing allows the sensors to resist repeated mechanical strain without degrading performance. Therefore, by taking into consideration these properties and their benefits, AMPS are incorporated in the PVA hydrogel for improving strain sensing [14].

1.3.4. Glycerol

Glycerol contains three hydroxyl groups making it a triol compound and well-known for its hygroscopic nature, contains plasticizing qualities that make it softer, flexible and simpler to process. In hydrogel-based strain sensors, it enhances stretchability, reduces fractures under high strains and improves sensitivity which enables the transmission of signals more efficiently. Due to its superior hydrophilicity, long-term stability and increased longevity in diversified environmental conditions and characteristics like non-toxic nature and reduced volatility make it ideal for wearable applications in human motion detection, soft robotics and flexible electronics. This distinctive combination of conductivity regulation and enhanced mechanical performance makes it an essential component of the next generation of hydrogel-based strain sensors [15].

1.3.5. N,N′-Methylenebisacrylamide (MBA)

MBA is a crosslinking agent employed in PVA based hydrogels as a covalent crosslinker by forming stable amide bonds between polymer chains. Several crucial elements of sensor performance are influenced by the degree and nature of crosslinking. Hydrogels that are crosslinked with MBA or ionic monomers, such as AMPS, can withstand high mechanical strains without fracturing, thereby guaranteeing uninterrupted operation in dynamic environments. The incorporation of MBA into sensors significantly improves its mechanical strength, flexibility, durability, and long-term stability by forming robust crosslinked network [16].

1.3.6. 2-Hydroxy-4'-(2-hydroxyethoxy)-2-methylpropiophenone (Irgacure)

Photoinitiators (PIs) are chemical compounds that convert light energy into reactive species like free radicals, anions or cations, that trigger polymerization. They are indispensable in the synthesis of UV-curable hydrogels, as they facilitate the rapid and precise crosslinking of polymer networks [17]. Irgacure is a popular photoinitiator in hydrogel-based sensors because of its strong absorption in UV range, low toxicity, and excellent efficiency. It absorbs UV radiation in the range of 250 nm-450 nm and decomposes into free radicals, which starts uniform crosslinking and fast polymerization. Here it combines with monomers like Acrylamide and AMPS to form polymer chains making it possible to create extremely elastic hydrogel for strain sensors. It controls how effectively the hydrogel network forms via UV polymerization. [18].

By leveraging the exceptional properties of these materials this research seeks to develop a strain sensor with superior toughness, electrical and self-healing properties. A smart functional hydrogel is created by copolymerizing monomers, Acrylamide and AMPS, resulting in Poly-Acrylamide-Co-AMPS for high performance strain sensing. These two monomers form the copolymer backbone which is responsible for the hydrogel's ionic conductivity, mechanical integrity and responsiveness to strain. Other constituent materials have been integrated to form a stable and 3D polymer network with improved mechanical strength, flexibility and self-healing. The fabricated sensor will contribute to next generation wearable electronics, paving the way for advancements in human motion detection, biomedical applications, flexible robotics and wearable devices.

1.4. Problem Statement

Conventional strain sensors often face significant challenges related to limited reliability, durability, stretchability, and self-healing capabilities due to the inherent constraints of the materials used. These limitations not only hinder their long-term effectiveness but also restrict their potential for applications requiring high flexibility, continuous operation, and adaptability under mechanical strain. As a result, their use in dynamic environments such as human motion detection, wearable devices, and medical

diagnostics has been constrained. This research aims to address these challenges by focusing on the fabrication and optimization of advanced strain sensors based on Poly-Acrylamide-Co-AMPS. This polymer offers unique advantages such as high stretchability, robust mechanical properties, and intrinsic self-healing abilities, making it an ideal candidate for next-generation strain sensor applications. By integrating this material, the project seeks to achieve enhanced sensitivity, high flexibility and stretchability, durability and self-healing properties.

1.5. Objectives of the Research

- Synthesize Poly-Acrylamide-Co-AMPS with tailored properties to ensure high sensitivity, stretchability, and durability.
- Fabrication of flexible and efficient strain sensors using synthesized material.
- Test the sensors for real-time human motion detection.

1.6. Significance of the Research

The research holds significant importance in biomedical technology, would be able to measure physiological parameters such as human motion and muscle activity with enhanced durability and performance thereby improving health care by early detection and diagnosis of various diseases. The flexibility and stretchability of the sensors ensures comfort, making them suitable for use in wearable devices. The high sensitivity will allow accurate monitoring of physiological signals, making it useful in tracking different body movements like muscle contractions, cardiovascular activity, and respiratory movements contributing to better health care. This research will push the boundaries of wearable and implantable medical devices enabling continuous real-time health monitoring and diagnostics, transforming patient care.

1.7. Applications for Strain Sensors

Strain sensors have many applications in various fields varying from material sciences, to detecting deformation in structural engineering, human motion detection, and medical diagnostics. In structural health and geotechnical monitoring, strain sensors are widely used for the detection of failures in structures including buildings and bridges and underground tunnels and prevention of other geotechnical conditions by the detection of stress aggregation and cracks. Strain sensors find their remarkable use in biomedical applications for detection of various physiological signals ranging from minor human motions such as heart rate, respiratory movement to large-scale human

joint motions and bending. They facilitate real time health monitoring by tracking human motion assisting in prosthetics, rehabilitation and wearable devices like fitness trackers. They are used in advanced robotics like soft and humanoid robots to mimic human motions as well as other industrial automation systems. Strain sensors find their promising applications in wearable electronics and smart textiles by embedding in e-clothing and smart gloves for virtual gaming and improves motion tracking experience. Due to the advancement in technology these sensors have become smart and find their promising use in IoT applications. The emergence of AI and machine learning algorithms integrated with strain sensors made an advancement in flexible intelligent monitoring and further improved the accuracy of these devices. The self-healable, stretchable and flexible nature strain sensors technology finds vast potential and paves the way for safer and smarter interactive environment [19]. The potential applications of wearable strain sensors in diverse fields are illustrated in Figure 1.4.

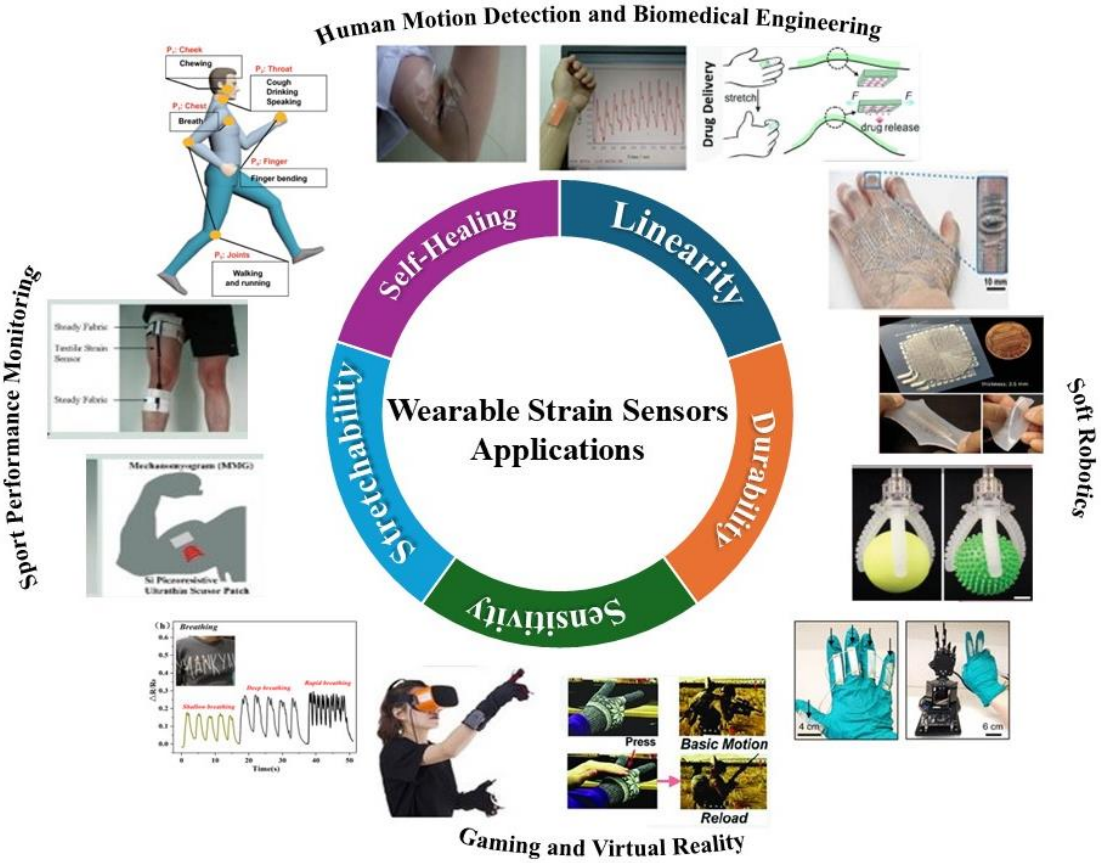

Figure 1.4: Potential applications of wearable strain sensors

1.8. Thesis Outline

The outline of my thesis is illustrated below.

Chapter. 1: This Chapter gives a brief introduction on nano technology and how it is revolutionized. Introduction to strain sensors and their significance in modern technology has been discussed. The key materials have been introduced briefly.

Chapter. 2: This Chapter presents a comprehensive background on sensor technology, different types of sensors. Strain sensors and evolution to flexible, stretchable and self-healing materials has been discussed.

Chapter. 3: This Chapter gives a Literature review of the proposed study by citing a number of recent papers. Different materials, fabrication techniques and performance evaluation have been discussed.

Chapter. 4: This Chapter discusses the synthesis, fabrication and characterization techniques employed in the research. From material composition to the device final product fabrication has been studied in detail.

Chapter. 5: This Chapter presents experimental results which are evaluated and discussed in detail with graphical visualizations and final images of fabricated product being tested for detection of human motion.

Chapter. 6: This Chapter presents the conclusive remarks on the proposed study with recommendations and some further research directions in the domain.

Chapter 2

Background

2.1. Historical Evolution of Sensors

The history of sensors started thousands of years ago in ancient times with the invention of sundials by the Egyptians who used sun position for time measurements. Following this concept, the Greeks and Romans improvised it using water clock to measure time by the flow of water, which they called as clepsydras. These were the initial attempts made to monitor the changes in environment and form the basis for sensor technology [20]. With the evolution in tools of civilization the first modern sensor idea came, which was to convert physical measurement signals to electrical signals with the invention of the very first gas temperature sensor in the 17th century by Galileo, marking the beginning for scientific measuring instruments. During the 18th-19th century industrial revolution came and the need for precise measuring tools spurred which led to the springing off the electromechanical sensors. Thomas Seebeck discovered Seebeck effect which laid the beginning of thermocouples. Then in 1843 Wheatstone bridge was developed for measuring strain and pressure. Similarly piezoelectric and photoelectric sensors were also invented in the late 19th century. These developments represented a substantial move in the electromechanical sensing leading to the foundation of modern sensor technology. The 20th century brought rapid advancements in sensor technology with the emergence of semiconductor-based sensors and piezoelectric quartz crystal by offering affordable, dependable, and small devices which are reliable and highly sensitive. MOSFETs, which are the most used and common transistors today, were invented back in 1959, a miniaturized sensor technology and paved the way for many semiconductor sensors such as MEMS in automobile and aerospace industries. From the 21st century the era of advanced and organic sensors began with the advancements in nanotechnology and flexible electronics. The notable breakthroughs include the OGFET with low cost of fabrication for medical diagnostics, various flexible and stretchable sensors in wearable and smart electronics for human motion detection and the integration of IoT and AI revolutionizing smart and autonomous systems [21].

The continuous quest for higher precision, escalating real time data collection and automation has been the driven force behind the evolution of sensor. Advances in

material science, microelectronics and computational techniques have consistently pushed the boundaries of sensing capabilities, from the unsophisticated mechanical instruments from ancient times to today's cutting-edge technology, AI driven tools and enhanced nanotechnology sensors. These modern sensors are not only compact, efficient and versatile but also have the ability to self-learn and make decisions by integration with AI. The future of sensor technology lies in bio-integrated devices, smart neuromorphic computing with potentially revolutionizing applications in smart infrastructure, autonomous systems, personalized healthcare, space exploration and interaction with digital and physical world to unlock unprecedented possibilities [22].

2.2. Sensors

Sensors are devices that receive and respond to a signal or a physical phenomenon which could be in the form of heat, light, electrical signal or motion. A sensor works by detecting these input signals and converting them into an analog or digital representation of that signal. Depending upon the working mechanism, how they are connected to the environment which they are measuring and different output types, sensors are classified into extensive categories such as passive and active sensors as well as analog and digital sensors [23].

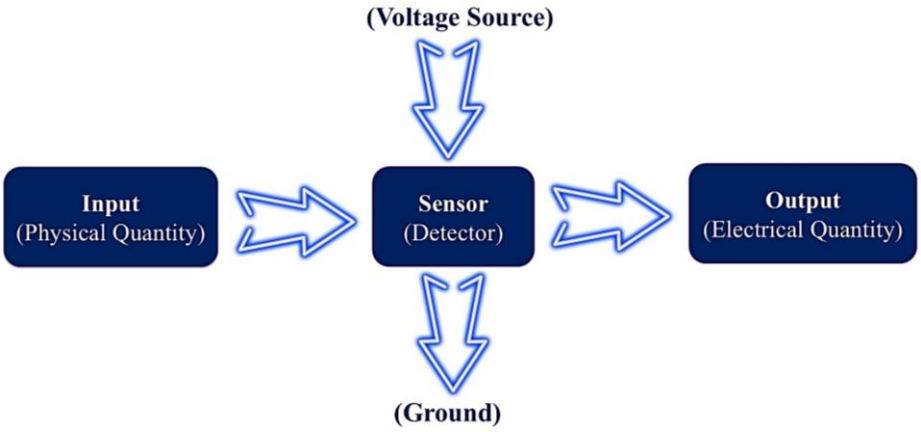

Figure 2.1: Block Diagram illustrating sensor working mechanism [23]

Passive sensors are the ones that do not require any external power supply for its operation instead they rely on the surrounding energy to produce a quantifiable reaction. They are frequently used in applications like remote environmental monitoring where low power consumption is required. Conversely, active sensors need an external power source to function which might be in the form of electrical power supplies or portable

batteries. They operate by the emission of energy waves and pick up the signals that are reflected or transmitted. Examples include radar which measures the distance and speed of the target object using electromagnetic waves and LIDAR that emits laser to measure distance [24]. The block diagram illustrating a general flow of operation of sensor is shown in Figure 2.1.

2.3. Types of Sensors

Sensors play a key role in modern technology, designed in such a way to detect and measure a specific quantity which could be in the form of light, heat, movement, humidity, pressure along with the physical, chemical, biological and electrochemical parameters. These quantities are converted into a measurable form such as an electrical signal usually in the form of voltage and current signals which enables signal monitoring and automation in various applications. There are various types of sensors such as temperature sensors, pressure sensors, gas sensors, humidity sensors, optical sensors, biosensors and strain sensors which are designed and used depending upon the applications and properties which need to be measured. These sensors are used to measure certain parameters with optimized properties for numerous applications such as health monitoring, robotics, various industrial processes and many more.

2.3.1. Temperature Sensor

Temperature sensors such as RTD (Resistance Temperature Detector), thermocouples, thermistors and infrared sensors are devices that are used to measure temperature changes by converting to electrical signals mainly in the form of voltage or resistance. They are utilized in computers, mobile phones, automobiles, in industrial processes and laboratory applications, for example temperature monitoring during different manufacturing processes and ensuring quality of food products [25].

2.3.2. Pressure Sensor

Pressure sensors are the devices that translate physical quantities like pressure or force of an object, gas or any type of fluid into corresponding electrical signals following the principle of piezoresistive or piezoelectric effect. These devices are used in a wide range of applications ranging from measuring fluid pressure in pipelines, to high pressure systems like boilers, controlling hydraulic and pneumatic systems as well as

in various medical devices such as in monitoring blood pressure and various diverse applications [26].

2.3.3. Gas Sensor

Gas sensors are devices used to detect the presence of various gas particles and their concentration. The sensors operate on different principles depending upon the type of technology used such as electrochemical gas sensors use a chemical reaction between target gas particles and electrodes to generate electrical signals in proportion to gas concentration, chemiresistive sensors like metal oxide semiconductors measure resistance, and optical sensors use IR absorption and laser spectroscopy. The applications of these sensors include air quality index, in scientific and medical applications like oxygen sensors and detection of various other toxic gases in specialized fields [27].

2.3.4. Humidity Sensor

Humidity sensors also known as Hygrometer are devices that detects the moisture or humidity levels present in the atmosphere. There are different types of humidity sensors based on their mechanism and working principles. Capacitive humidity sensors change the dielectric constant of the material to produce a humidity-proportional output signal, while resistive ones use ion particles in salt medium to change electrode resistance. These sensors operate by measuring humidity in terms of relative humidity, absolute humidity or dew point depending upon their working and application. They ensure optimum humidity levels and play a vital role in a wide range of applications which include weather monitoring, greenhouses, industrial and medical applications, and HVAC systems [28].

2.3.5. Optical Sensors

An optical sensor collects and measures light changes and converts them into electrical impulses for research and development, medical diagnostics, environmental monitoring and motion detection [29]. The system of these sensors includes a light source, a sensing medium that detects light reflection, transmission or absorption, photo detectors that convert light into electrical signals, and a signal processing unit that analyzes the electrical signals to provide data. Optical sensors are classified by light

interaction and properties of the target material such as photodetectors or photodiodes, fiber optic sensors, image sensors, LASER sensors and LIDAR [30].

2.3.6. Strain Sensors

Strain sensors are devices that are designed to measure mechanical deformations such as bending, twisting and stretching of an object when subjected to an external force or stress. These deformations lead to changes in electrical properties such as resistance, capacitance or optical characteristics which are then analyzed to quantify the amount of applied strain. Resistive, capacitive, piezoelectric and piezoresistive sensors are the most common types of strain sensors. The simplicity and cost-effectiveness of resistive strain sensors make them a popular choice for measuring strain through changes in electrical resistance. Capacitive sensors detect fluctuations in capacitance that result from modifications in the distance or area between electrodes during stretching. Piezoresistive sensors demonstrate an increase in electrical resistance because of the internal strain-induced alteration in their conductive pathways, whereas piezoelectric sensors generate electric charges in response to applied mechanical stress. Each type is selected based on the specific application's needs for sensitivity, durability and environmental compatibility [31]. Figure 2.2 shows the operation of resistive and capacitive strain sensors as the fiber-based conductive network deforms.

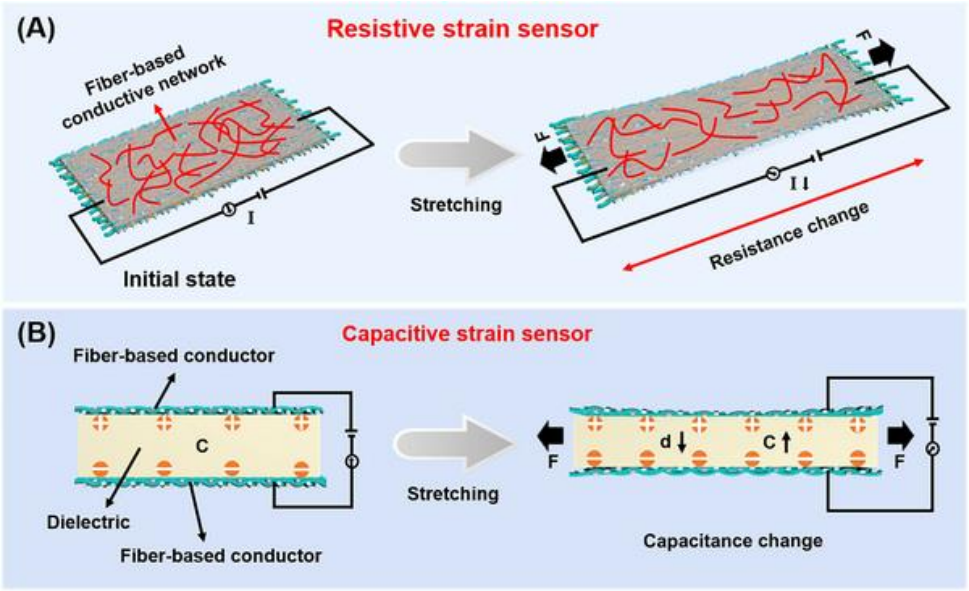

Figure 2.2: Working Mechanism of Strain Sensors **(A)** Resistive and **(B)** Capacitive [32]

The efficiency of the sensor is determined by the performance parameter gauge factor which indicates the sensitivity to deformation. The main focus and challenge of the researchers during manufacturing is this parameter which could be tuned by optimization of sensor geometry, material composition, and utilizing controlled microcrack mechanism. Another important metric on which strain sensor performance depends is the response time which tells how quickly the sensor responds to the input parameter which is crucial in real time applications. Moreover, there are other important frameworks like linearity over repeated strain levels, hysteresis indicating the repeatability and stability of the sensor which need to be optimized with the passage of time to meet application demands [33].

2.4. Flexible and Stretchable Strain Sensors

With the ongoing advances in material sciences and microelectronic technology novel strain sensitive materials, signal conditioning and acquisition systems need to be updated. Traditional strain sensors had to face certain challenges like low sensitivity, slow response, size restrictions, high expenses and vulnerability to temperature changes. The materials were extensively studied by the researchers to meet the demands of unique application needs and environmental conditions. Technological innovations particularly in wearable electronics, bio-integrated devices and human machine interaction have led to the development of flexible and stretchable sensors which can easily conform to irregular surfaces without effecting performance. The ultra-stretchability of these sensors makes them resilient and flexible just like human skin and tissues.

The growing demand for adaptable, lightweight, portable and non-toxic sensing solutions that can seamlessly integrate with textiles, irregular surfaces and human skin is the driving force towards the trend in stretchable and flexible strain sensors with increased sensitivity, durability and self-healing capabilities. Flexible strain sensors are suited for real-time motion tracking and medical diagnostics due to their excellent mechanical regulation, reliability and reusability. Furthermore, self-healing materials prolong sensor lifespan while cutting waste and manufacture expenses. The development of next generation intelligent systems depends on the transition of stretchable sensors which are smart and flexible [33]. The stretchable and flexible strain sensors with different characteristics are shown in Figure 2.3.

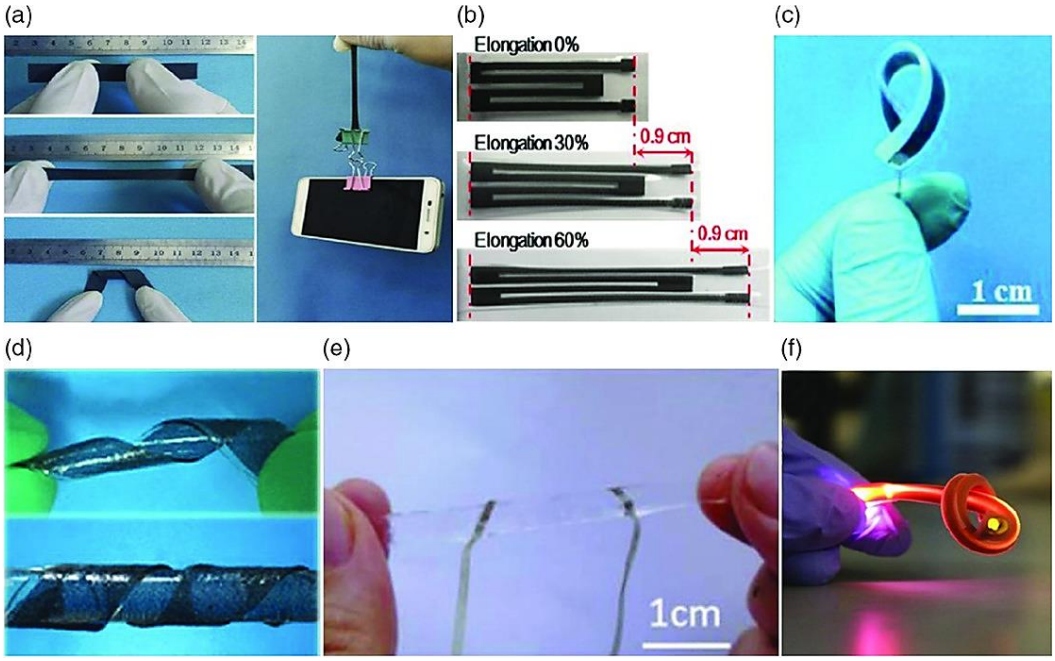

Figure 2.3: Different types of Stretchable, flexible and skin mountable strain sensors [33]

2.4.1. Materials for Stretchable Strain Sensors

Stretchable and flexible strain sensors use varied and developing materials. One of the pivotal factors in the development of stretchable strain sensors is the selection of materials which have direct impact on stretchability, flexibility, electrical conductivity and durability. Stretchable sensors are typically fabricated using advanced polymer materials, nanocomposites consisting of conductive fillers as well as hybrid materials. They have been broadly classified into two classes i.e. elastomeric (flexible) substrates and conductive (functional/active) materials. Here is the list of different categories of materials which can be employed for the production of this cutting-edge technology.

- **Elastomeric substrate** serves as a matrix that retains the conductive phase and transfers strain during deformation. Fundamental materials include Polydimethylsiloxane (PDMS), Thermoplastic polyurethane (PU) and Ecoflex which have high stretchability, biocompatibility and low modulus [34].
- **Conductive materials** act as a sensing element of the sensor and are responsible for detecting changes during deformation. They include carbon-based fillers like CNTs and graphene, metal nanoparticles such as nickel, gold, silver and emerging 2D materials like MXenes [35].

- **Conductive polymers** are a novel class of materials that intrinsically form a conductive or sensing layer without additional fillers. Polyaniline (PANI), poly(3,4-ethylenedioxythiophene) (PEDOT) and polypyrrole (PPy) can be engineered to have conductivity while maintaining stretchability [36].
- **Hybrid Composites** balance electrical conductivity and mechanical stretchability, formed by blending elastomers and conductive fillers. These composites can be designed to have a tunable working range, gauge factor and sensitivity by manipulating the microstructure, concentration, dispersion and type of fillers. For example, CNT-PDMS composites offer high sensitivity and durability [37].
- **Conductive Hydrogels and Ionogels** are gaining popularity in biological friendly strain sensors because of the softness, conductivity and mechanical compatibility. The materials have polymeric networks that are distended with water or ionic liquids and doped with conductive components that improve the performance of stretchable strain sensors [38].

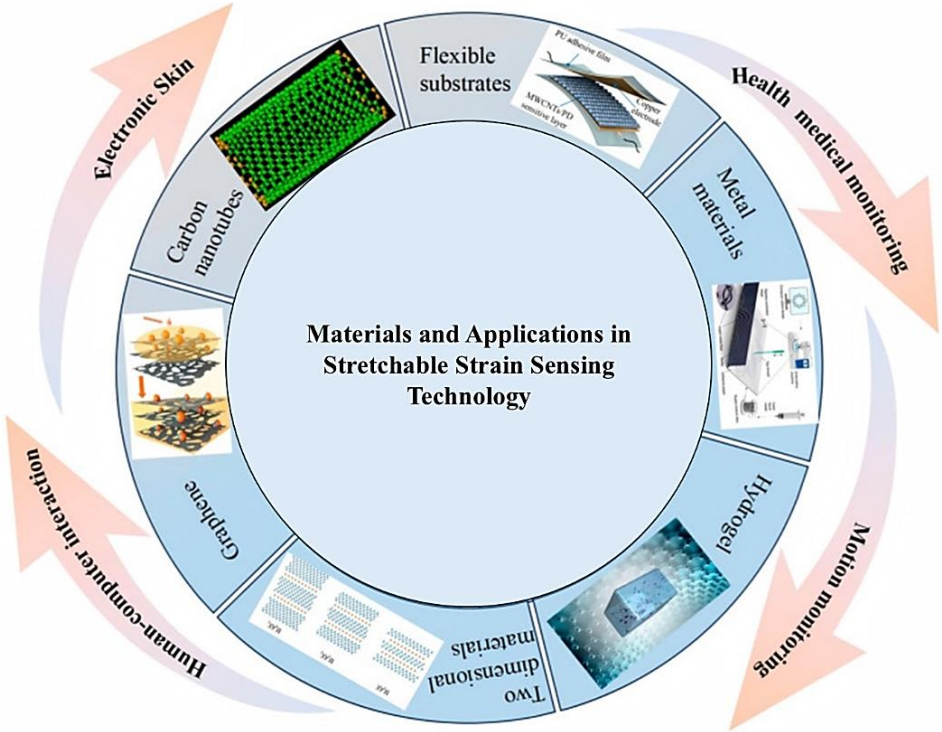

Figure 2.4: Different types of materials used in Stretchable Strain Sensors [39]

2.5. Self-Healing Mechanisms

Due to the built-in mechanism some materials have the capacity to repair themselves after damage or internal fracture caused by a force or stress. They are the smart class of materials with physical and chemical bonding and reactions contributing to recovering damages. Due to different operating mechanisms self-healing could be intrinsic, extrinsic and microcapsule based. Intrinsic self-healing involves chemical reactions like polymerization or cross-linking and bonds such as hydrogen, ionic and dynamic covalent bonds which are alterable and repairs damage spontaneously whereas external self-healing requires an external stimulus for repairing like polymers as healing agents or catalysts which promotes the formation of chemical bonds and facilitates healing repairing damages [40].

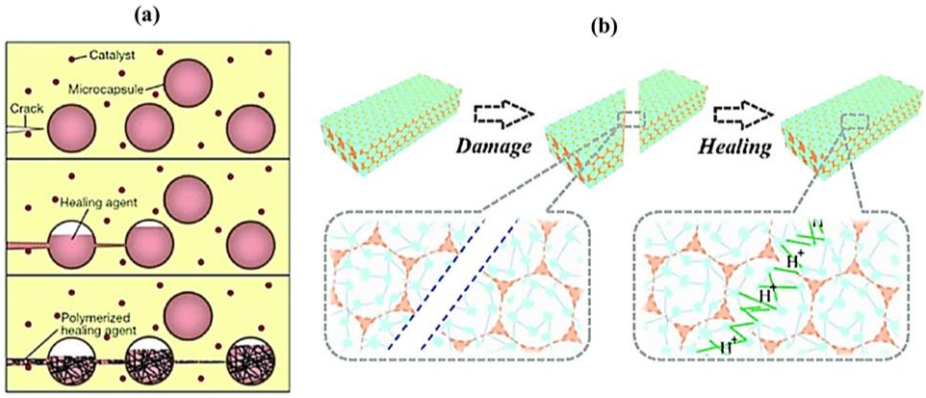

Figure 2.5: (a) Extrinsic Self-healing Process **(b)** Intrinsic Self-Healing Process [41]

The ability and effectiveness of self-healing is determined by different characterizations done before and after damage such as spectroscopic analysis to study chemical composition and structures at molecular level, imaging techniques like SEM [42], TEM [43], AFM [44] and other techniques like thermal analysis in which we study thermal stability and conductivity. These characteristics help to study the behavior and properties of material after self-healing and evaluate its efficiency [45]. The self-healing process involved in both extrinsic and intrinsic self-healing materials is demonstrated in Figure 2.5.

Self-Healing Materials

- **Ceramics and Concrete:** Ceramics work by oxidation reactions and diffusion of healing agents at sites to recover damage while self-healing concrete

materials contain bacteria or encapsulated healing agents which produce calcium carbonate to seal cracks upon water exposure [46].

- **Metals:** There are self-healing metals including some shape memory alloys like nickel titanium (NiTi) which recover their original shape after mechanical deformation either by oxidation process or by heating at reverse transformation temperature [47].
- **Polymers and Hydrogels:** Polymers like PDMS, shape memory polymers and thermoplastic polymers exhibit self-healing properties due to the formation of intermolecular bonds, diffusion of healing agents or reversible bonding mechanisms.

Key Self-Healing Polymers and Hydrogels:

- **Polyethylene Glycol (PEG) and Polypropylene (PP):** Hydrophilic polymers with moderate self-healing abilities and widely used in biomedical applications [48].
- **Polyamides (Nylon)** are polymers made of repeatable amide groups with the most common type Nylon. They are significantly found in 3D printing materials with high geometrical stability, versatility and mechanical strength [49].
- **Polyvinyl Alcohol (PVA):** PVA is a synthetic polymer with high amount of water retention and finds its use in wound healing and various industries including textiles, coatings, packaging, laundry detergent products [10].
- **Poly (acrylamide-co2-acrylamido-2-methylpropane sulfonic acid):** It is a hydrophilic copolymer with high ionic conductivity, used in diverse fields because of excellent self-healing abilities, mechanical properties and biocompatibility [50].
- **Chitosan, Alginate and Silk Fibroin based hydrogel** are natural polymer hydrogels which are bio-degradable and non-toxic, ideal for wound dressing, in drug delivery and tissue engineering [51], [52].
- **Hyaluronic acid** is a biocompatible material and commonly utilized in skin care. It forms a solid hydrogel by chemically cross-linking with other agents and can be employed in joint lubrication and tissue engineering [53].

Chapter 3

Literature Review

M. Vahdani et al. fabricated strain sensors using environmental-friendly and bio-disintegrable materials like sodium carboxymethyl cellulose (NaCMC), glycerol, and polyvinyl alcohol (PVA) along with sensing materials for conductivity. With a failure strain of ~330%, gauge factor of 1.7, and 2000 stretch and release cycles, the sensor proved efficient in applications with good stretchability, piezoresistive behaviors and the highest sensitivity achieved with Au thickness of 60 nm and was successfully tested for monitoring human motion [54]. The sensor decomposes after 9 hours in deionized water at room temperature, dissolves in 5 minutes and breaks down completely at 95° C in water within 25 minutes as shown in Figure 3.1.

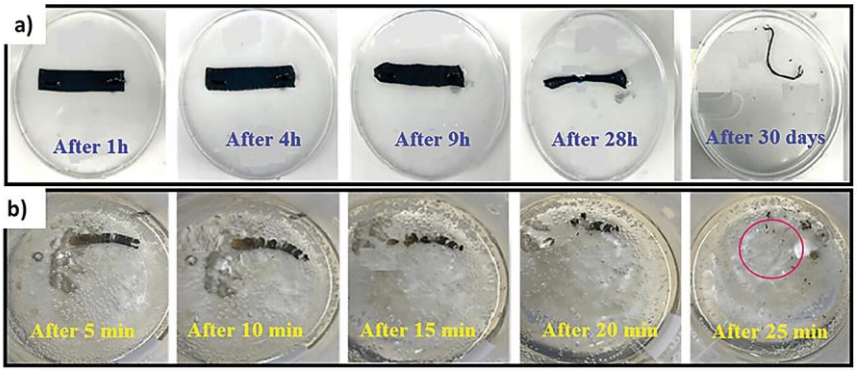

Figure 3.1: (a) and **(b)** Represents the decaying process of the strain sensor in deionized water at room temperature and 95 °C respectively [54]

R. Yang et al. fabricated a wearable strain sensor using conductive hydrogel materials to address the issue of mechanical toughness, low sensitivity and strain ranges with an advance 3D printing technique in a macrostructure design like meshes. The developed strain sensor was based on polyvinyl alcohol, tannic acid and polyacrylamide (PVA/TA/PAM) and its customizable mesh structure improved sensitivity, achieving a GF=32.95 at low strains (3.5%-5%) and GF=21.5 at high strains (100%-120%) with good mechanical strength. The sensor exhibited a stable and repeatable response tested for over 500 cycles and was effective in detecting both small (facial, pulse) and large (joint bending) body movements [55]. The mesh structured models under stress distribution are shown in Figure 3.2.

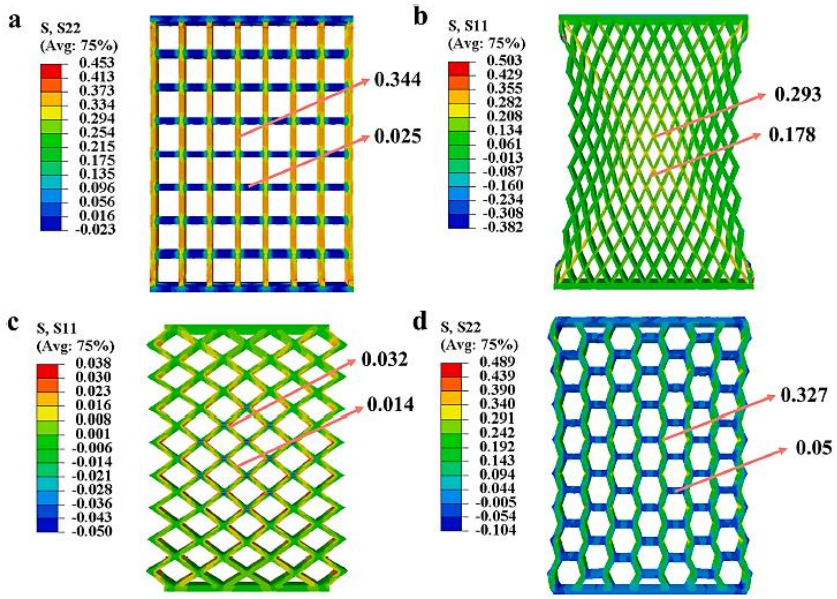

Figure 3.2: Stress distribution for four mesh structured models under 10% tensile strain showing directional load variation [55]

P. Kateb et. al utilized the vapor-phase polymerization technique to create a capacitive strain sensor for textile and wearable applications. The polymerization of polypyrrole in the vapor phase was employed to create conductive textiles. For the insulation layer, dip coating was used to deposit polyurethane (TPU), polystyrene-block-polyisoprene-block-styrene (SIS) and barium titanate ($BaTiO_3$) to form a dielectric layer with mechanical resistance. The sensor was fabricated using twisted yarns, which improves sensitivity and enables efficient tracking of strain throughout the yarn. The sensor's efficacy was evaluated in real-world applications with the implementation of a machine learning model that accurately classified 12 distinct hand gestures with 100% accuracy [56].

P. Shukla et al. fabricated a multilayer strain sensor based on PDMS/graphene/PDMS layers with graphene ink deposition through drop-casting onto the layer of PDMS substrate. This layered device uses graphene as a conductive material and PDMS as a stretchable flexible substrate that showed increased sensitivity with GF= 850 and wide strain range of 60%, a fast response time and tested for cyclic stability of approximately 1000 stretching-releasing cycles. The sensor response to different frequencies was investigated and validated by tracking human physiological motions, making them suitable for wearable applications [57].

W. Hong et al. made a notable contribution in high performance, stretchable, durable and eco-friendly sensors with the fabrication of a strain sensor composed of graphene/multi-walled carbon nanotubes and polymer composites. The dual layered biologically inspired stretchable strain sensor mimics human finger print pattern and fiber arrangement within lotus root structure to demonstrate good sensitivity of 35.33 (GF), strain range (0–145%), stretchability (145%), rapid and stable response with exceling in applications like monitoring human micro-expression, sign language recognition and Morse code detection showing great potential for electronic skin applications [58]. The preparation process of the sensor with stretching and flexibility of the product is shown in Figure 3.3.

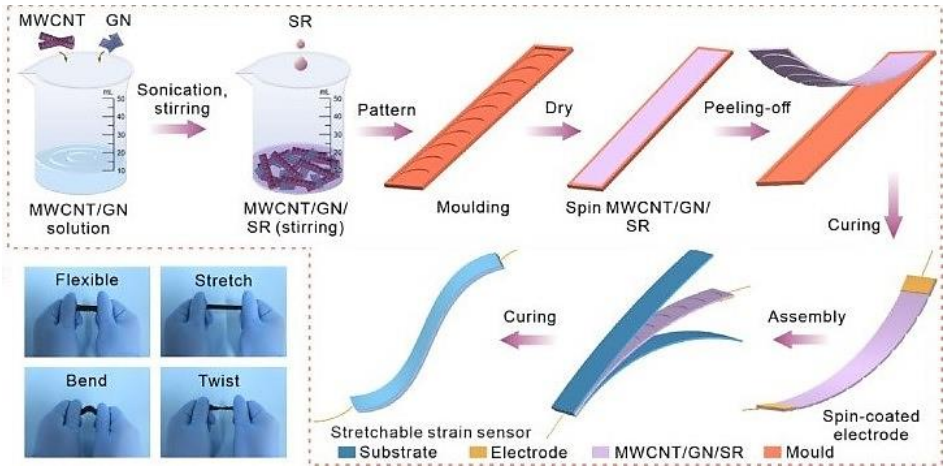

Figure 3.3: Preparation process and physical demonstration showing flexibility, stretching, bending and twisting of the sensor[58]

X. Boa et al. fabricated a 3D conducting polymer gel composed of polyaniline (PANI) polyvinyl alcohol (PVA) and cellulose nanocrystal (CNC) to enhance dispersal of nanoparticles and improve mechanical properties. The resulting composite gel sensor demonstrated remarkable properties including stretchability (550 %), fast response (~105ms), high GF of up to 20.7, stability and anti-freezing properties making it suitable for use in wearable electronics under dynamic conditions [59]. The schematic representation depicting the fabrication process and PPC ink printed on different substrates (PET, PVDF, PI and Glass) along with customizable design are shown in Figure 3.4.

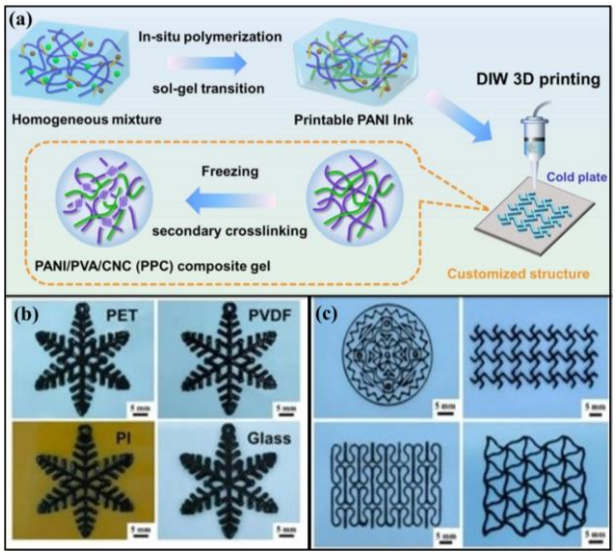

Figure 3.4: (a) A schematic representation demonstrating the fabrication process of PANI/PVA/CNC (PPC) composite gel. **(b)** Printed pattern of the gel on different substrates. **(c)** Customized structure of printed PPC ink [59]

Z. Wu et al. illustrated the properties of ionic conductive hydrogels with the fabrication of strain sensor based on the polymer materials PAM and PVA by introduction of sodium casein (SC). Compared to PAM/PVA based sensor the addition of SC resulted in good conductivity due to the large number of free ions. This dual network hydrogel demonstrated excellent mechanical properties with maximum strain and stress limitation of 719 % and 444.3kPa respectively. The electrical properties were also good with GF of 2.17 under a wide strain detection range. Sensor was tested for monitoring real world human motion by integrating with the digital power meter and monitoring the displayed resistance change [60].

H. Wu et al. fabricated a superhydrophobic strain sensor inspired by butterfly wing architecture. The dual conductive layer was made using GNS and MWCNT materials on a PDMS substrate and then pre-stretching created wrinkled features, enabling strain detection of up to 50%. The sensor possessed features like a water contact angle of 167.5°, making it successful for underwater detection. The performance of this sensor was evaluated by integrating it with robotic grippers for detection of objects of varying different sizes and underwater applications by attaching it to robotic fish that are controlled at varying speeds [61].

A.K. Padhan et al. fabricated an ionically crosslinked polymer ionogel which is composed of polyvinylimidazol (PVIM) and polyphosphoric acid (PPA) through the

sonication process. The designed ionogel based sensor exhibited good tensile strength, excellent toughness and stretchability (140%) along with purely intrinsic flexibility, transparency and repeatability. Additionally, the mechanical properties and ionic conductivity of the polymer were further enhanced by the incorporation of Ca-ions into PVIM–PPA ionogels with 5 times increase in conductivity and 90% recovery after self-healing [62].

D. Chen et al. fabricated a multi-crosslinked double network ionic conductive hydrogels with an eco-friendly approach. From the research analysis it was seen that the conventional ionic conductive hydrogels preparation process is complex and involves toxic photoinitiators. To overcome this, a hydrogel was prepared through UV irradiation using polyvinyl alcohol (PVA) containing (PVA-SbQ), styryl pyridinium groups and sodium alginate (SA), with the immersion in ferric chloride ($FeCl_3$) and glycerol (Gly). The synergistic approach introduces tensile strength (2.489 MPa) and elongation at break (1452 %). Moreover, the resulting sensor exhibited anti-freezing capabilities, electrical stability, gauge factor of 2.49 along with remarkable flexibility allowing it to conform to various body movements with ease and comfortability. The transmittance of hydrogel is also evaluated by varying material composition [63].

K. Wang et al. focused on developing a conductive hydrogel strain sensor with crosslinked network to enhance the mechanical toughness with multiple functionalities. The author used glycerol, magnesium acrylate and varying contents of PANI to make a composite PAMgA/Gly/PANI with APS and TEA for initializing polymerization process. The sensor exhibited water retention and self-healing performance due to hydrogen bonding between glycerol, water molecules and segments of chain in PAMgA [64].

T. Truong and J. Kim created a shape-memory polymers (SMP) with blended carbon nanotubes (CNTs) for high sensitivity. The characterization results of the fabricated sensor showed high sensitivity (GF of 20 at 5% strain), suitable to sense subtle movements such as human breathing. The durability test was validated for 1000 cycles of stretching at the strain of 4% showing consistent performance and retains stretchability up to 140% with good electrical response, flexibility, high reversibility and reduced hysteresis [65]. The sensor was used for detecting respiration movement using Fourier transform (FT) analysis and power spectrum density (PSD) and

transmitting the signals wirelessly to computer for data processing as shown in Figure 3.5.

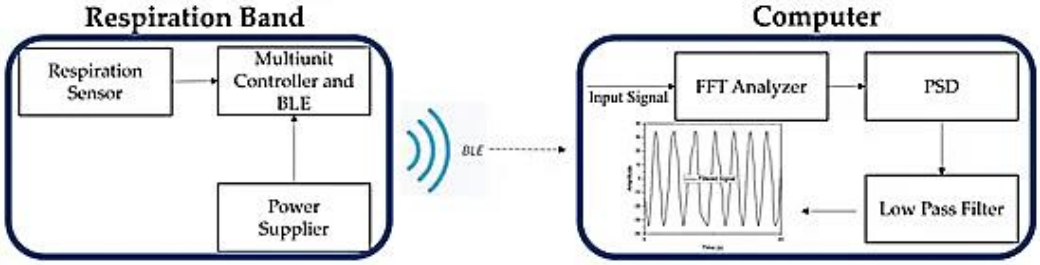

Figure 3.5: Block Diagram representing Respiration Monitoring System using the fabricated sensor [65]

H. Cheng et al. contributed by fabricating a strain sensor to overcome the limitations of previous wearable devices like their low sensitivity, adhesiveness, and impermeability based on the composite polymer and conductive materials; with the incorporation of TPU for flexibility, PDA and MXene ($Ti_3C_2T_x$) for adhesiveness and good electrical conductivity respectively. The approach used wet spinning process yielding a high gauge factor of 57.15 in a wide strain detection range and mechanical stability over repeatable use. Despite these advancements there are certain challenges in the research which need to be addressed like signal drift, environmental stability and hysteresis [66].

R. Wang et al. developed a strain sensor with fibers possessing faster response and reduced hysteresis. Researchers developed an approach which improves scalability in manufacturing and accomplished an improvement in mechanical robustness and faster signal response with response time of less than 30ms, resolution of 0.015%, stability (16000 cycles) by optimizing composition and including nanomaterials. A common drawback in fiber strain sensor is low hysteresis which affects accuracy and consistency in performance was successfully addressed in the research [67].

L. Guo et al. developed an integrated wearable collaborative strain sensor (IWCSS), with the coating of a conductive double-cross-linked hydrogel consisting of a superhydrophobic layer. The prepared sensor could restore its performance and hydrophobicity and the layer acts as a barrier against water infiltration and provides improved environmental durability and protection against liquid corrosion which ensures stable sensing. This sensor gives response time of 70ms, sensitivity coefficient of 0.8, a strain sensing range of up to 30%, and excellent stretchability of 150% with

good self-healing capabilities making this technology useful for accurately monitoring human movements with high accuracy and stability even in demanding environments [68]. The self-healing behavior of the sensor at room temperature is illustrated in Figure 3.6.

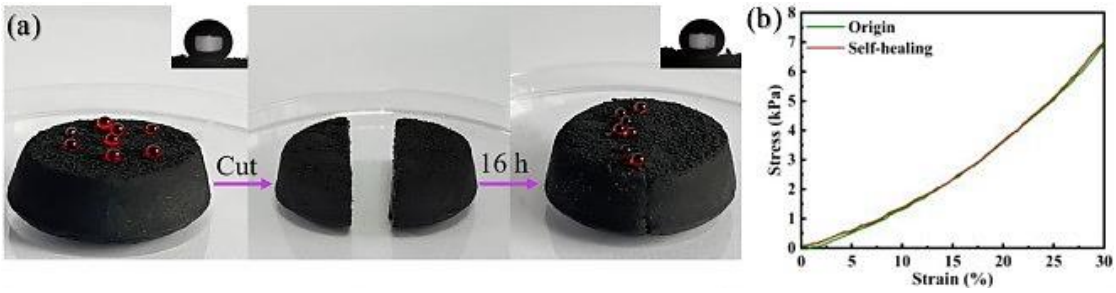

Figure 3.6: (a) Experimental representation of the self-healing ability **(b)** Stress versus strain plot of the original versus self-healed sensor [68]

X. Dai et al. contributed to the field of self-powered electronic skin and addressed the limitations of reduced performance of previous sensors in diverse environmental conditions like water exposure, varying pH levels and extreme temperatures. The self-healing polyurea and silver conductive nanowire sensor converts mechanical energy to electrical energy utilizing triboelectric effect, making it self-powered. The proposed sensor demonstrated excellent performance without signal distortion and enhanced durability of the device opening new avenues in scenarios where environment resilience is of paramount significance [69]. The sensor with AgNWs arranged in 3x3 array structure and two sandwiched layers of polyurea for measuring the sweat tolerance are illustrated in Figure 3.7.

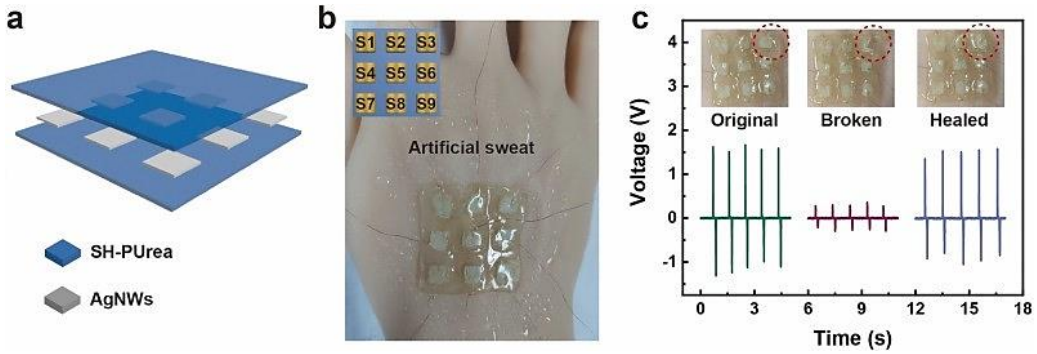

Figure 3.7: Sensor attached to the back of hand with artificial sweat particles sprayed and comparison of output voltage signals of original and healed sensor [69]

N. Sanandiya et al. addressed the escalating issue of EMI interference due to increasing electronic devices by developing chitosan-based electroconductive ink. The performance of commercial and military equipment suffers significantly due to this radiation. The study introduced 3D printing ink, by leveraging biopolymers— chitosan as a binder, silk fibroin as structural stabilizer and carbon fillers for electroactive fillings. The developed structure blocks incoming waves up to 99.9% with electromagnetic shielding power of 30-31 dB, preventing unwanted exposure to radiation and signal disruption. This highlights the ink's strong potential for use in sensing applications for protection against EMI, thereby maintaining signal fidelity and device efficiency [70].

W. Zhong et al. introduced a novelty in strain sensors with the introduction of multilayered polyurethane fiber prepared sensor (MPF) by integrating PU and CNTs coated through wet spinning onto an elastic electrode. The technique utilizes a multi-layer entanglement process to enhance the conductive pathways and stretchability. The sensor is intended to detect human motion by achieving a tunable sensitivity and an expanded working range. It achieves a high sensitivity factor of up to 127.74 and range of up to 58% making it highly effective for detection of subtle and large-scale human motions. The importance of this research lies in how it addresses the persistent challenge of the trade-off between sensitivity and strain range in the field of flexible and wearable strain sensors [71].

C. Zhang et al. proposed research on capacitive type strain sensors which are fiber based utilizing the advantages of capacitive properties instead of resistive ones. The researchers address the issues of limited stretchability and delamination by utilizing direct ink writing method for fabrication. The product has high sensitivity (0.924), consumes less power, exhibits excellent mechanical stability, wide detection range of 178%, low hysteresis (1.44%) and effectively tested in real world applications showing its potential advantages in smart textiles of next generation and implantable electronics [72].

M.N. Alam et al. introduced an approach resulting in an increasing toughness of silicone nanocomposites using multiwalled carbon nanotubes (MWCNTs) and molybdenum disulfide (MoS_2). Individual MWCNTs and MoS_2 exhibit polymeric properties. This synergistic effect technique overcomes the mechanical limitations of

previous sensors based on just polymers. The CNT-MoS_2 hybrid filler offered improve fracture strain compared to single filler systems, enhanced toughness and established a trend towards multi-dimensional fillers for enhanced durability and flexibility [73].

Y. Chen et al. contributed to real world biosensor applications by developing a strain sensor with the incorporation of carboxymethyl chitosan (CMCS) into gellan gum/polyacrylamide (GG/ PAM). CMCS provides antibacterial properties and combined effect of GG and PAM enhanced the performance of the sensor by optimizing the amounts of CMCS and GG. The sensor monitored large movements and subtle facial micro-expressions with short response time [74].

T. Jamatia et al. introduced a highly flexible strain sensor using styrene-b-(ethylene-co-butylene)-b-styrene triblock copolymer (SEBS) and carbon black (CB) using a simple and cost-effective solvent-processing method. The introduction of CB in SEBS polymer enhanced piezoresistive properties and prepared prototype exhibited high resilience to stress and strain, with good flexibility, conductivity and a linear dependence on the applied strain. It can monitor body motions like breathing and walking when sewn onto clothing therefore is poised for applications in healthcare, smart textiles and robotics [75].

Chapter 4

Experimental Tools and Techniques

There are several techniques available for synthesizing and preparing polymer nanocomposite solutions. The use of the technique depends on the type of material, their properties and characteristics, requirements of a specific application, scale of manufacturing, budget availability etc. This section discusses briefly the fabrication and characterization methods employed to develop and investigate the device under test. Different tools and techniques utilized in the process for the proposed research have been discussed in the underlying section.

4.1. Material Synthesis

4.1.1. Probe Sonicator

Probe sonicator is a laboratory device used for dispersing and breaking down large particles in a solution to nanoscale ones and homogenizing them. A probe sonicator operates using sound energy or ultrasonic waves with frequency greater than 20kHz to agitate, loosen particles stuck to surfaces and breaking of aggregates, consisting of a probe which is emersed in a sample at an amplitude. These waves generate cavitation, which creates strong shear forces that effectively disperse materials, shatter cell walls and cause disruption of particles [76].

4.1.2. Bath Sonicator

A bath sonicator is also referred to as ultrasonic cleaner or ultrasonic bath which generates sound waves with high frequencies (>20kHz) through ultrasonic transducer. These waves create very small bubbles called cavitation bubbles in microscopic form in a liquid solution. It consists of a tank which is filled with water or a cleaning solution with sample which needs to be processed immersed inside. When the device is activated, it dislodges contamination particles, breaks agglomeration or degas to remove dissolved gases from liquids using the principle of acoustic cavitation. Bath sonicator ensures homogeneous dispersion of materials, removes unwanted particles and is used for cleaning in sensor technology [77].

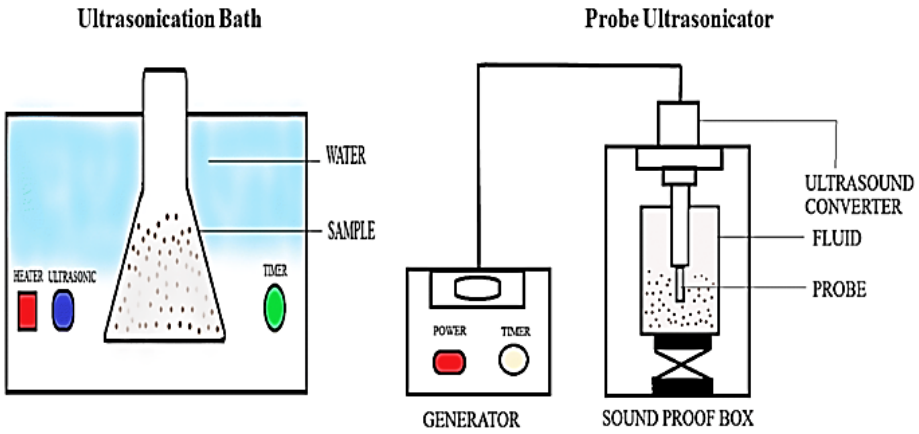

Figure 4.1: Schematic view of Ultrasonic Bath and Probe Sonicator [78]

4.1.3. Magnetic Stirrer

A magnetic stirrer is a frequently used laboratory instrument that is employed to efficiently mix liquid solutions by means of a magnetic stir bar. After calculating and choosing the concentration of each material, the solution is set to mixing forming a homogeneous mixture. Magnetic stirrer works by utilizing either a stationary or rotating magnetic field to rotate a stir bar inside a vessel. These stir bars are typically coated with PTFE (Teflon) or Glass and come in different shapes and sizes. Stir bars are magnetically linked to the external rotating magnet which is present beneath the container. It starts to rotate as the magnetic field is activated that thoroughly agitates the liquid resulting in consistent and homogeneous solutions. Magnetic stirring is employed for complete dissolution and uniform distribution of materials involved including photoinitiators, crosslinkers, monomers and plasticizers. The speed of stirring is not fixed, it depends upon the material utilized, their quantity and concentration. In the case of hydrogel-based synthesis moderate speed is best for uniform dissolution of particles without destroying bonding of incorporated materials [79].

Magnetic stirrers have extensive applications in the fields of chemistry, biology, and material sciences where they are utilized to combine solutions, mix suspended particles, and other liquid substances. They have several advantages over conventional mechanical stirring methods such as their improved consistency, minimum contamination risk, silent operation, and precise speed control. Additionally, advanced magnetic stirrer models are equipped with integrated heating capabilities that enable mixing of solutions and temperature regulation at the same time. This feature is

essential for processes such as synthesis of polymers, solubility studies, and various biochemical reactions. They have become indispensable in modern laboratories since they enable high-quality research and experimentation, as well as reliable, efficient, and easy to use [80].

Figure 4.2: Magnetic stirrer [81]

4.2. Device Fabrication Techniques

4.2.1. Spin coater

A spin coater is a device used in various scientific and industrial applications such as in microfabrication's to apply a uniform, homogeneous thin film coating of liquid solutions onto flat substrate through a process known as spin coating. In the process a liquid solution is dispensed in controlled amount on to the center of the substrate and is rapidly spun, the liquid spreads evenly onto the substrate material due to centrifugal force which spreads the liquid outward. The thickness of the developed films depends on several key factors including speed of spinning, time duration for the process and deposited solution viscosity. Lower spin produces thicker films whereas higher speed results in thinner uniform films. This technique is preferred due to its ability to yield thin films with high uniformity and thickness variations of less than 1% [82].

Figure 4.3: Spin Coater [83]

4.2.2. Magnetron Sputtering

Magnetron sputtering is a vapor phase deposition technique used to deposit thin films onto various substrates. Plasma is generated in vacuum chamber where positively charged ion particles are accelerated towards negatively charged particles. The target material is negatively charged, which is the material to be deposited. The bombardment of high energy ions within the plasma causes the ejection of atoms from the target which are deposited travelling through vacuum environment on to a substrate too form thin films. The presence of a magnetic field near the target improves the sputtering process by restricting electrons. This results in an increase in the ionization rate of the plasma leading to better film quality and higher deposition rates. This method is preferred due to its ability to generate films with exceptional adhesion, uniform thickness, and significant purity. The technique plays an important role in the development of strain sensors by enabling the deposition of sensitive thin film material onto a flexible substrate for studying electrical properties and performance of the sensor [84]. A pictorial view of the general process involved in magnetron sputtering is shown in Figure 4.5.

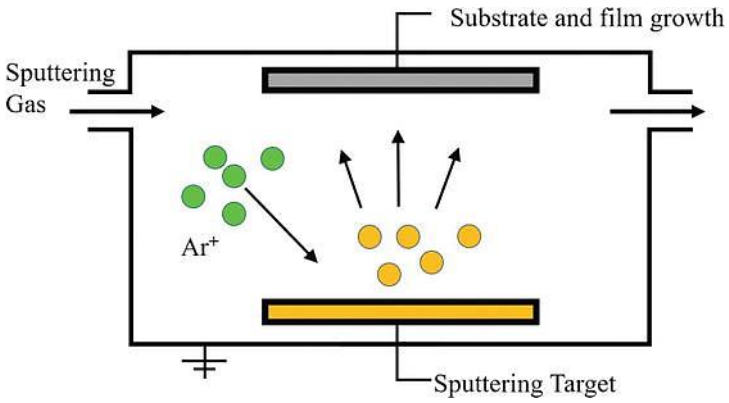

Figure 4.4: Magnetron Sputtering [85]

4.2.3. UV Curing

UV treatment or UV curing is a photochemical process that hardens or cures coating, adhesives, inks and other materials with the exposure to high intensity UV light. UV light has wavelength ranging from 100-400 nm which is further divided into three main types i.e., UVA (315-400 nm) and UVB (280-315 nm) which are both used for curing applications such as coatings and polymer crosslinking, and UVC (100-280 nm) is effective for sterilization and disinfection purposes. In material synthesis UV treatment plays a crucial role, when UV light is incident, it is absorbed by photoinitiators initiating a polymerization process and transforming the liquid form into a solid film within seconds. The rapid process offers certain advantages than conventional techniques such as low energy utilization, mechanically robust coating, ensures uniform and durable product and reduced environmental impact. In the production of strain sensors UV treatment plays a pivotal role for the formation of polymer-based conductive films, encapsulation layers, and structural reinforcements, where it solidifies polymer networks [86]. The process involved in UV curing is illustrated in Figure 4.6.

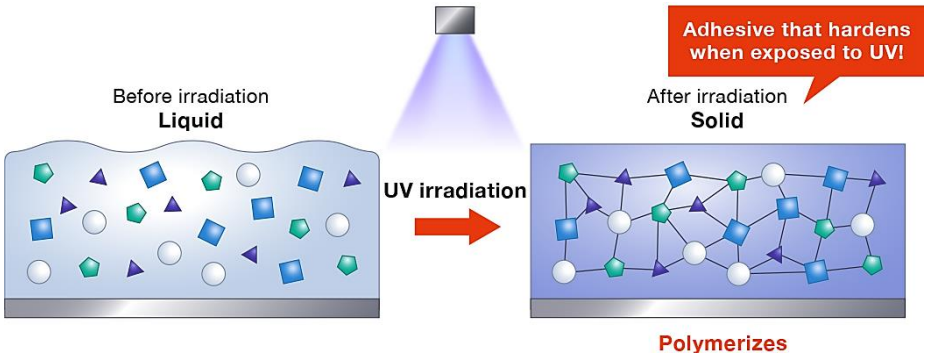

Figure 4.5: UV curing process [86]

4.3. Characterization Techniques

4.3.1. Scanning Electron Microscopy (SEM)

Scanning electron microscopy (SEM) is an imaging technique that produces images of target sample by scanning with focused beam of electrons. The scanned sample is present in a vacuum chamber and mounted on a movable stage. It consists of an electron gun made of tungsten filament to generate a high energy beam of electrons which by passing through electromagnetic lenses is directed towards sample. Upon interaction, this beam produces different types of signals including backscattered and secondary electrons along with X-rays which are finally converted to high resolution images. SEM is typically used to analyze microstructure, chemical composition and topography of sample with very high resolution to the scale of nanometers. It is a technique which is widely used in material sciences, biological sciences, nanotechnology and electronics for material characterization at different stages of research, to provide detail insights into surface features and fine structures. In strain sensors SEM is beneficial to study the morphology, dispersion and uniformity of conductive fillers and polymeric materials. Moreover, it helps to identify defects, cracks and evaluate adhesion issues at interface of composite sensors in order to get optimized performance [42][87].

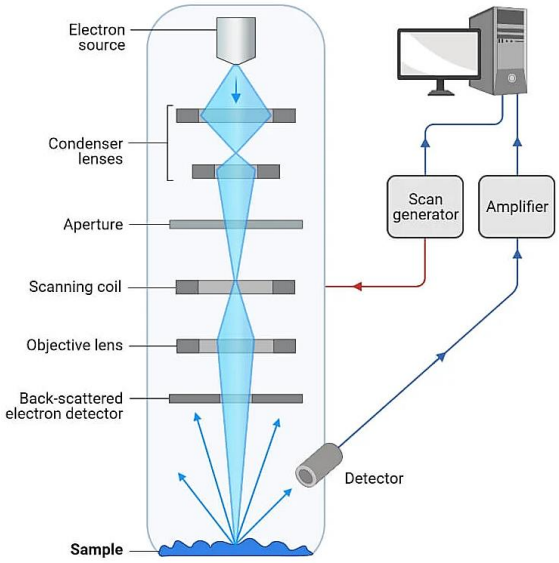

Figure 4.6: Scanning Electron Microscopy [42]

4.3.2. Electrical Characterization

i. IV Characterization

Current-Voltage characterization or IV Characterization is a fundamental electrical test used to determine the relationship between current and voltage of strain sensors. It evaluates the response of sensors to different values of applied voltages by recording electrical signals. By looking at the IV data we can analyze and provide insights to various parameters such as conductivity and resistance which can be easily calculated through the current and voltage data using Ohm's Law.

$$V = IR$$

Moreover, linearity in sensor performance can be analyzed through current-voltage data. These metrics are crucial for sensor performance. Current values can be determined under various strain levels which can help to optimize and fine tune the sensor design and fabrication technique. By examining resistance change with applied strain researchers can figure out the degree to which the sensor effectively converts mechanical deformation into electrical signals and analyze sensor sensitivity. Researchers use this information in real-time strain monitoring, biomedical applications and wearable devices to ensure accuracy and reliability of the product [88], [89].

4.3.3. Mechanical Characterization

i. Stability Test

The stability of the sensor is evaluated to monitor strain sensor performance and see how it changes over time under varying and harsh environmental conditions like temperature, humidity and shock. With the passage of time sensor functionality degrades and there could be drift in output signal which can lead to inaccurate readings. With the help of stability and cycle tests this performance degradation can be detected earlier. Stability test ensures sensors remain operative for prolonged use and are functional with consistent performance for real world implementation. Sensors that show stable cycles upon testing ensure stability, reduce risk of failure in environmental conditions and are reliable for long term use. Stability cycles help with fine tuning sensor performance to enhance durability and longevity [90], [91]. Here sensor stability was tested for 100 cycles at 20% stretching.

ii. Sensitivity

Sensitivity refers to how effectively a device or sensor output changes in response to the change in the physical quantity which is to be measured. In the case of strain sensor, it tells effectiveness to detect mechanical deformation like bending, stretching or compressing and converting that to electrical signals. Depending on the type and mechanism on which the sensor operates there are different measurable quantities to find sensitivity including resistance, capacitance or voltage. The importance of this performance metric is to find the precision and accuracy of the measuring device. The more sensitive device will be better suitable for real world applications. In resistive type strain sensors, it is measured in terms of gauge factor by calculating change in resistance with respect to the applied strain [92]. The sensitivity of the resistive type strain sensors can be calculated using the following equation:

$$GF = \frac{\frac{\Delta R}{R_0}}{\epsilon} \tag{4.1}$$

The strain applied ϵ can be calculated using the equation:

$$\epsilon = \frac{\Delta L}{L_0} \tag{4.2}$$

Where ΔR, R_0 and ϵ are the change in resistance, initial resistance and strain applied respectively, ΔL and L_0 are the length change on applied strain and initial length of the fabricated sensor respectively.

iii. Stretching Test

Stretching test is used to analyze mechanical deformation in response to strain applied. It tells how sensor behaves under tensile and compressive forces. When the sensor is stretched, its electrical resistance changes because of the change in dimensions and microstructure. The internal structure of the device in turn causes changes in electrical and mechanical properties. This test tells at what length the fabricated sensor be able to stretch or elongate with respect to the original before it breaks. To conduct stretching test a controlled stretching force is applied after clamping the sensor on both sides. The testing of this parameter is critical in the case of flexible and stretchable sensors where it conforms to different irregular surfaces and other applications in wearable electronics, structural health monitoring and soft robotics to support durability,

wearability, and enhance performance [93]. Stretchability is expressed in percentage of the original sensor length:

$$Stretchability(\%) = \frac{\Delta L}{L_0} \times 100 \quad (4.3)$$

Where L_0 and ΔL represents the initial and final length of the sensor respectively.

iv. Self-Healing Test

Self-healing is the ability of the sensor to recover or repair to its original electrical and mechanical properties after controlled damage. The self-healing test evaluates the sensor to recover to original properties after physical damage like cuts or stretching beyond limit. Different types of bonds including dynamic, hydrogen and ionic bonding are responsible for material recovery after damage or repeatable use. In self-healing the damaged sensor is tested for healing by tracking its recuperation process over time. Performance is evaluated by monitoring characteristics like device sensitivity, conductivity, stretchability and recovery time. Here the sensor will be sliced and then attached to evaluate the performance by stretching after intrinsic healing and calculating recovery time. The thorough understanding of this parameter is crucial in the case of applications in biomedical, infrastructure and soft robotics to assess the durability and longtime use [94].

4.4. Characterization Tool

For the electrical and mechanical evaluation of the developed hydrogel strain sensor, a pre-developed automated characterization tool available at CAEPE Lab, IIUI was used. This automated tool consists of gripping stage, an actuator system, and integrated electronic modules that enable programmable and controlled testing of flexible devices. The system supports multiple functionalities including IV-characterization, measuring unknown resistances, and various mechanical performance tests such as bending, relaxing, cycle test, and stretchability evaluations. It has precise motor-based mechanisms which allow accurate strain sensing and have highly conductive electrode grips to ensure noise-free signal acquisition and accurate electrical signals during dynamic tests. Furthermore, the tool enables angle-dependent testing, which is especially relevant for simulating joint-like motions in wearable sensor applications. This DIY platform proved to be cost-effective, efficient, and highly adaptable for

characterizing next-generation flexible sensors. It is crucial in validating sensor performance parameters such as sensitivity, durability, self-healing behavior, and response consistency under repetitive deformation cycles.

4.5. Real Time Implementation

The self-healing, stretchable strain sensor demonstrates strong potential for real-time human motion detection applications by mounting across various body parts such as the wrist, finger, elbow and knees. When mounted on these areas, it can accurately monitor joint movements, muscle activity and motion timelines. Its ability to recover after damage ensures long-term durability and reliable performance, making it suitable for continuous healthcare monitoring. The sensor's high stretchability and sensitivity allows for detection of both subtle and extensive movements. It can track physiological movements like blinking, facial expressions, respiration and muscle contractions, making it highly suitable for applications in wearable healthcare, rehabilitation and human-machine interfacing thus contributing to improved diagnostic accuracy and treatment outcomes [95].

Chapter 5

Result and Analysis

5.1. Optimization Strategy and Baseline Reference

The optimization study conducted in this research work is based on a hydrogel formulation which was previously developed. The strain sensor was tested for basic sensing functionalities and needed further optimization. This composition serves as the reference point for further optimization of target parameters. In this research, to achieve optimal performance of the hydrogel-based strain sensor, six constituent materials: Glycerol, 2-Hydroxy-4'-(2-hydroxyethoxy)-2-methylpropiophenone (Irgacure), Acrylamide (AM), N,N′-Methylenebisacrylamide (MBA), 2-Acrylamido-2-methylpropane sulfonic acid (AMPS) and Polyvinyl Alcohol (PVA) concentrations have been systematically varied. The optimization approach has been followed with each material concentration individually varied while keeping the other five material concentration constant. The selected baseline formulation is listed in Table 5.1.

Table 5.1: Base Concentration of Materials Used for Optimization

Material	Base Concentration
Glycerol	0.5 mL
Irgacure	0.0331 g
AM	0.8775 g
MBA	0.000681 g
AMPS	0.2625 g
PVA	0.1 g

Each material will be varied across four concentrations which have been selected as 1x, 2x, 3x, and 4x of the base value and its impact evaluated based on five key performance parameters. The optimal value for each material selected is based on the balanced performance across all parameters:

- Resistance variation with applied strain
- Stability Cycles
- Sensitivity (Gauge Factor)
- Stretchability
- Self-healing

After tuning these parameters for material composition, strain sensor performance is further optimized by varying dimensions including width, length and thickness and effect is monitored across the same performance metrics to get the final device.

5.2. Material Synthesis Process

The hydrogel-based strain sensors have been synthesized via UV initiated free-radical polymerization. The general procedure is mentioned below:

1. Firstly, measure PVA which is in powdered form with the help of a weighing machine. Add 5 g of PVA in 150 mL distilled water with solution placed on hot plate and magnetic stirrer. The temperature of hot plate is set to 80℃ and continuous stirring is done at the speed of 750 RPM for 1 hour so that all PVA particles are well dissolved and forms a uniform solution.
2. For each batch 3 mL of the PVA stock which is equivalent to the ratio of 0.1 g of PVA with respect to 3 mL of DW is extracted from the previously synthesized solution.
3. Measure all the remaining materials using a precise weighing machine and break them into small particles with the help of probe sonicator for uniform dispersion.
4. Take a beaker, add 3 mL of the prepared PVA solution and heat it at 80℃ on magnetic stirrer for 10 minutes with stirring speed of 750 RPM.
5. Turn off the heat and allow the solution to cool down to room temperature.
6. Once at room temperature, gradually add glycerol according to the pre-defined value into the PVA solution while continuously stirring at 750 RPM for 10 minutes. The stirring speed should be the same throughout the entire process.
7. Incorporate the remaining materials in the following order: Irgacure, MBA, Acrylamide and AMPS, according to the specified weights, ensuring that each component is completely dissolved before introducing the next. Continue

stirring the solution for 1 hour or until all material particles are well dissolved, forming a homogenous solution for hydrogel.

8. Place the solution in bath sonicator for removing air bubbles and forming homogeneous solution.

- **Fabrication**

- Put the synthesized solution into the mold using a spin coater to coat a uniform layer of solution, then expose it to UV light to initiate polymerization process until a soft, flexible and transparent gel is formed.
- For the fabrication process magnetron sputtering is utilized to form contacts on both terminals of the active layer. Fabricated devices are finally employed for testing mechanical, electrical and self-healing properties.

To ensure a controlled study of material composition, the synthesis process, sensor geometry and physical dimensions (Width: 1 cm, Length: 7 cm, Thickness: 3 mm) remain the same throughout the entire optimization process, only the concentration of each material is varied across four levels which are selected as 1x, 2x, 3x, and 4x of the base value and impact is evaluated based on five key performance parameters one at a time. The optimal value for each material selected is based on the balanced performance across all parameters.

Figure 5.1 shows the experimental steps involved in the synthesis of hydrogel-based strain sensor

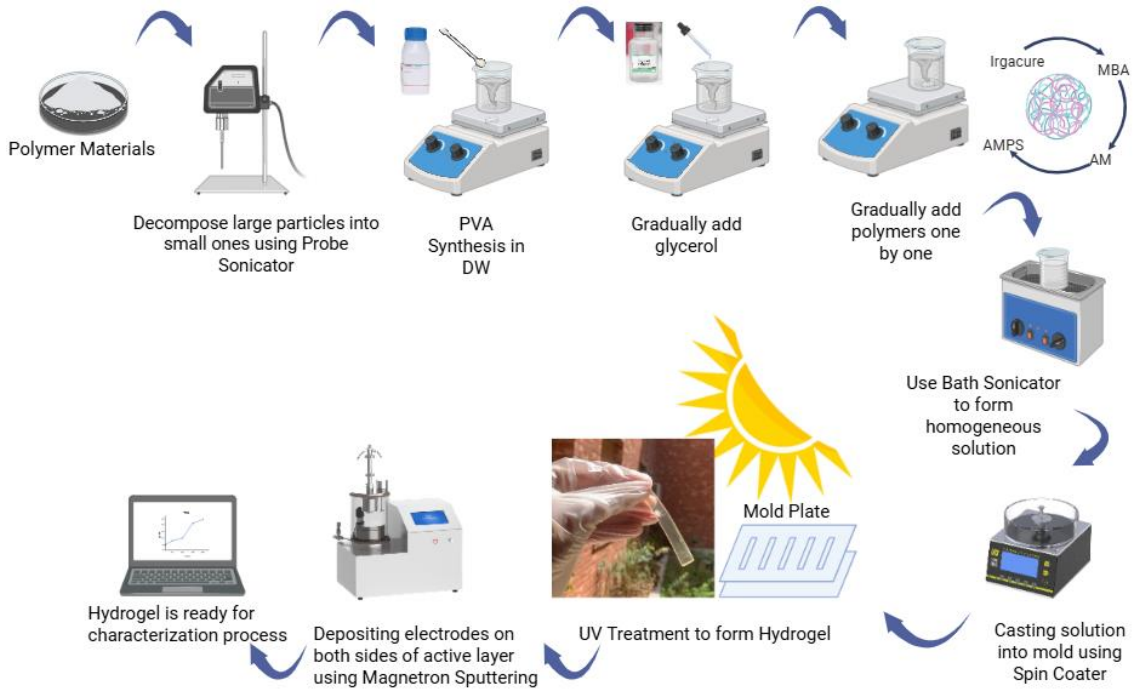

Figure 5.1: Synthesis Process

5.3. Material Composition Optimization

5.3.1. Optimization of Glycerol

During the optimization process, initially Glycerol has been varied from 0.5 mL to 2.0 mL (1x → 4x) while other materials concentrations kept constant and 4 sensors have been synthesized. Glycerol concentration of 0.5 mL gave the smoothest and well cured sensor. However, the 1.5 mL and 2 mL samples were unable to cure completely under UV treatment as the concentration increased. This is because glycerol is a hygroscopic material, which results in a higher moisture content, making it difficult to set completely as can be seen in Figure 5.2.

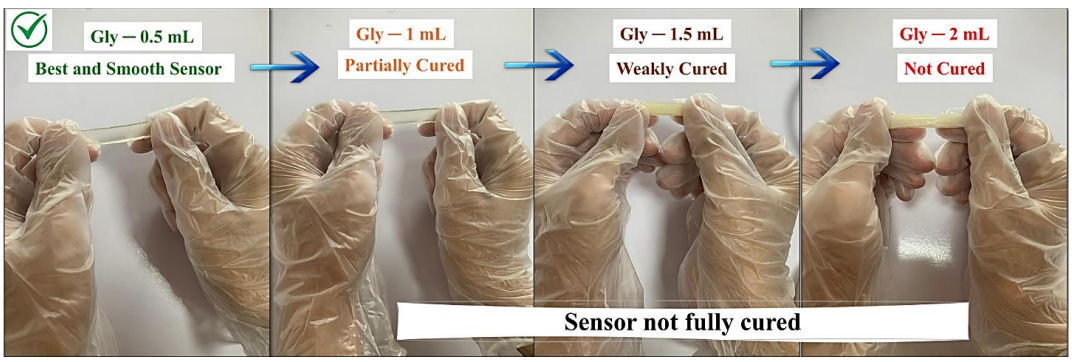

Figure 5.2: Glycerol Synthesized Sensor with Varying Concentration

It has been observed that increasing glycerol content softens the network, limiting its mechanical integrity and resistance. Higher concentrations improve sensitivity due to high ionic mobility, but they compromise linearity and signal clarity during stretch/release cycles. The results of parameters tested are presented in Figure 5.3.

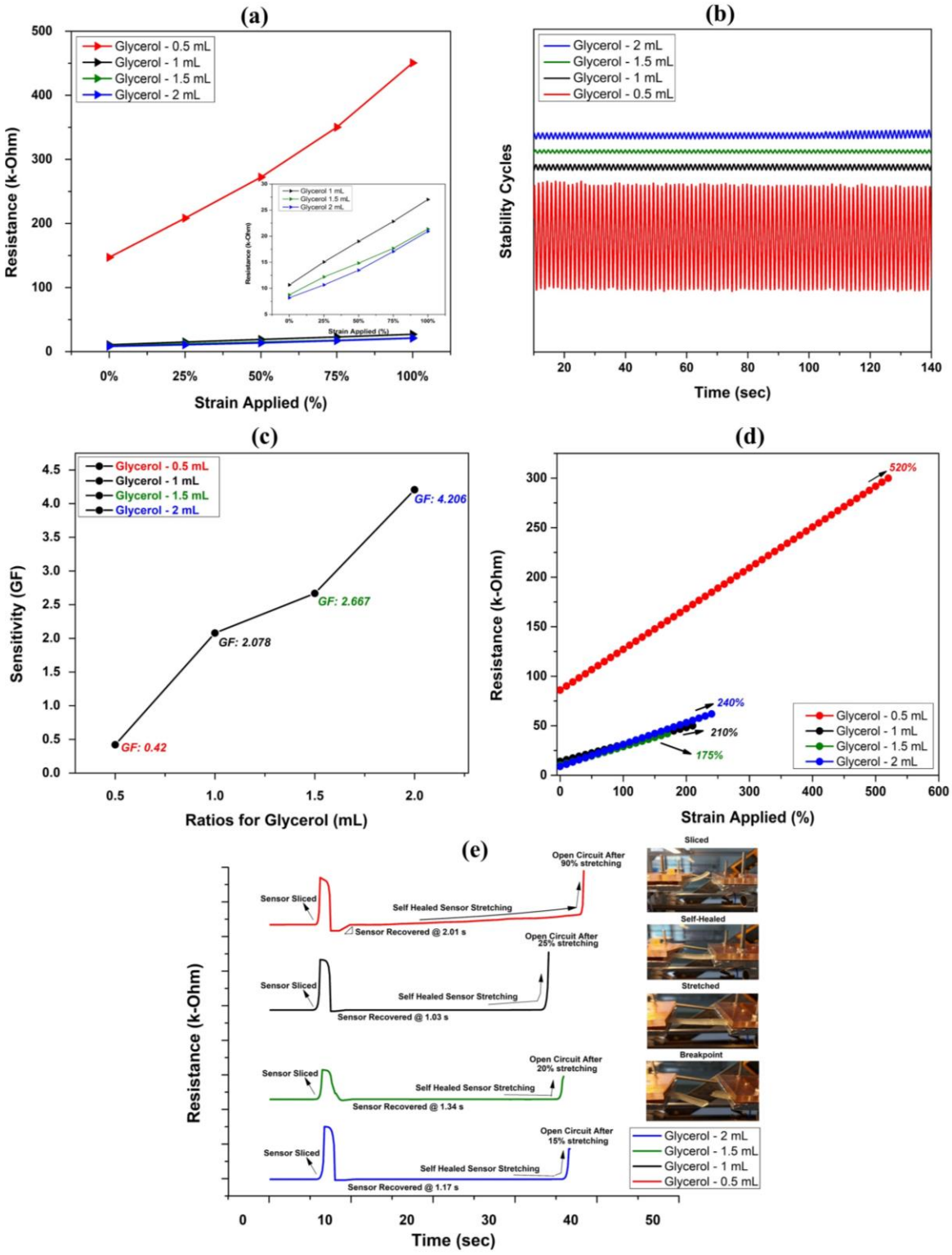

Figure 5.3: Strain sensor graphs with varying concentrations of Glycerol: 0.5mL, 1mL, 1.5mL and 2mL. **(a)** Resistance versus Applied Strain **(b)** Stability Cycles **(c)** Sensitivity **(d)** Stretching **(e)** Self-Healing

Considering all parameters and mechanical results, Sensor 1 with 0.5 mL glycerol concentration showed the best result because of linear resistance variation and consistent performance across stability cycles with higher amplitude and better-defined cycles, providing moderate and balance sensitivity while maintaining its mechanical integrity. The sensor achieved the highest stretchability (520%) and recovered up to 90% stretching after self-healing, which has been the best among the four tested compositions. This composition maintains an optimal balance between mechanical flexibility, electrical performance and self-healing abilities and thus fixed for subsequent experiments. The summarized performance trends for varied Glycerol concentrations are shown in Table 5.2.

Table 5.2: Summary of the performance trends for varying Glycerol Concentration

Sr. No.	Glycerol (mL)	Resistance verses Strain (%) Curve	Stability Cycles	Sensitivity (GF)	Stretchability (%)	Stretching after Self-Healing
1	0.5	Linear	Good	0.42	520	90% in 2.01s
2	1	Linear	Small	2.078	210	25% in 1.03s
3	1.5	Linear	Small	2.667	175	20% in 1.34s
4	2	Linear	Small	4.206	240	15% in 1.17s

5.3.2. Optimization of Irgacure

The optimization of Irgacure has been conducted by varying concentration from 0.0331g to 0.1324g (1x → 4x) and 4 sensors have been synthesized. During the synthesis process it was observed that as Irgacure concentration increases beyond 0.0331 g, there is polarity issue in the polymer matrix which resulted in non-uniform mixture, therefore, to overcome this issue temperature of 40℃ was provided to facilitate crosslinking and form homogeneous solution. The four synthesized sensors are represented in Figure 5.4.

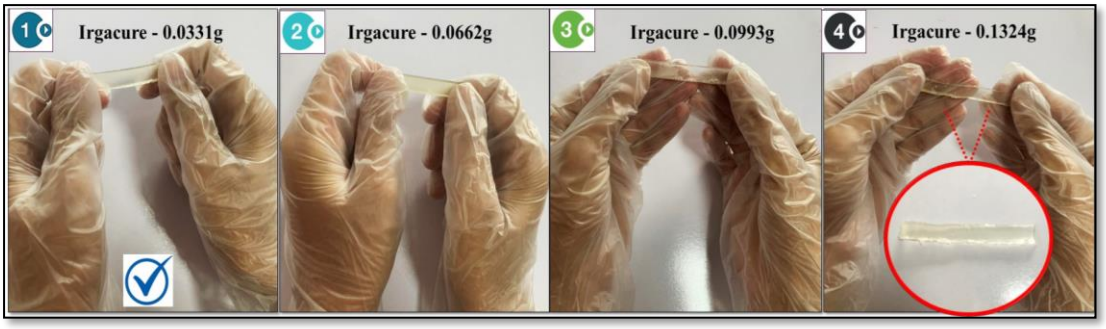

Figure 5.4: Irgacure Synthesized Sensor with Varying Concentration

Due to limited crosslinking Irgacure concentration of 0.0331g provides relatively low sensitivity but has a highly linear resistance response on applied strain. Higher Irgacure concentrations resulted in improved sensitivity with a maximum GF of 4.54 at 0.0993 g. However, they introduced processing challenges like poor solubility and reduced flexibility, reliability and performance of the sensor. Excessive crosslinking and over polymerization at higher concentrations also led to sensor brittleness and inconsistent recovery due to restricted polymer chain mobility. The performance results for the 4 synthesized sensors are reflected in Figure 5.5.

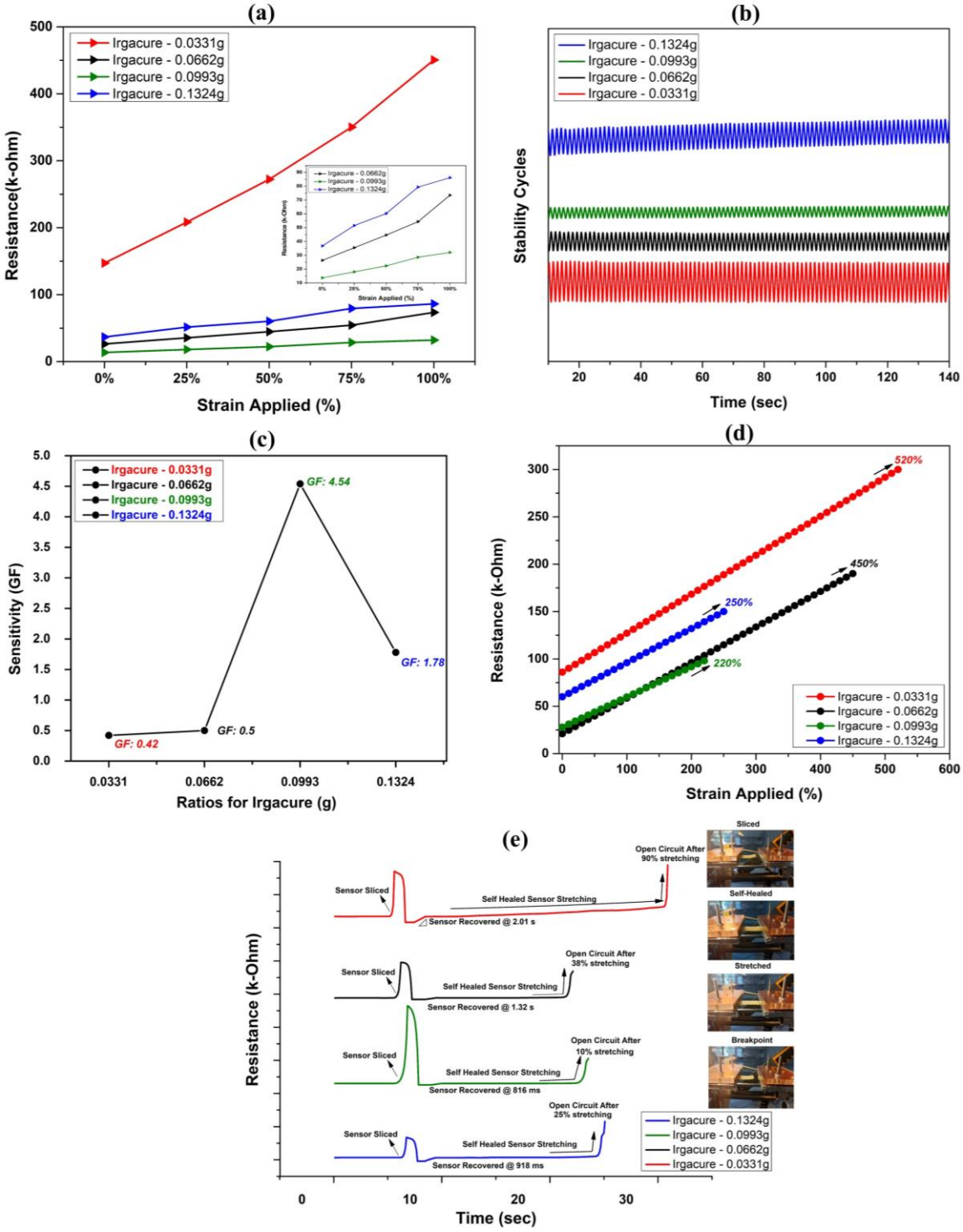

Figure 5.5: Strain sensor graphs with varying concentrations of Irgacure: 0.0331 g, 0.0662 g, 0.0993 g and 0.1324 g. **(a)** Resistance versus Applied Strain **(b)** Stability Cycles **(c)** Sensitivity **(d)** Stretching **(e)** Self-Healing

From the results, 0.0331 g is selected as the optimized Irgacure concentration due to the balanced radical generation resulting in proper polymerization and well-connected

conductive network and most favorable overall performance with maximum durability, excellent stretchability (520%) and good self-healing capabilities with stretching after damage up to 90%. Glycerol and Irgacure baseline concentrations gives the best results. The summary of performance for varying Irgacure concentration is represented in Table 5.3.

Table 5.3: Summary of the performance trends for varying Irgacure Concentration

Sr. No.	Irgacure (g)	Resistance versus Strain (%) Curve	Stability Cycles	Sensitivity (GF)	Stretchability (%)	Stretching after Self-Healing
1	0.0331	Linear	Good	0.42	520	90% in 2.01s
2	0.0662	Non-Linear	Stable	0.5	450	38% in 1.32s
3	0.0993	Non-Linear	Small	4.54	220	10% in 816ms
4	0.1324	Non-Linear	Stable	1.78	250	25% in 918ms

5.3.3. Optimization of Acrylamide (AM)

After getting the optimized value for Glycerol and Irgacure, optimization of Acrylamide is done by varying its value from 0.8775g to 3.51g (1x → 4x) following the previous strategy and synthesizing 4 sensors for performance testing. The results show that AM concentration of 0.8775 g and 1.755 g produced smooth, flexible and stretchable sensors. As concentration increases beyond 1.755 g i.e. 2.6325 g and 3.51 g, sensors lose their flexibility and result in hard and rigid ones. The synthesized sensors are shown in Figure 5.6.

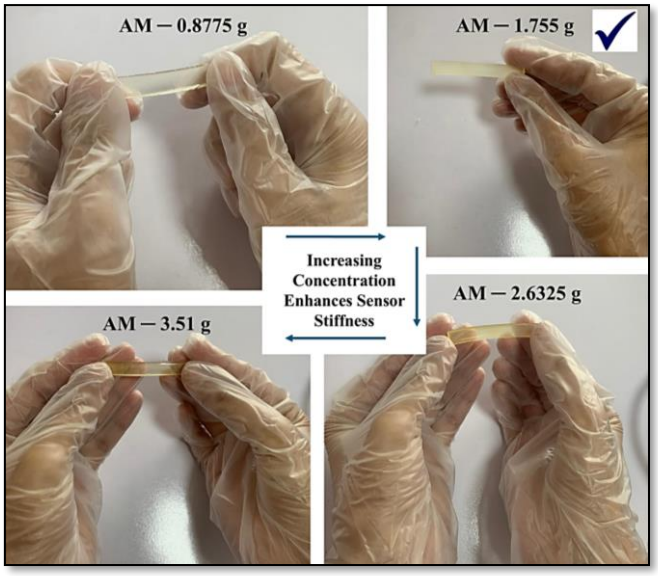

Figure 5.6: Acrylamide Synthesized Sensor with Varying Concentration

The sensor with an Acrylamide concentration of 1.755 g (2x times) shows linearity compared to Acrylamide concentration of 0.877 g and as value increases beyond 1.755 g, the resistance curve becomes less flexible, indicating reduced elasticity and shows less responsiveness to changes in strain. Sensor 1 and Sensor 2 shows excellent stability cycles maintaining consistent resistance values. Sensor 4 is extremely rigid that its sensitivity again increases since small strain may lead to microcracks increasing change in resistance thus sensitivity making it less suitable for strain sensing applications. The comparison of performance metrics is illustrated in Figure 5.7.

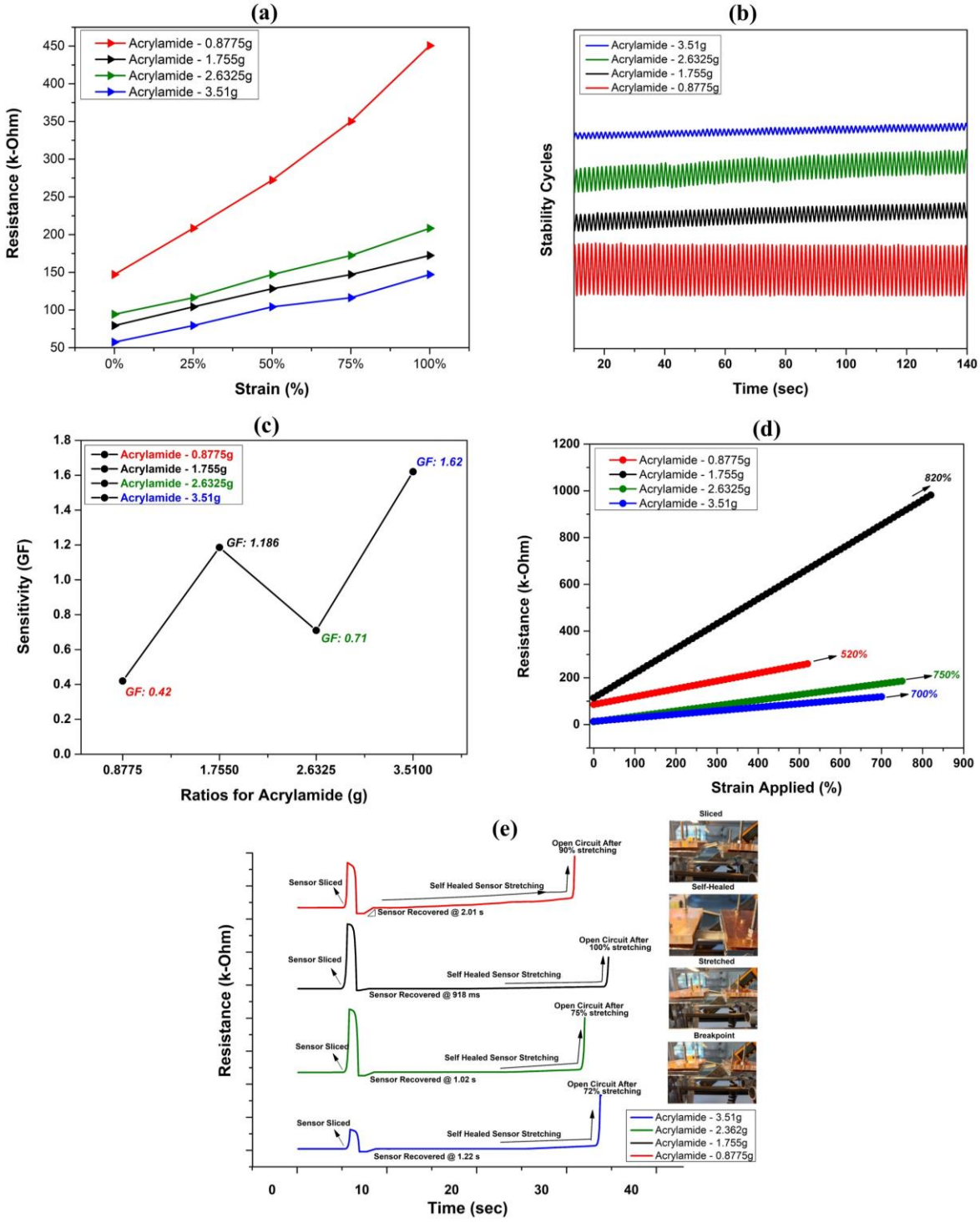

Figure 5.7: Strain sensor graphs with varying concentration of Acrylamide 0.8775 g, 1.755 g, 2.6325 g and 3.51 g. **(a)** Resistance versus Applied Strain **(b)** Stability Cycles **(c)** Sensitivity **(d)** Stretching **(e)** Self-Healing

The mechanical, electrical and self-healing properties of Sensor 2 with 1.755 g Acrylamide concentration emerges as the best performing sensor with good sensitivity

(GF=1.186), the highest stretching of 820%, the fastest self-healing time which is within just 918ms and good self-healing efficiency indicated by stretching up to 100% after healing, creating a best trade-off across all parameters. The comparison of varying Acrylamide concentration on its performance is shown in Table 5.4.

Table 5.4: Summary of the performance trends for varying Acrylamide Concentration

Sr. No.	AM (g)	Resistance versus Strain (%) Curve	Stability Cycles	Sensitivity (GF)	Stretchability (%)	Stretching after Self-Healing
1	0.8775	Linear	Good	0.42	520	90% in 2.01s
2	1.755	Linear	Stable	1.186	820	100% in 918ms
3	2.6325	Linear	Unstable	0.71	750	75% in 1.02ms
4	3.51	Non-Linear	Small	1.62	700	72% in 1.22s

5.3.4. Optimization of N,N′-Methylenebisacrylamide (MBA)

To optimize the crosslinking density in the hydrogel network the optimization of the fourth material i.e. MBA (N,N′-Methylenebisacrylamide) is done by varying its value from 0.000681g to 0.002724g (1x → 4x) following the previous strategy and synthesizing 4 sensors for performance testing. The results indicate that higher concentration of MBA leads to more stretchable and soft sensors but when concentration exceeds double (0.001362g) of the original sensor the synthesized sensor shows rigidness and non-uniform structure because of the denser crosslinked networks. The synthesized samples are shown in Figure 5.8.

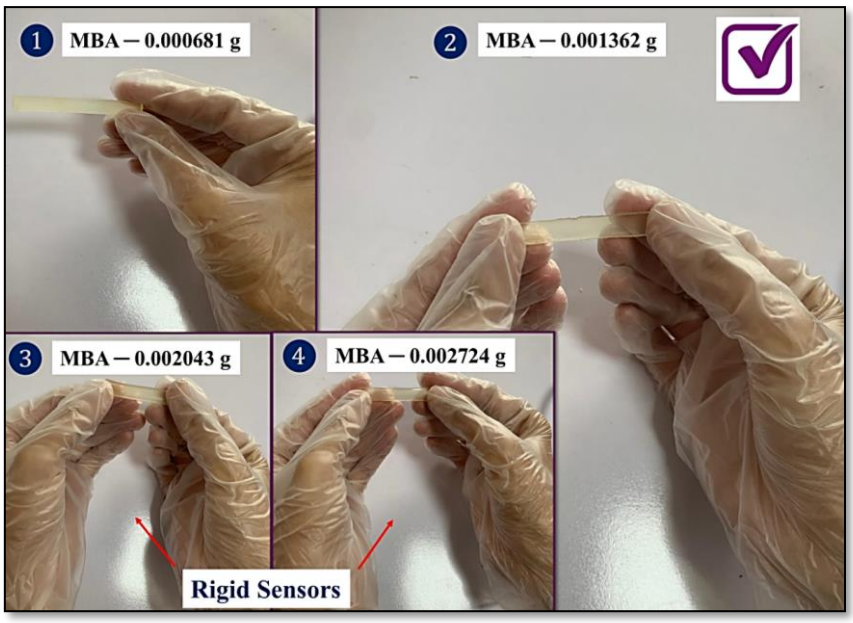

Figure 5.8: MBA Synthesized Sensor with Varying Concentration

Among the tested samples, MBA concentration of 0.001362 g (2x base value) shows the most linear and balance resistance change with respect to the applied strain indicating predictable sensing behavior and good cyclic stability with minimum resistance fluctuation whereas the 0.002724 g MBA sample shows instability because of the microcrack and increased stiffness. The sensitivity curve also shows that it is good compared to higher concentrations. The self-healing performance of the sensor illustrates that as MBA increases; self-healing has slow response because of the insufficient polymer mobility preventing restoration of bonds before breaking. Higher concentrations cause the sensor to make bonds quickly therefore resulting in non-uniform and inconsistent sensors. The performance comparison is shown in Figure 5.9.

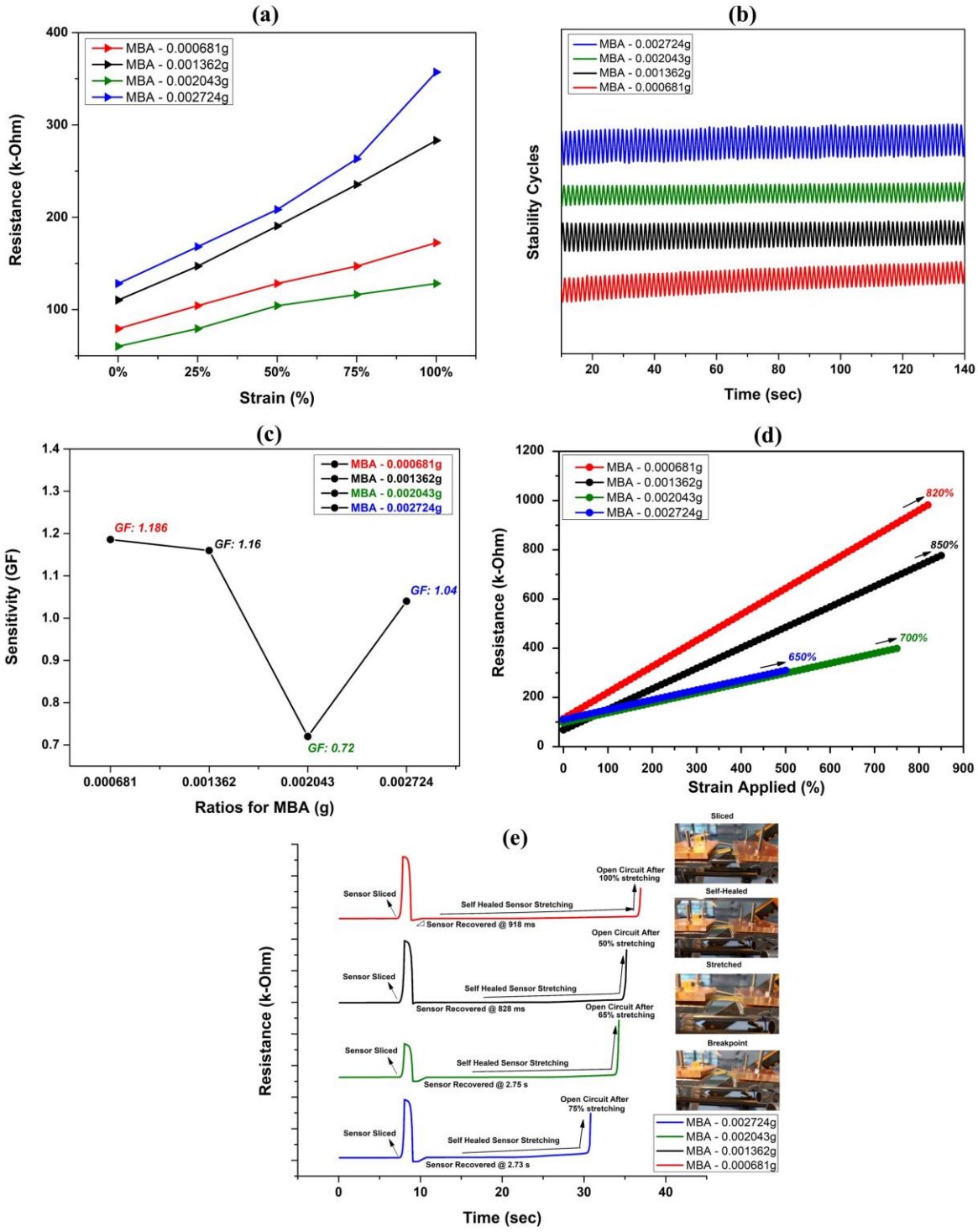

Figure 5.9: Strain sensor graphs with varying concentration of MBA: 0.000681 g, 0.001362 g, 0.002043 g and 0.002724 g. **(a)** Resistance versus Applied Strain **(b)** Stability Cycles **(c)** Sensitivity **(d)** Stretching **(e)** Self-Healing

After considering every factor, the MBA concentration is optimized at 0.001362g, regulating all parameters. It has good cyclic stability, linearity, sensitivity (GF=1.16),

the highest stretchability of 850% and provides 50% stretching within just 828ms following damage recovery. Due to dense networks and quick bond formation, excessive MBA content stiffens and impairs stretchability and healing, affecting sensory performance. The comparison of varying MBA concentration on its performance is shown in Table 5.5.

Table 5.5: Summary of the performance trends for varying MBA Concentration

Sr. No.	MBA (g)	Resistance versus Strain (%) Curve	Stability Cycles	Sensitivity (GF)	Stretchability (%)	Stretching after Self-Healing
1	0.000681	Linear	Stable	1.186	820	100% in 918ms
2	0.001362	Linear	Stable	1.16	850	50% in 828ms
3	0.002043	Non-Linear	Stable	0.72	700	65% in 2.75s
4	0.002724	Non-Linear	Slight drift	1.04	650	75% in 2.73s

5.3.5. Optimization of 2-Acrylamido-2-Methylpropane Sulfonic Acid (AMPS)

Following the optimization of Glycerol, Irgacure, Acrylamide and MBA, AMPS concentration is varied while maintaining the material composition that is previously optimized to check the influence on performance. The synthesized sensors show that as AMPS concentration increases sensors become softer and more stretchable. The synthesized samples are shown in Figure 5.10.

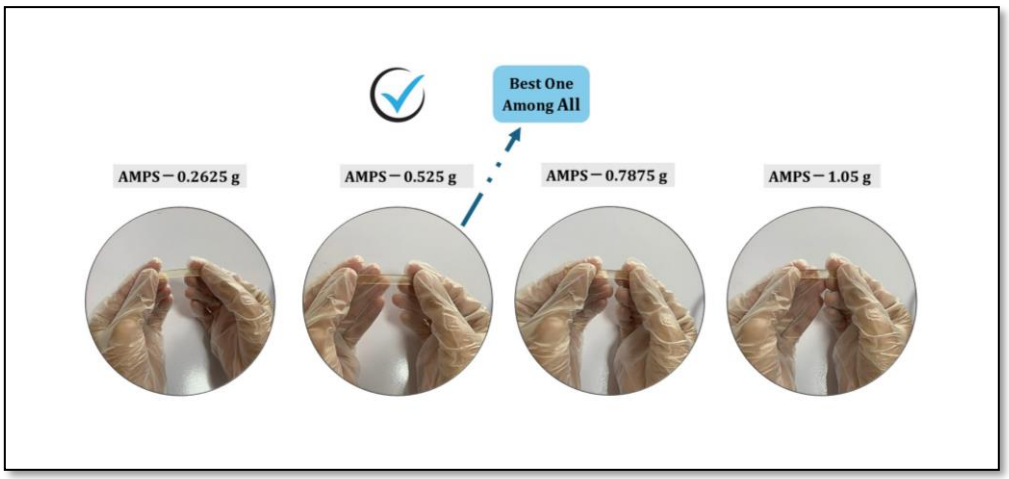

Figure 5.10: AMPS Synthesized Sensor with Varying Concentration

It is observed that as AMPS amount increases in the composition the resistance of the sensor decreases, indicating an increase in conductivity due to the sulfonic acid group and makes the sensor more sensitive to external stimulus by enabling ion transport. The stability trend of AMPS shows that Sensor 2 and Sensor 3 with the concentration of 0.525g and 0.7875g respectively has the most stable stretch/release cycles where Sensor 2 exhibits the highest sensitivity that decreases with concentration. The reason is that initially increasing AMPS enhances ionic conductivity but beyond a certain threshold, saturation of conductive pathways occurs which lowers sensitivity and makes sensor mechanically weak. The stretching trend shows that as the ratio is doubled from 0.2526 g to 0.525 g, stretching increases from 850% to 900% but after a certain limit excessive crosslinking stiffens the synthesized hydrogel sensor. Self-healing indicates that as AMPS ratio increases sensors become too stiff thus chains cannot move freely to reconnect thereby decreasing self-healing performance. The performance comparison of AMPS is shown in Figure 5.11.

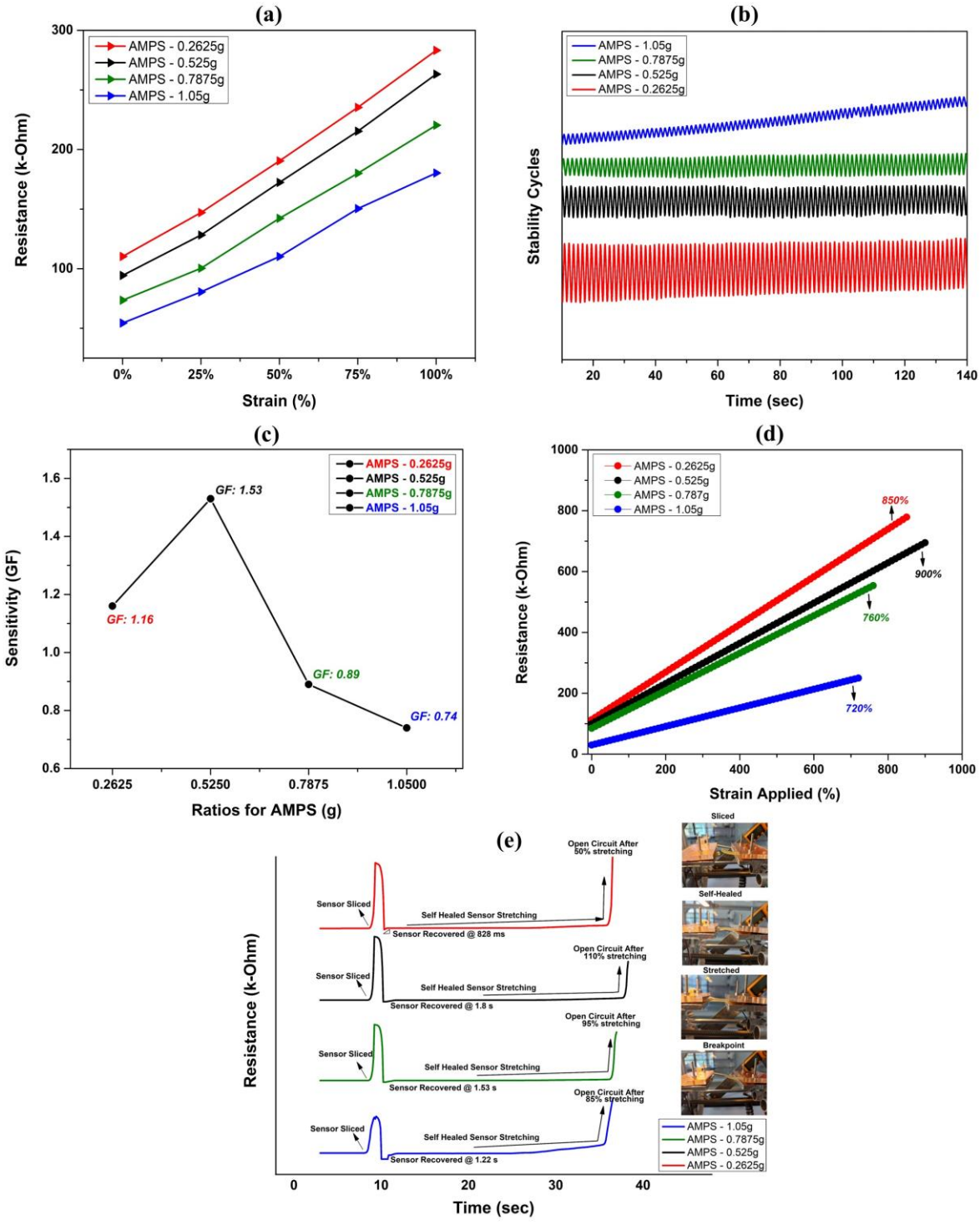

Figure 5.11: Strain sensor graphs with varying concentration of AMPS: 0.2625 g, 0.525 g, 0.7875 g and 1.05 g. **(a)** Resistance versus Applied Strain **(b)** Stability Cycles **(c)** Sensitivity **(d)** Stretching **(e)** Self-Healing

Based on the result, the optimal AMPS concentration is Sample 2 with the ratio of 0.525 g giving the well-balanced combination for all tested parameters with superior

uniformity and surface quality. Sensor with too low AMPS concentration results in poor conductivity and mechanical strength and too high concentration decreases sensitivity and self-healing properties. The comparison of performance metrics for AMPS is illustrated in Table 5.6.

Table 5.6: Summary of the performance trends for varying AMPS Concentration

Sr. No.	AMPS (g)	Resistance versus Strain (%) Curve	Stability Cycles	Sensitivity (GF)	Stretchability (%)	Stretching after Self-Healing
1	0.2625	Linear	Less Stable	1.16	850	50% in 828ms
2	0.525	Linear	Good	1.53	900	110% in 1.8s
3	0.7875	Non-Linear	Stable	0.89	760	95% in 1.53s
4	1.05	Non-Linear	Small	0.74	720	85% in 1.22s

5.3.6. Optimization of Polyvinyl Alcohol (PVA)

The final component PVA is optimized by varying its value while keeping all previously determined values fixed. Due to the high viscosity of PVA, increasing its concentration leads to thicker sensor solution, forming bubbles making it difficult to synthesize a uniform hydrogel. The images of synthesized samples are illustrated in Figure 5.12.

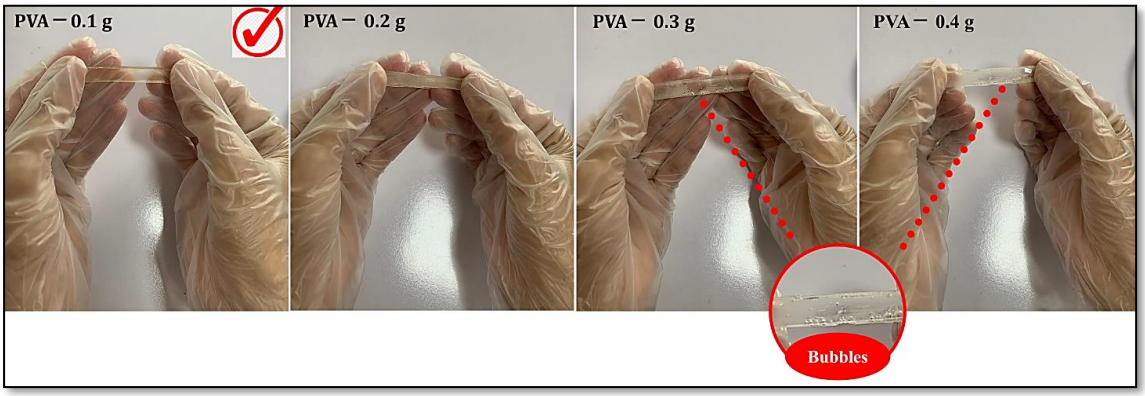

Figure 5.12: PVA Synthesized Sensor with Varying Concentration

PVA with the concentration of 0.1 g has the most linear and balance change in resistance with minimal drifts. It exhibits the highest sensitivity and the greatest stretchability, representing it as the most ideal composition. The sensitivity and stretchability of the sensor decreases as PVA concentration is increased due to the strong crosslinking and excess hydrogen bonding, making sensors bond denser and stiffer. Self-healing time improves with higher PVA concentrations because of the increase in bonding sites which allow broken bonds to recombine faster but at the cost of reducing flexibility and stretchability. Excessive PVA also resulted in poorer conductivity and mechanical handling properties. The results are shown in Figure 5.13.

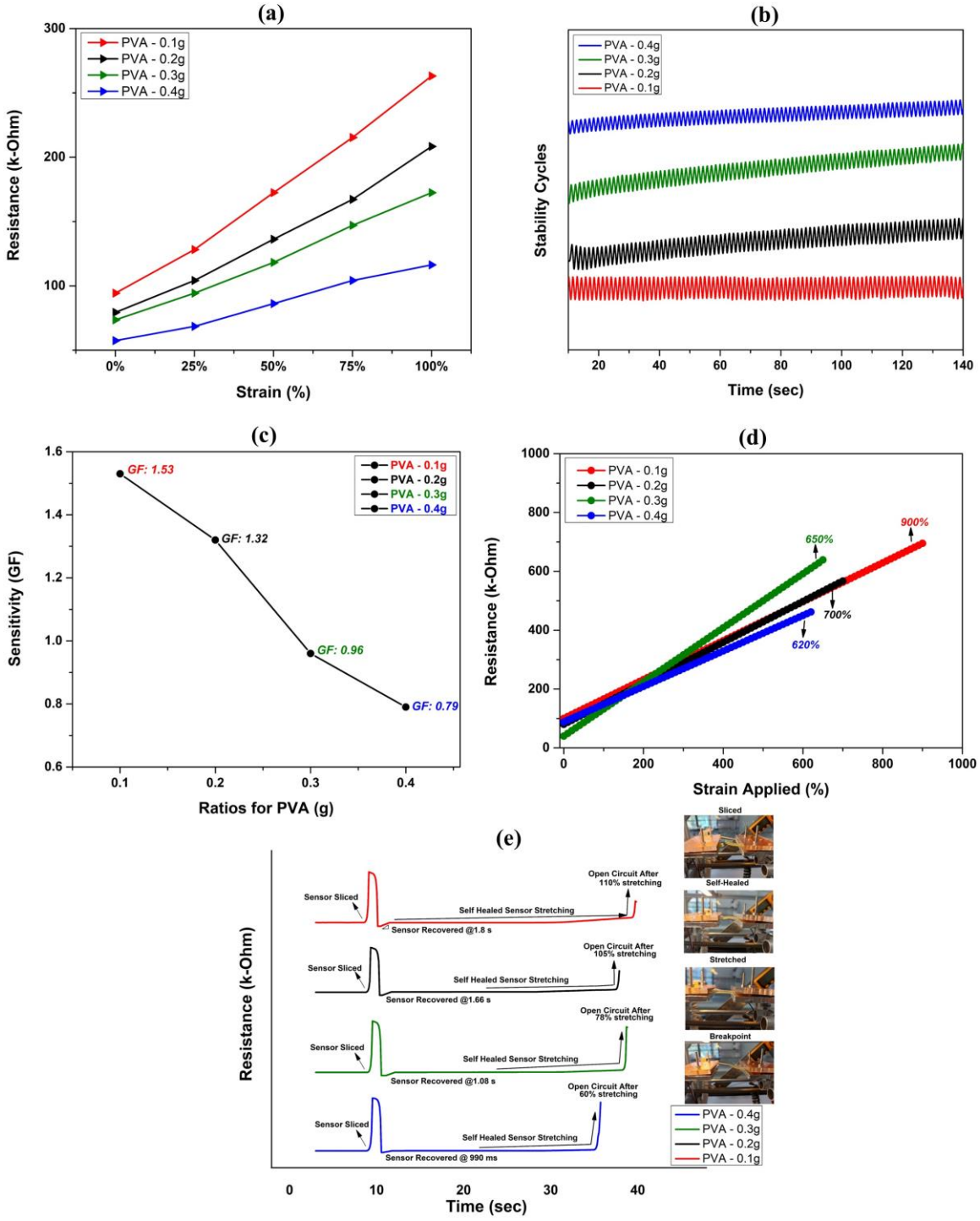

Figure 5.13: Strain sensor graphs with varying concentration of PVA: 0.1 g, 0.2 g, 0.3 g and 0.4 g. **(a)** Resistance versus Applied Strain **(b)** Stability Cycles **(c)** Sensitivity **(d)** Stretching **(e)** Self-Healing

Considering all the parameters, the observation tells that PVA is fixed at 0.1 g which is the baseline value. The comparison of performance metrics for PVA is illustrated in Table 5.7.

Table 5.7: Summary of the performance trends for varying PVA Concentration

Sr. No.	PVA (g)	Resistance versus Strain (%) Curve	Stability Cycles	Sensitivity (GF)	Stretchability (%)	Stretching after Self-Healing
1	0.1	Linear	Good	1.53	900	110% in 1.8s
2	0.2	Non-Linear	Unstable	1.32	700	105% in 1.66s
3	0.3	Non-Linear	Unstable	0.96	650	78% in 1.08s
4	0.4	Non-Linear	Small	0.79	620	60% in 990ms

5.3.7. Final hydrogel strain sensor with optimized composition of Materials

Based on the comprehensive evaluation of six key components ─ Glycerol, Irgacure, Acrylamide, MBA, AMPS and PVA, a systematically optimized composition has been developed for the hydrogel-based strain sensor. Each material has been varied individually while keeping the others constant to assess its effect on five critical performance parameters i.e. resistance-strain linearity, cyclic stability, sensitivity, stretchability and self-healing ability. The optimized concentrations of material for hydrogel strain sensor are indicated in Table 5.8.

Table 5.8: Optimized Composition

Material	Concentration
Glycerol	0.5 mL
Irgacure	0.0331 g
AM	1.755 g
MBA	0.001362 g
AMPS	0.525 g
PVA	0.1 g

This composition exhibited linear resistance (conductivity) response under applied strain varied at 0%, 25%, 50%, 75% and 100%. Stable and repeatable cyclic performance tested for 100 cycles, excellent strain sensitivity (GF=1.53), stretchability of up to 900%. It also demonstrated fast self-healing behavior with minimal structural compromise, stretching up to 110% after intrinsic healing in 1.8 s.

Figure 5.14 shows the resistance versus applied strain plot for the final composition.

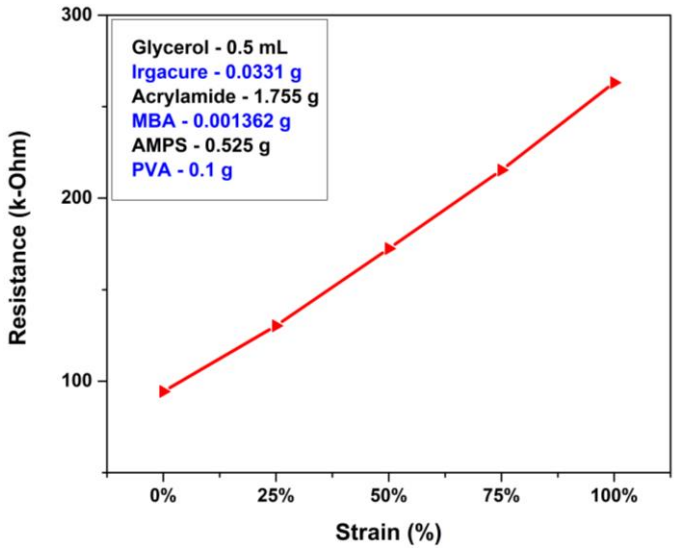

Figure 5.14: Resistance versus Applied Strain (%)

Figure 5.15 represents the stability cycles for the final composition.

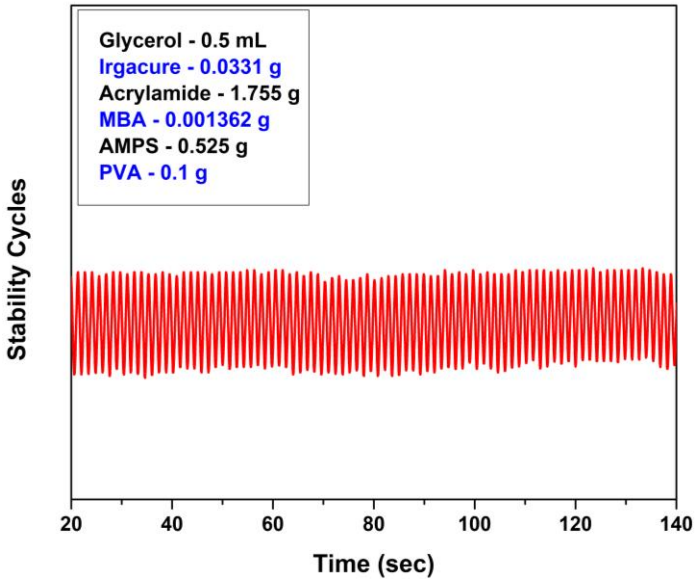

Figure 5.15: Stability Cycles

Figure 5.16 shows the sensitivity represented by the gauge factor of the device for the final composition.

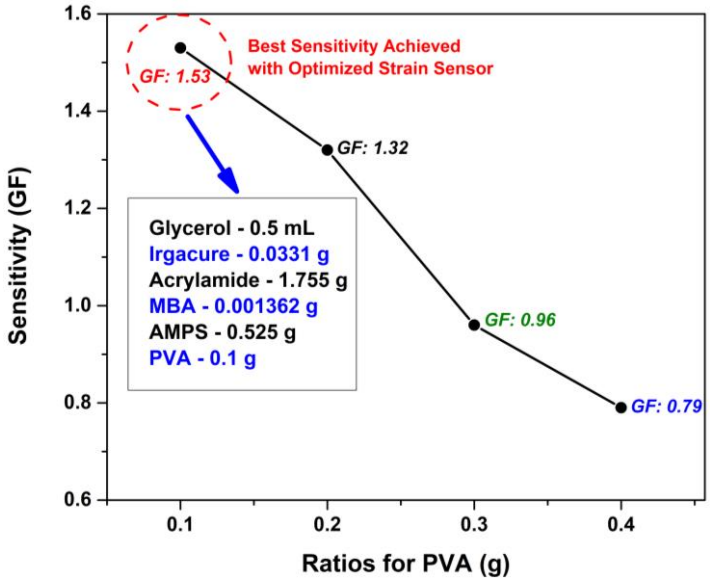

Figure 5.16: Sensitivity represented with Gauge Factor

Figure 5.17 shows the stretchability for the final composition.

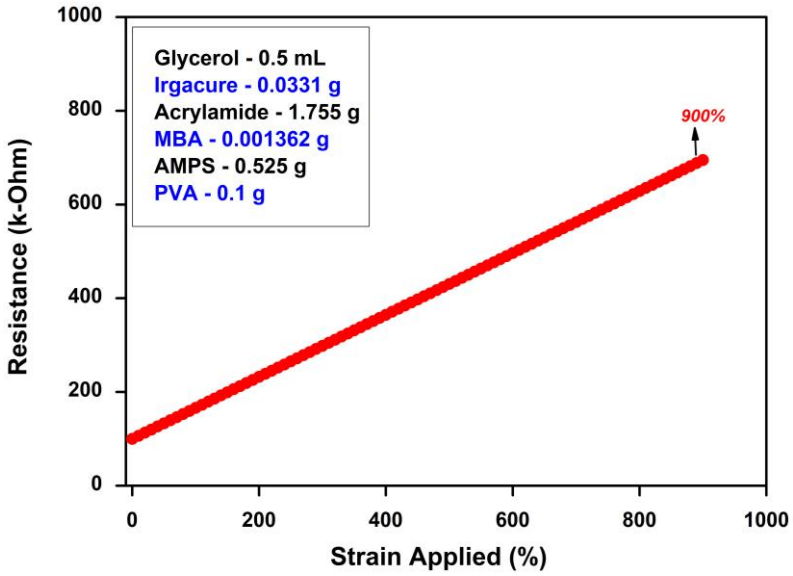

Figure 5.17: Stretchability

Figure 5.18 shows the self-healing performance of the final composition.

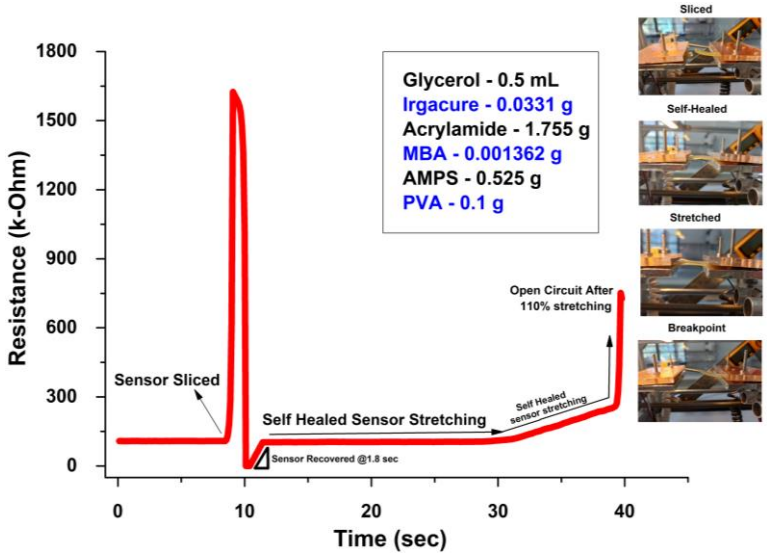

Figure 5.18: Self-healing Performance

The final hydrogel formulation combines high conductivity, durability, sensitivity, flexibility and automating healing capacity, making it ideal for applications in wearable electronics and human motion detection. This optimization provides a foundation for device integration and real-world deployment of the strain sensor by further tuning the dimension parameters including length, width and thickness for efficient strain sensing in practical environment.

5.4. Dimensional Optimization of the Strain Sensor

After fixing the optimal material composition in Section 5.3, performance for hydrogel strain sensor has been further enhanced through proper tuning of dimensions. The geometrical parameters of the sensor specifically its width, length and thickness have a profound effect on the electrical and mechanical behavior of the sensor therefore the goal is to get the optimized parameters for dimensions by varying these parameters one at a time and analyzing its effect. The fabricated strain sensors are synthesized using previously optimized formulation for material composition. The synthesis procedure, curing process and protocol remained the same across all samples and followed as described in section “Material Composition Optimization”. The only difference is the use of molds during casting solution at varying dimensions.

- **Influence of Geometry on Resistance**

The resistance of hydrogel-based strain sensor depends on both materials utilized and geometry of the sensor. It is represented as

$$R = \frac{\rho L}{A} \tag{5.1}$$

Where R is the electrical resistance, ρ is the resistivity of the sensor, length of the sensor and A is the cross-sectional area which is further expressed in

$$A = W \times t \tag{5.2}$$

W and t are the width and thickness of the sensor respectively.

5.4.1. Optimization of Width

As width increases, the cross-sectional area becomes larger which creates more path for the flow of ions and allows more current to flow through the device. This in turn results in a decrease in resistance as shown by equation (5.1) and an increase in conductivity. Width also has a direct impact on stability response of the sensor; wider sensor provides a sufficient area for even distribution of strain over the entire surface of the device resulting in stability over repeated stretch/release cycles and increase mechanical durability whereas too small geometries are more sensitive to defects and tears. The dimensions taken for width variations with length and thickness taken as constant are as indicated in Table 5.9.

Table 5.9: Width Variation

Sr. No.	Width (cm)	Length (cm)	Thickness (mm)
1	1	7	3
2	1.5	7	3
3	2	7	3
4	2.5	7	3

The synthesized sensors in a mold of four different widths keeping length and thickness constant are shown in Figure 5.19.

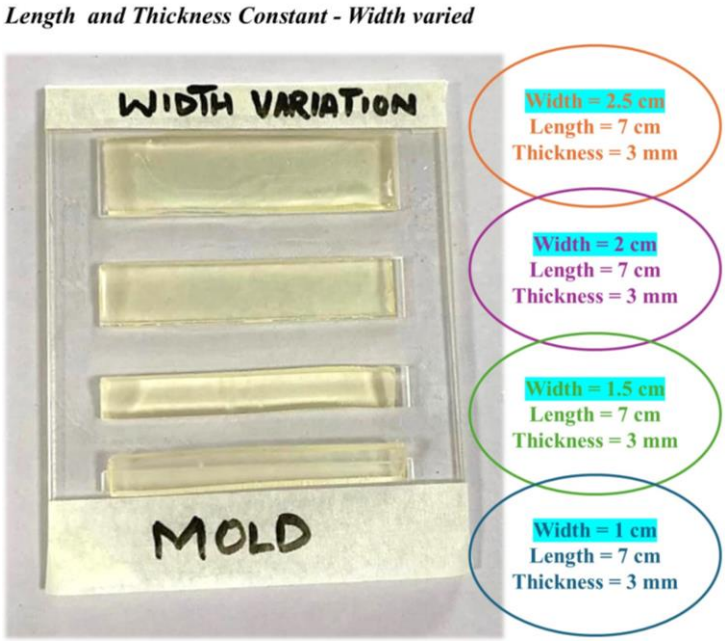

Figure 5.19: Synthesized Sensor with Four Width Variations

It is observed that smaller widths exhibit greater resistance variations, and the 1 cm wide sensor shows the highest resistance change (95 kΩ to 270 kΩ) with a linear and stable response under 0–100% strain, indicating superior sensitivity and effective piezoresistive behavior. Stability cycles confirm their consistent waveform patterns with minimal noise. Conversely, the 2.5 cm width sensor shows a flatter resistance curve due to lower resistance and distribute strain deformations across increased cross-sectional areas. Stretchability is observed to be higher at 1 cm and 1.5 cm because of better flexibility and decreased mechanical stiffness. All sensors heal successfully with narrower sensors being healed faster due to smaller damaged areas and more interfacial bonding across cut areas. The results of performance metrics with varying widths are shown in Figure 5.20.

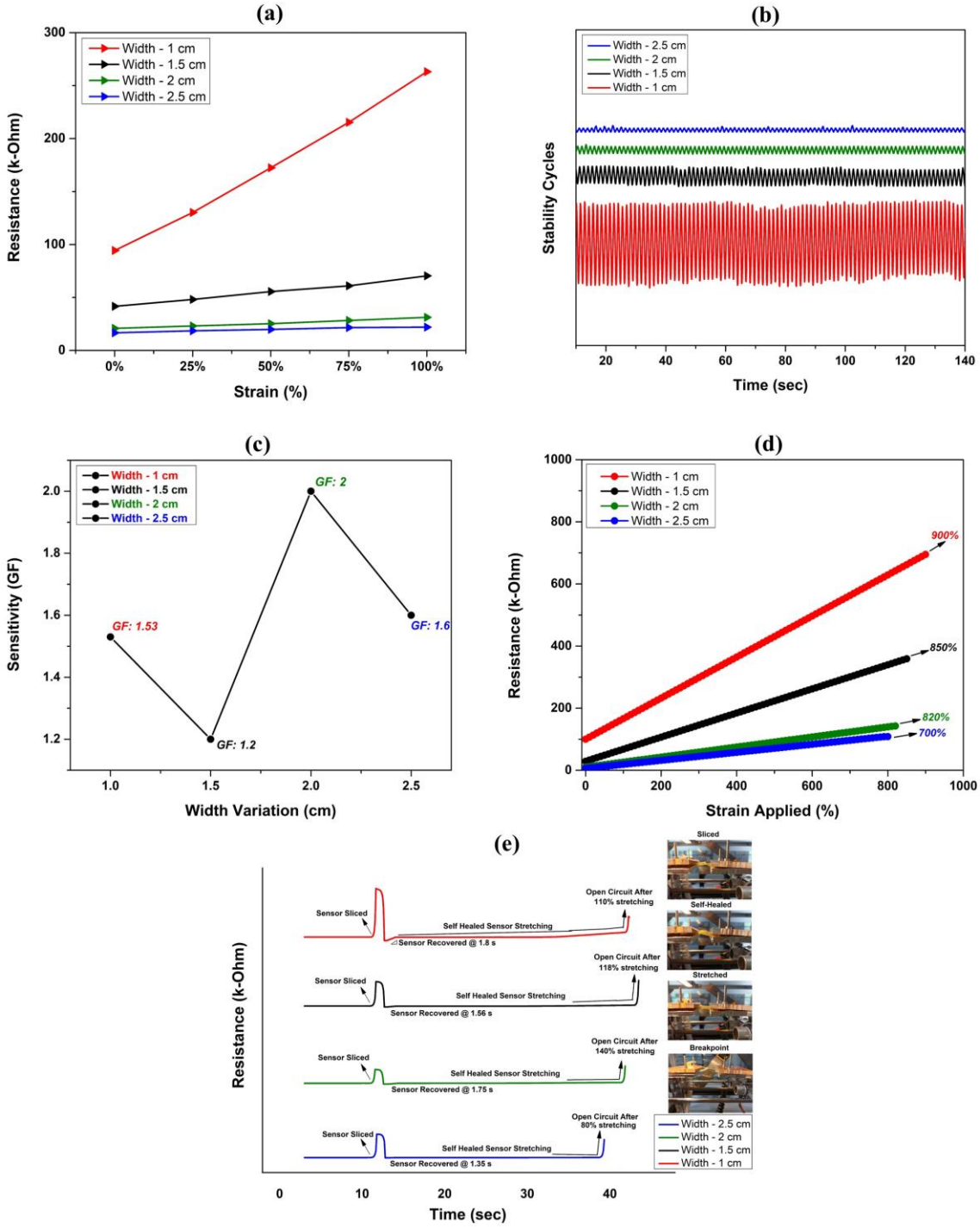

Figure 5.20: Strain sensor graphs with variation in width: 1 cm, 1.5 cm, 2 cm and 2.5 cm. **(a)** Resistance versus Applied Strain. **(b)** Stability Cycles **(c)** Sensitivity Trend **(d)** Stretching **(e)** Self-Healing

Based on performance curve analysis, the 1 cm wide sensor demonstrates the most consistent and reliable cyclic behavior during repeated stretching. Its compact size enhances flexibility and conformability on body joints providing 900%

stretchability with the sensitivity (GF) of 1.53 and the self-healing capability of 110% stretching achieved after recovery in 1.8 s. The ideal width is 1 cm, which balances sensitivity, flexibility and healing. The summarized characteristics of each width variation-based strain sensor are illustrated in Table 5.10.

Table 5.10: Summary of the performance parameters for Varying Width

Sr. No.	Width (cm)	Resistance versus Strain (%) Curve	Stability Cycles	Sensitivity (GF)	Stretchability (%)	Stretching after Self-Healing
1	1	Linear	Stable	1.53	900	110% in 1.8s
2	1.5	Linear	Stable	1.2	850	118% in 1.56s
3	2	Linear	Small	2	820	140% in 1.75s
4	2.5	Linear	Small	1.6	700	80% in 1.35s

5.4.2. Optimization of Length

The relation of equation (5.1) suggests that increase length has a direct impact on resistance and longer sensors exhibit large resistance variations upon strain applied which in turn improves sensitivity of the device, but too large sensors may compromise structural integrity due to the exposure of large surface area to deformation. The dimensions of mold taken for length variations with the selected optimized width of 1 cm and thickness taken as constant are as indicated in Table 5.11.

Table 5.11: Length Variation

Sr. No.	Width (cm)	Length (cm)	Thickness (mm)
1	1	7	3
2	1	8	3
3	1	9	3
4	1	10	3

The synthesized hydrogel solution is placed into the mold of variable length: 7 cm, 8 cm, 9 cm and 10 cm. These mentioned dimensions are for the molds in which the hydrogel solution has been cast but when mounted on DIY characterization tool the active length of the sensor reduces from the original synthesized sensor with remaining length utilized for depositing electrodes. Therefore, the actual length of fabricated sensors are **2 cm, 3 cm, 4 cm** and **5 cm**. The synthesized sensor in a mold of four varying lengths are shown in Figure 5.21.

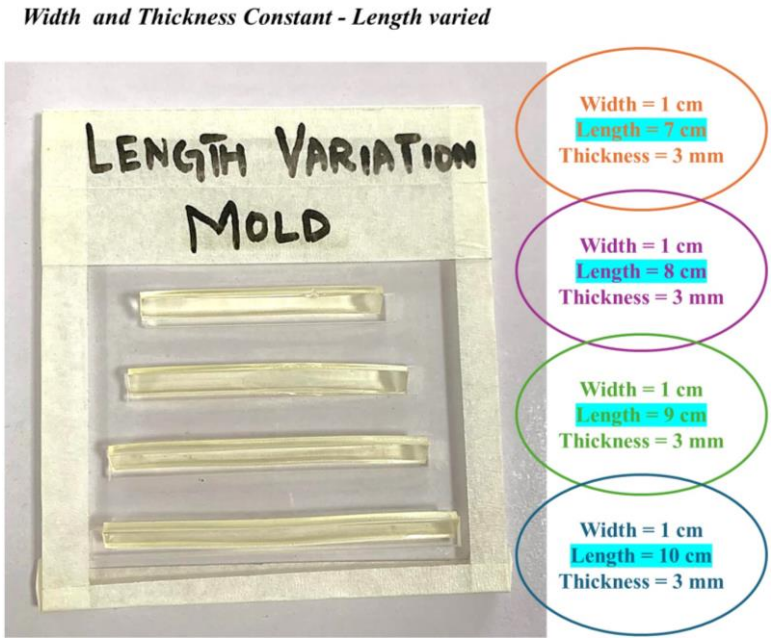

Figure 5.21: Synthesized Sensor with Four Length Variations

As the length of the sensor increases from 7 cm to 10 cm (active lengths 2–5 cm), the resistance increases gradually due to the longer ion transport path where Sensor 1 showed the lowest resistance whereas Sensor 4 has the highest resistance. Moreover, sensors with longer lengths distributes strain more evenly reducing damages. The sensitivity shows a non-linear trend with the highest sensitivity achieved by the Sensor 4 (10cm). The stretchability and self-healing capability of the sensor also improves with length due to strain accommodation over a larger area. The stretching after self-healing of Sensor 4 is the highest in larger sensors with more polymer chain diffusion and network reformation. The results with varying lengths are shown in Figure 5.22.

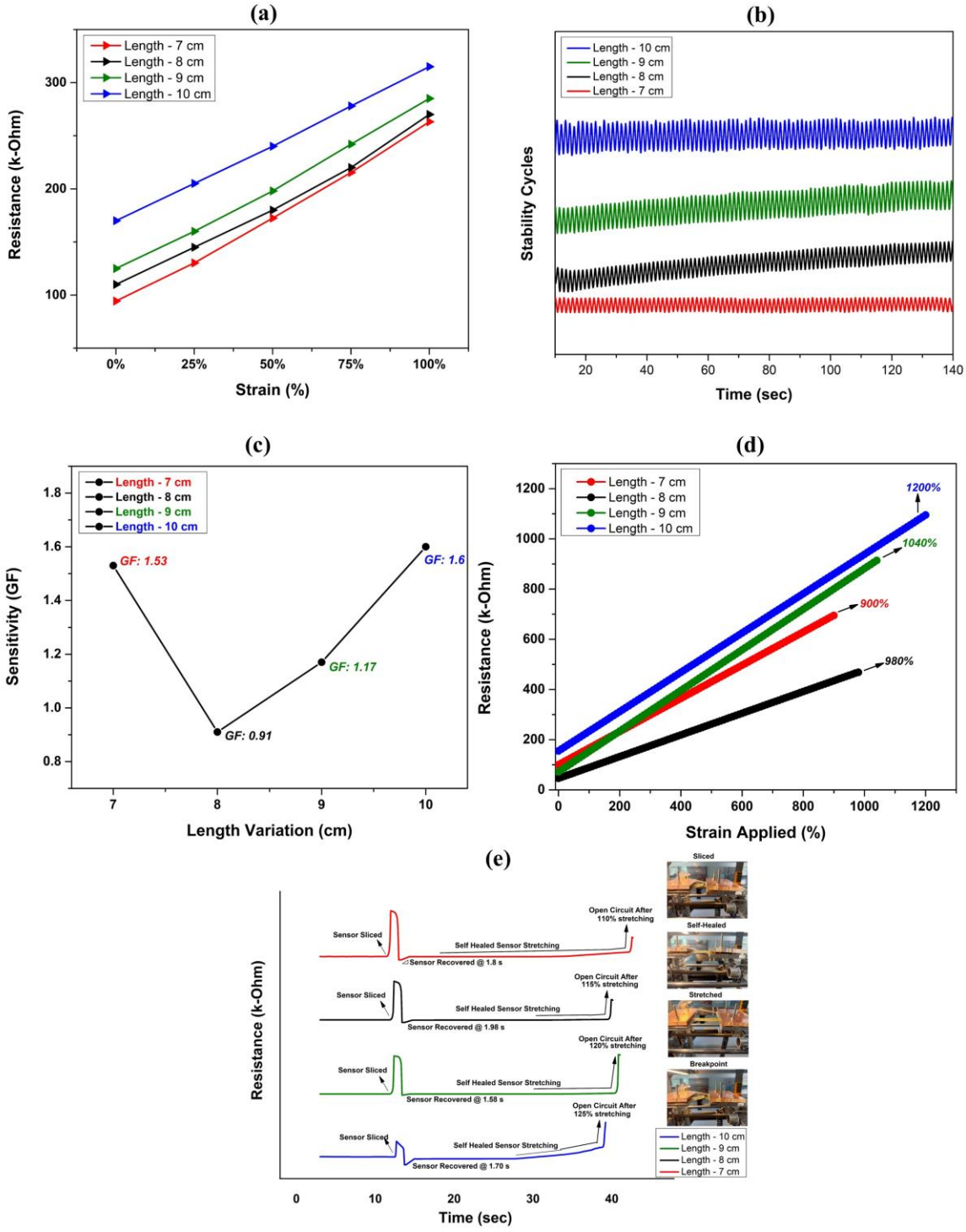

Figure 5.22: Strain sensor graphs with variation in length: 7 cm, 8 cm, 9 cm and 10 cm. **(a)** Resistance versus Applied Strain **(b)** Stability Cycles **(c)** Sensitivity **(d)** Stretching **(e)** Self-Healing

On analyzing the overall performance, the 10 cm sensor demonstrated optimal performance across key metrics with consistent and reliable cyclic behavior, excellent

linearity and optimal sensitivity with a gauge factor of 1.6. It shows superior stretchability up to 1200% and efficient self-healing with 125% stretch recovery in 1.7s. The summarized characteristics of the four length variation strain sensors are illustrated in Table 5.12.

Table 5.12: Summary of the performance parameters for Varying Length

Sr. No.	Length (cm)	Resistance versus Strain (%) Curve	Stability Cycles	Sensitivity (GF)	Stretchability (%)	Stretching after Self-Healing
1	7	Linear	Stable	1.53	900	110% in 1.8s
2	8	Non-Linear	Unstable	0.91	980	115% in 1.98s
3	9	Non-Linear	Unstable	1.17	1040	120% in 1.58s
4	10	Linear	Stable	1.6	1200	125% in 1.70s

5.4.3. Optimization of Thickness

Thickness is inversely proportional to resistance like the width of the sensor as indicated by equation (5.1). Thicker sensors resist deformation more so have reduced flexibility and stretchability whereas thinner sensors offer more sensitivity to strain changes. However extremely thinner ones are mechanically fragile and may easily break. The dimensions taken for sensor thickness variations are as indicated in Table 5.13 with the selected optimized values for width and length.

Table 5.13: Thickness Variation

Sr. No.	Width (cm)	Length (cm)	Thickness (mm)
1	1	10	3
2	1	10	4
3	1	10	5
4	1	10	6

The synthesized solution is placed into the molds of dimensions as mentioned in Table 5.12 with thickness: **3 mm, 4 mm, 5 mm and 6 mm** as could be seen in Figure 5.23.

Figure 5.23: Synthesized Sensor with Four Thickness Variations

Sensor thickness significantly impacts the performance of the sensor. Due to larger deformation, thinner sensors (3 mm) exhibit a higher initial resistance and a greater resistance variation under strain, which leads to increased sensitivity and stretchability whereas stretchability decreases progressively with thickness since thicker sensors being stiffer which hinders their ability to stretch. Although broader sensors exhibit superior self-healing capabilities, their overall performance is inferior making them unsuitable for practical applications. The performance comparison for varying thickness with width and length kept constant are illustrated in Figure 5.24.

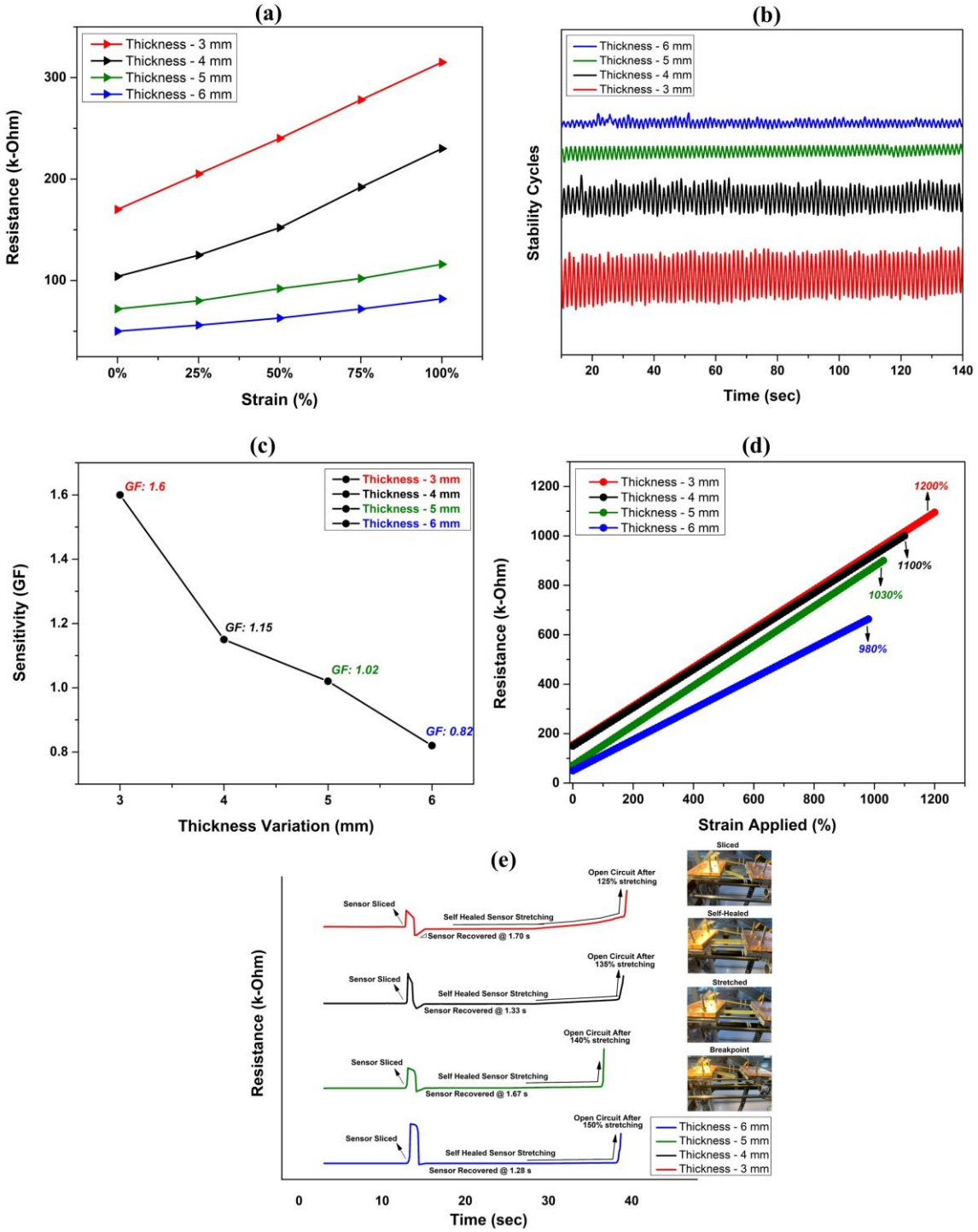

Figure 5.24: Strain sensor graphs with variation in thickness such as 3 mm, 4 mm, 5 mm and 6 mm. **(a)** Resistance versus Applied Strain **(b)** Stability Cycles **(c)** Sensitivity **(d)** Stretching **(e)** Self-Healing

The 3 mm thick sensor demonstrated the most consistent and repeatable performance, with the highest sensitivity (GF 1.6) achieved, excellent stretchability (1200%) and

good self-healing (125% recovery in 1.7 s). Overall, the 3 mm thick sensor demonstrated the optimal balance of responsiveness, sensitivity, mechanical flexibility and healing ability, making it the optimal choice. The summary of performance for variable thickness is represented in Table 5.14.

Table 5.14: Summary of the performance parameters for Varying Thickness

Sr. No.	Thickness (mm)	Resistance versus Strain (%) Curve	Stability Cycles	Sensitivity (GF)	Stretchability (%)	Stretching after Self-Healing
1	3	Linear	Stable	1.6	1200	125% in 1.70s
2	4	Non-Linear	Unstable	1.15	1100	135% in 1.33s
3	5	Linear	Stable	1.02	1030	140% in 1.67s
4	6	Linear	Unstable	0.82	980	150% in 1.28s

5.5. Final Strain Sensor after both Material and Dimensional Optimization

After structural and systematic optimization of both the material composition and geometry of the sensor, the final strain sensor with the optimum blend of PVA, Glycerol, Irgacure, AM, MBA and AMPS and dimensions that are width, length and thickness of 1 cm, 10 cm and 3 mm respectively has been selected based on the superior performance in electrical and mechanical testing. The sensor meets the requirements for biomedical strain sensing with excellent stretchability for large scale human movements.

The performance metrics result for the final fabricated high performance strain sensor are as shown below:

i. Resistance versus applied strain for optimized strain sensor

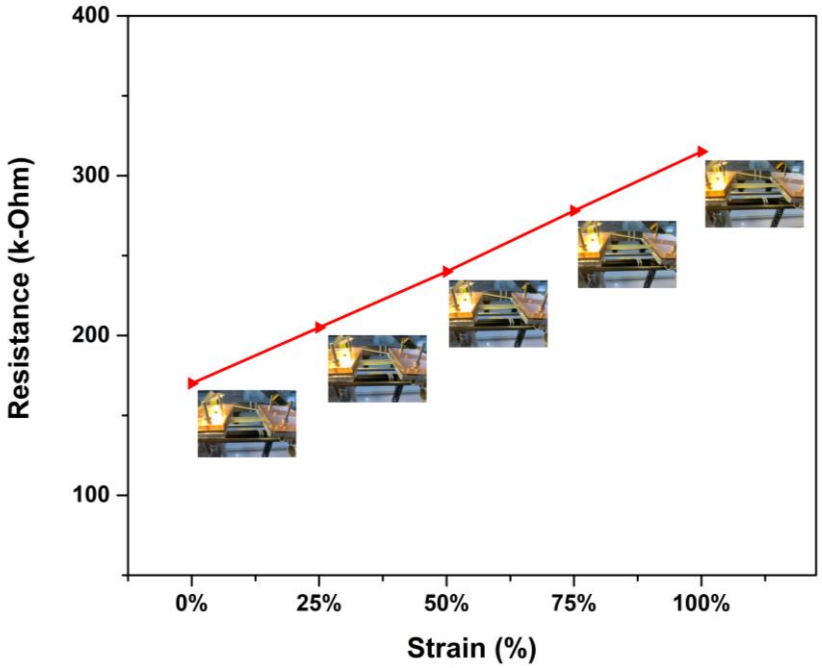

Figure 5.25: Resistance versus Applied Strain (%) for final device

ii. Stability Cycles for optimized strain sensor

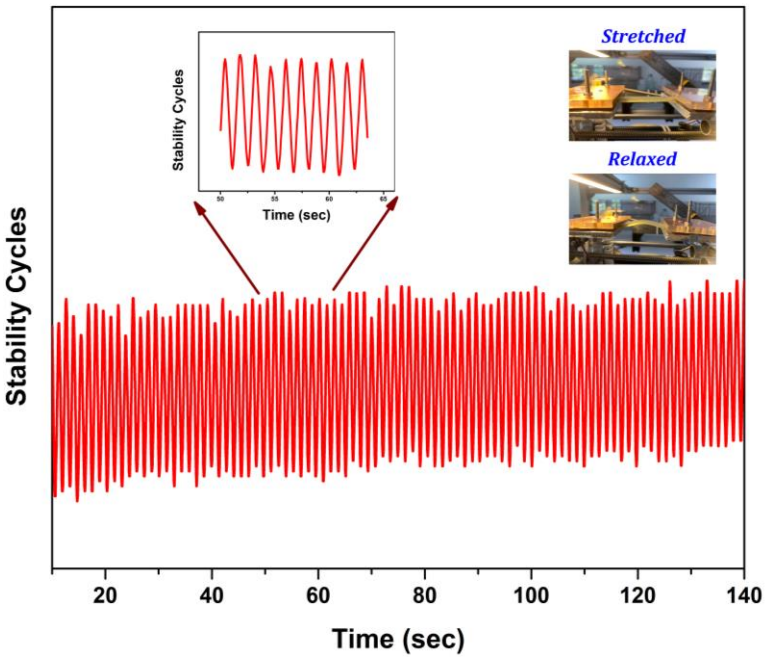

Figure 5.26: Stability Cycles of final device

iii. Sensitivity achieved with optimized strain sensor

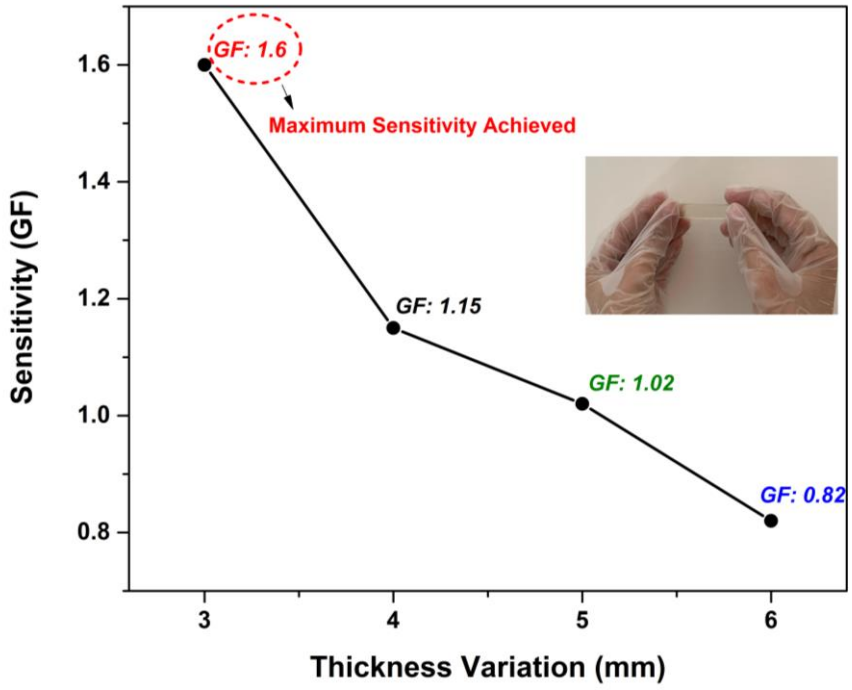

Figure 5.27: Best Sensitivity of final device

iv. Stretching achieved with optimized strain sensor

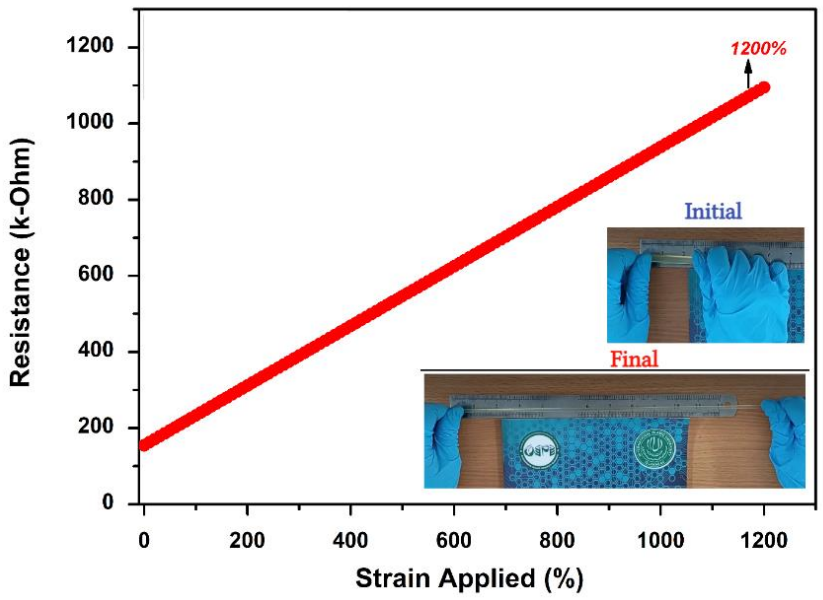

Figure 5.28: Stretching result achieved for final device

v. Self-healing achieved with optimized strain sensor

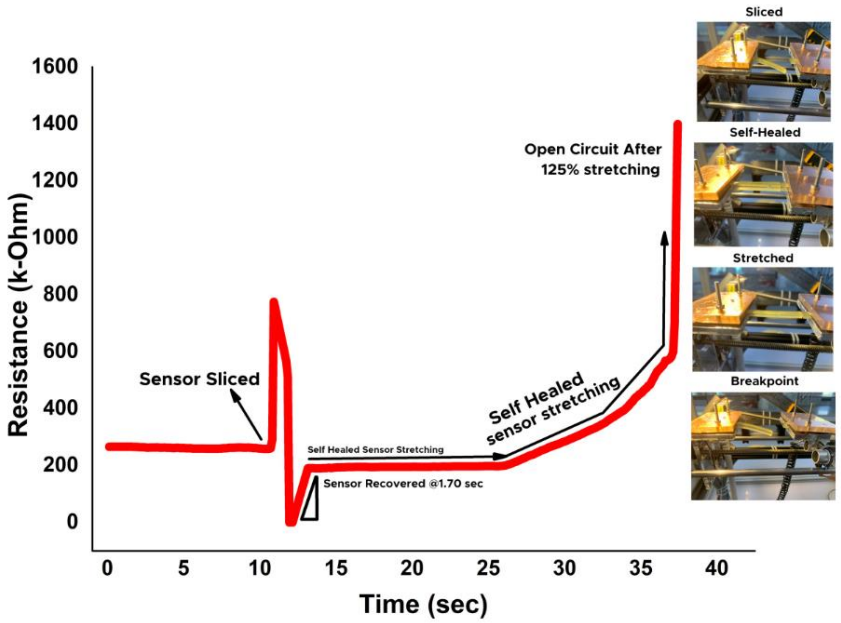

Figure 5.29: Self-healing of final device

The fabricated strain sensor exhibits outstanding conformability and durability under various mechanical deformations including twisting, stretching, and bending which facilitates real world dynamic human motions. Its transparency allows minimal visual obstructions, and self-healing capability is evident from rejoined interface after physical damage. Images of high-performance fabricated hydrogel strain sensor with mechanical and self-healing capabilities are shown in Figure 5.30.

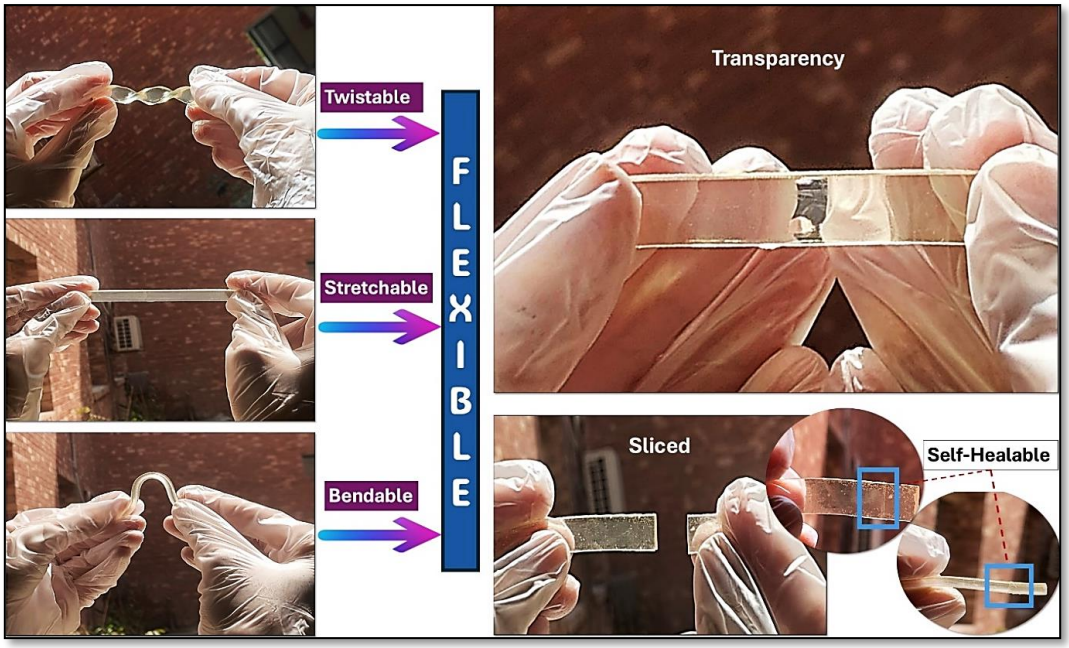

Figure 5.30: Final hydrogel-based strain sensor

5.6. Scanning Electron Microscopy (SEM) Analysis of Optimized Strain Sensor

The surface morphology of the hydrogel-based strain sensor has been examined using Scanning Electron Microscopy (SEM) with a resolution of 10 micrometers as shown in Figure 5.31. The SEM image of optimized hydrogel strain sensor reveals a surface that is smooth and homogeneous without any visible cracks, voids, or structural defects as can be seen in Figure 5.31 (a). This suggests that the sensor is structurally stable and fabricated uniformly. The polymer components were thoroughly mixed and fully dissolved during synthesis as indicated by the absence of microfractures or surface irregularities. This well-integrated structure contributes to the sensor's mechanical integrity and operational reliability. Figure 5.31 (b) shows SEM image of self-healed strain sensor after cut, which shows that the sensor successfully reconnects after cut and regains its structural integrity. These results confirm that the sensor is not only mechanically reliable but also exhibits strong self-healing ability, ensuring consistent performance, enhanced durability, and a low risk of mechanical failure over repeated use, making it an appropriate candidate for long-term wearable monitoring applications.

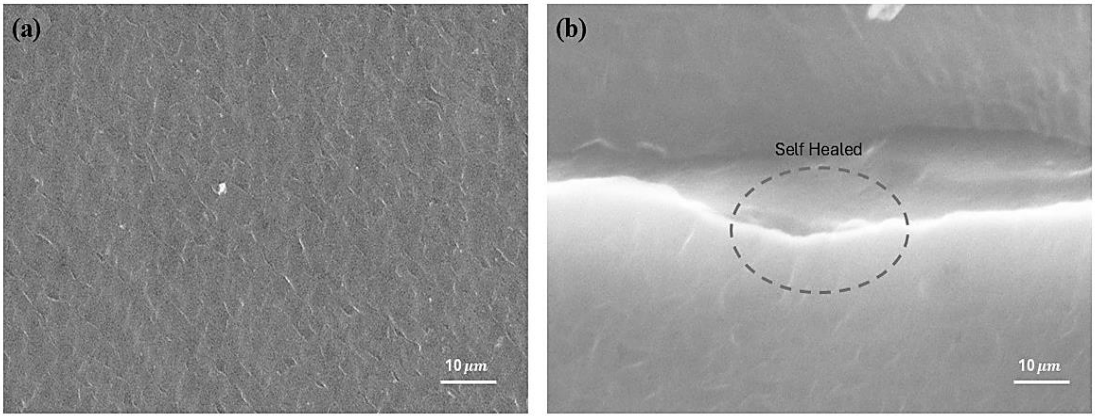

Figure 5.31: (a) SEM image of Optimized hydrogel-based strain sensor (b) Self-Healed strain sensor after cut

5.7. Real Time Implementation

5.7.1. LED Glow Test for Conductivity and Self-Healing

To show the designed strain sensor practical performance, a series of electrical tests were carried out by integrating the sensor into a closed circuit with four LEDs. As shown in Figure 5.32 (a), LEDs are connected in series with the fabricated strain sensor and LEDs glow serve as an immediate visual indicator of current flow through the sensor. This is due to the effective charge transport across the device confirming sensor's low resistance and stable conductivity in its pristine form. When the sensor was partially mechanically damaged with scissors it initiated microstructural disruption within the polymer matrix. Despite the damage LEDs continued to glow with minor flickering since conducting paths remained intact due to the elastic and conductive properties of the polymer matrix which demonstrates sensor resilience to minor physical damage as depicted in Figure 5.32 (b). An open circuit resulted from the electrical pathway being totally cut off after the sensor was fully severed. All LEDs shut off as a result, demonstrating the total lack of conductivity and preventing electricity flow as illustrated in Figure 5.32 (c). The sliced parts were then brought into contact under ambient conditions, allowing the hydrogel to autonomously reform its internal bonds after a brief healing period. The polymeric network restored both mechanical adhesion and electrical conductivity, allowing current to flow and re-illuminating the LEDs as shown in Figure 5.32 (d). The strain sensor stretching test was also conducted which demonstrated excellent conductivity of the sensor in the initial

state, which lit up LEDs brightly without any strain due to intact conductive path. Upon stretching the conductive network deformed, increasing resistance and dimming the LEDs as depicted in Figure 5.32 (e-f). This simple LED test demonstrates the sensor's great strain sensitivity, making it perfect for wearable motion detection applications.

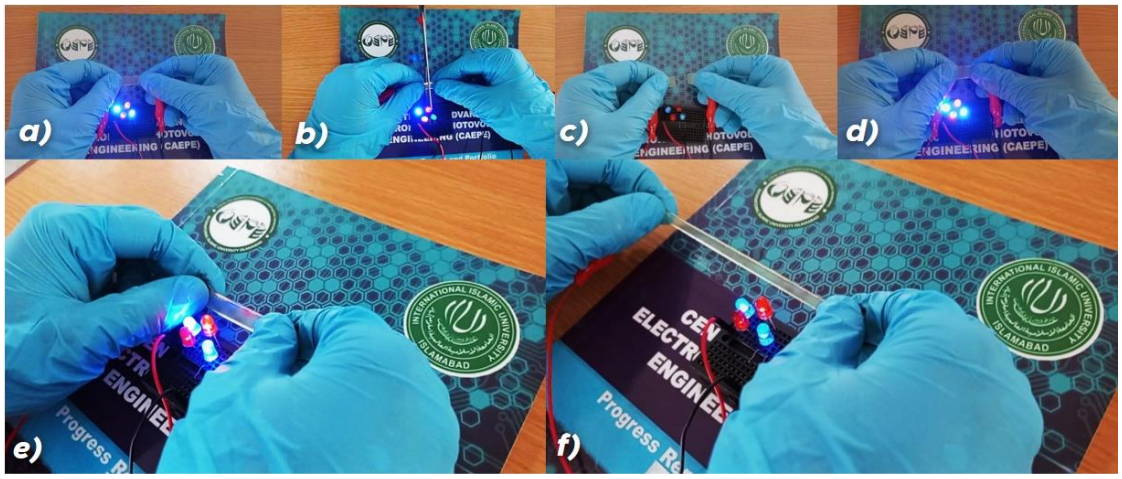

Figure 5.32: Electrical series circuit test along with 4 LEDs to evaluate electrical conductivity of self-healing strain sensor

5.7.2. Sensor Mounted on Human Body for Motion Detection

The fabricated strain sensor with optimized material recipe is mounted on different parts of the human body for real world monitoring of human motion. The sensor efficiently detects and converts mechanical deformations into electrical impulses in real time when put on dynamic body parts like finger, wrist, elbow, or knee. The piezoresistive principle, which states that resistance varies in response to mechanical strain, forms the basis of the fundamental sensing process. Each bending motion caused a distinct increase in resistance due to the elongation of the sensor material, which resulted in disruption in the conductive network. Conversely, relaxation led to a rapid decrease in resistance, indicating the structural recovery of the sensor. The repeatable and consistent peaks across multiple stretch/release cycles validate the sensor's mechanical stability, reversibility, and sensitivity under dynamic strain. The sharp transitions between bending and relaxing phases further confirm the sensor's fast response and excellent recovery behavior. The results demonstrate that the optimized sensor is highly suitable for human motion monitoring, particularly in applications such as gesture recognition, rehabilitation monitoring, and analyzing joint motion in real time as shown in Figure 5.33.

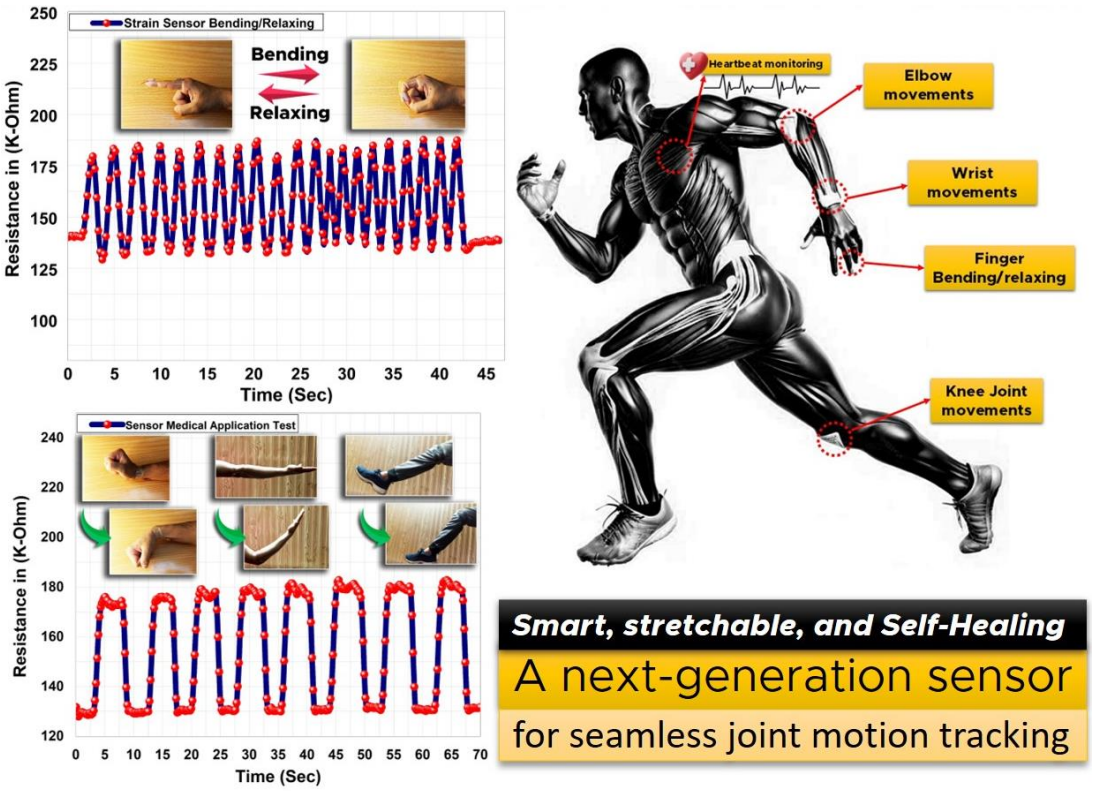

Figure 5.33: Flexible, stretchable and self-healable strain sensor mounted on different body joints for monitoring human motion

Chapter 6

Conclusion and Future Work

6.1. Conclusion

This research focused on the fabrication of high-performance strain sensor based on pure polymer materials with targeted application for real time human motion detection. A systematic experimental approach developed a stretchable, self-healable and biocompatible hydrogel-based strain sensor fabricated using simple processing methods. Through the optimization strategy, each material was independently varied and its effects on five key performance parameters were analyzed to determine the optimal formulation. This provides a strain sensor with stable and linear resistance variation, sensitivity represented by GF of 1.53, stretchability of 900% and self-healing achieved in 1.8s. Furthermore, this sensor geometry was optimized to get a final device for real world applications. The strategy helped to determine the optimized device with self-healing within 1.7s ensuring its lifespan and reliability even in difficult operating conditions. It has an exceptional stretchability of 1200% and possessed extreme flexibility owing to its utilization in monitoring large scale human motions involved in various physical activities and making it conformable to mount on irregular surfaces. The sensor exhibited good stability and endurance, maintaining its consistent performance tested for 100 stretch/release cycles thus making it ideal for high and frequent mechanical stress. The dimensional optimization further enhanced the sensitivity of this hydrogel strain sensor achieving a gauge factor of 1.6 making it usable for strain sensing on various body parts like finger, elbow, knee, wrist etc. The sensor's high strain sensitivity, detection accuracy and transparency make it beneficial for medical diagnostics, enabling timely identification of abnormalities and facilitating targeted treatment. This ultimately enhances patient outcomes and reduces healthcare expenses.

To demonstrate practical utility, the sensor was tested in real-time scenarios by twisting, bending, and stretching confirming its flexibility and robustness. The developed sensor was tested by mounting onto different parts of the body such as finger, elbow and knee to detect human movements efficiently. A simple LED conductivity test further validated its functionality by showing instantaneous current flow on stretching

indicating its good strain sensitivity. These demonstrations proved the strain sensor's ability to monitor subtle physiological movements like joint flexion and pulse, as well as large-scale motion, making it highly relevant for healthcare monitoring, rehabilitation, and soft robotics.

6.2. Future Work

The developed sensor has promising performance in terms of sensitivity, stretchability and durability and great potential for the future. Further improvements can be made with the integration of conductive fillers such as nanomaterials to improve conductivity and environmental stability. Performance can be further improved by incorporating encapsulation techniques which help to retain moisture in the hydrogel strain sensor, preventing dehydration, and protecting the sensor from environmental factors. Future research may also focus on advance fabrication techniques such as 3D printing or microfluidic patterning to create highly precise and miniaturized sensor architectures. Additionally, developing wireless communication modules or integrating the sensor with flexible circuits can facilitate its use in wearable systems for real-time health monitoring. Future work may also focus on expanding the sensor's capability to detect other physical parameters such as temperature or pressure and could pave the way for multifunctional healthcare platforms.

Comparison with reported work

Table 6.1: Comparison of gauge factor, stretchability and self-healing of strain sensors

Material Used	Gauge Factor	Stretchability	Self-Healing	References
$Ti_3C_2T_x$ MXene/AgNWs/liquid metal	3.22	440%	12 h	2023 [96]
Au-CNFs/NaCMC/PVA/glycerol	1.7	330%	_	2024 [54]
LiF/MWCNT/MXene/PVA/AM hydrogel	0.8	150%	16 h	2024 [68]
LiCl and SBMA incorporated into PVA/TA/PAM	0.6024	1000%	72 h	2024 [97]
DA/Py/AM	3.05	660%	1.5 h	2024 [98]
PVA/PEDOT: PSS	0.67	_	5 min	2024 [99]
GelMA/PNAGA/PVA/borax-NaCl (GNPB)	3.28	160%	24 h	2025 [100]
GA/PVA/ CNC/ PEDOT:PSS	2.5	580%	3s	2025 [101]
PVA/AMPS/AM/MBA/Irgacure /Glycerol	1.6	1200%	1.7 s	**This work**

References

[1] L. Duan, D. R. D'hooge, and L. Cardon, "Recent progress on flexible and stretchable piezoresistive strain sensors: From design to application," *Prog Mater Sci*, vol. 114, p. 100617, 2020.

[2] Y. Xia, Q. Zhang, X. E. Wu, T. V Kirk, and X. D. Chen, "Practical and durable flexible strain sensors based on conductive carbon black and silicone blends for large scale motion monitoring applications," *Sensors*, vol. 19, no. 20, p. 4553, 2019.

[3] B. Zazoum, K. M. Batoo, and M. A. A. Khan, "Recent Advances in Flexible Sensors and Their Applications," *Sensors 2022, Vol. 22, Page 4653*, vol. 22, no. 12, p. 4653, Jun. 2022, doi: 10.3390/S22124653.

[4] D. Y. S. Low *et al.*, "Self-healing synthetic rubber composites: review of recent progress and future directions towards sustainability," *Materials Today Sustainability*, vol. 24, p. 100545, Dec. 2023, doi: 10.1016/J.MTSUST.2023.100545.

[5] X. Huang *et al.*, "High-stretchability and low-hysteresis strain sensors using origami-inspired 3D mesostructures," *Sci Adv*, vol. 9, no. 34, p. eadh9799, Aug. 2023, doi: 10.1126/SCIADV.ADH9799.

[6] F. Mo *et al.*, "Advances in ionic conductive hydrogels for skin sensor applications," *Materials Science and Engineering: R: Reports*, vol. 165, p. 100989, Jul. 2025, doi: 10.1016/J.MSER.2025.100989.

[7] T. C. Ho *et al.*, "Hydrogels: Properties and Applications in Biomedicine," *Molecules*, vol. 27, no. 9, p. 2902, May 2022, doi: 10.3390/MOLECULES27092902.

[8] Z. Ye, H. Lu, G. Chai, C. Wu, J. Chen, and L. Lv, "Glycerol-modified poly (vinyl alcohol)/poly (ethylene glycol) self-healing hydrogel for artificial cartilage," *Polym Int*, vol. 72, no. 1, pp. 27–38, 2023.

[9] L. Zhao, Y. Zhou, J. Zhang, H. Liang, X. Chen, and H. Tan, "Natural Polymer-Based Hydrogels: From Polymer to Biomedical Applications," Oct. 01, 2023, *Multidisciplinary Digital Publishing Institute (MDPI)*. doi: 10.3390/pharmaceutics15102514.

[10] M. M. Rahman Khan and M. M. H. Rumon, "Synthesis of PVA-Based Hydrogels for Biomedical Applications: Recent Trends and Advances," *Gels*, vol. 11, no. 2, p. 88, Feb. 2025, doi: 10.3390/GELS11020088.

[11] X. Liang *et al.*, "Polyvinyl alcohol (PVA)-based hydrogels: Recent progress in fabrication, properties, and multifunctional applications," *Polymers (Basel)*, vol. 16, no. 19, p. 2755, 2024.

[12] G. Sennakesavan, M. Mostakhdemin, L. K. Dkhar, A. Seyfoddin, and S. J. Fatihhi, "Acrylic acid/acrylamide based hydrogels and its properties - A review," *Polym Degrad Stab*, vol. 180, p. 109308, Oct. 2020, doi: 10.1016/J.POLYMDEGRADSTAB.2020.109308.

[13] Y. He, J. Xiong, Y. Hu, Z. Guo, S. Wang, and J. Mao, "AM/AMPS delignified wood-based hydrogel with enhanced mechanical strength and fatigue resistance for wearable

strain sensing and energy harvesting," *Polymer (Guildf)*, vol. 320, Feb. 2025, doi: 10.1016/J.POLYMER.2025.128075.

[14] H. S. Seo, J. Y. Bae, K. Kwon, and S. Shin, "Synthesis and Assessment of AMPS-Based Copolymers Prepared via Electron-Beam Irradiation for Ionic Conductive Hydrogels," *Polymers 2022, Vol. 14, Page 2547*, vol. 14, no. 13, p. 2547, Jun. 2022, doi: 10.3390/POLYM14132547.

[15] D. Hardman, T. George Thuruthel, and F. Iida, "Self-healing ionic gelatin/glycerol hydrogels for strain sensing applications," *NPG Asia Mater*, vol. 14, no. 1, Dec. 2022, doi: 10.1038/s41427-022-00357-9.

[16] J. Zhang, D. Qu, S. Wang, S. Qi, and H. Zuo, "Structure, Property Optimization, and Adsorption Properties of N,N′-methylenebisacrylamide Cross-Linked Polyacrylic Acid Hydrogels under Different Curing Conditions," *Polymers 2024, Vol. 16, Page 1990*, vol. 16, no. 14, p. 1990, Jul. 2024, doi: 10.3390/POLYM16141990.

[17] W. Tomal and J. Ortyl, "Water-Soluble Photoinitiators in Biomedical Applications," *Polymers 2020, Vol. 12, Page 1073*, vol. 12, no. 5, p. 1073, May 2020, doi: 10.3390/POLYM12051073.

[18] K. Long *et al.*, "Anti-freezing, adhesive and conductive hydrogel for flexible sensors and deep learning assisted Triboelectric nanogenerators," *Chemical Engineering Journal*, vol. 513, p. 162828, Jun. 2025, doi: 10.1016/J.CEJ.2025.162828.

[19] S. Liu *et al.*, "Machine-learning integrated strain/pressure dual-mode flexible sensor for assistance of unable-phonation scenarios," *Chemical Engineering Journal*, vol. 503, p. 158364, 2025.

[20] "A Walk Through Time - Early Clocks | NIST." Accessed: Feb. 24, 2025. [Online]. Available: https://www.nist.gov/pml/time-and-frequency-division/popular-links/walk-through-time/walk-through-time-early-clocks

[21] "History and Evolution of Sensors." Accessed: Feb. 24, 2025. [Online]. Available: https://www.monolithicpower.com/en/learning/mpscholar/sensors/intro-to-sensors/history-and-evolution

[22] A. Bin Rashid and A. K. Kausik, "AI revolutionizing industries worldwide: A comprehensive overview of its diverse applications," *Hybrid Advances*, p. 100277, 2024.

[23] "20 Different Types of Sensors Used in Industry | Definition & Applications." Accessed: Feb. 25, 2025. [Online]. Available: https://dipslab.com/sensor-types/

[24] "Passive vs. Active Sensors - Electrical and Control Systems." Accessed: Feb. 25, 2025. [Online]. Available: https://www.electricalandcontrol.com/passive-vs-active-sensors/

[25] "Classes, Types, and Applications of Temperature Sensors." Accessed: Jan. 29, 2025. [Online]. Available: https://www.iqsdirectory.com/articles/thermocouple/temperature-sensors.html

[26] "An Overview of Pressure Sensors | Same Sky." Accessed: Jan. 29, 2025. [Online]. Available: https://www.sameskydevices.com/blog/an-overview-of-pressure-sensors

[27] “Understanding Gas Sensors: Types, Working Principles, and Applications.” Accessed: Jan. 30, 2025. [Online]. Available: https://components101.com/articles/introduction-to-gas-sensors-types-working-and-applications

[28] “Humidity Sensor Basics - Types, Working, Applications, Projects.” Accessed: Feb. 02, 2025. [Online]. Available: https://www.electronicsforu.com/tech-zone/electronics-components/humidity-sensor-basic-usage-parameter

[29] H. Gu and L. Wang, “A High-Detection-Efficiency Optoelectronic Device for Trace Cadmium Detection,” *Sensors*, vol. 22, no. 15, Aug. 2022, doi: 10.3390/S22155630.

[30] F. F. Martín *et al.*, “Optoelectronic instrumentation and measurement strategies for optical chemical (bio) sensing,” *Applied Sciences*, vol. 11, no. 17, p. 7849, 2021.

[31] S. Ma, J. Tang, T. Yan, and Z. Pan, “Performance of Flexible Strain Sensors With Different Transition Mechanisms: A Review,” *IEEE Sens J*, vol. 22, no. 8, pp. 7475–7498, Apr. 2022, doi: 10.1109/JSEN.2022.3156286.

[32] “Classification and mechanism of strain sensors: (A) resistive sensor,... | Download Scientific Diagram.” Accessed: May 12, 2025. [Online]. Available: https://www.researchgate.net/figure/Classification-and-mechanism-of-strain-sensors-A-resistive-sensor-B-capacitive_fig7_380993206

[33] H. Souri *et al.*, “Wearable and stretchable strain sensors: materials, sensing mechanisms, and applications,” *Advanced Intelligent Systems*, vol. 2, no. 8, p. 2000039, 2020.

[34] G. Ghosh *et al.*, “Tough, transparent, biocompatible and stretchable thermoplastic copolymer with high stability and processability for soft electronics,” *Materials Today*, vol. 57, pp. 43–56, Jul. 2022, doi: 10.1016/J.MATTOD.2022.05.019.

[35] V. Orts Mercadillo *et al.*, “Electrically Conductive 2D Material Coatings for Flexible and Stretchable Electronics: A Comparative Review of Graphenes and MXenes,” *Adv Funct Mater*, vol. 32, no. 38, p. 2204772, Sep. 2022, doi: 10.1002/ADFM.202204772;JOURNAL:JOURNAL:10990712;PAGE:STRING:ARTICLE/CHAPTER.

[36] H. T. Tazwar, M. F. Antora, I. Nowroj, and A. Bin Rashid, “Conductive polymer composites in soft robotics, flexible sensors and energy storage: Fabrication, applications and challenges,” *Biosens Bioelectron X*, vol. 24, p. 100597, Aug. 2025, doi: 10.1016/J.BIOSX.2025.100597.

[37] J. Du *et al.*, “Optimized CNT-PDMS Flexible Composite for Attachable Health-Care Device,” *Sensors (Basel)*, vol. 20, no. 16, p. 4523, Aug. 2020, doi: 10.3390/S20164523.

[38] V. Patel, E. Das, A. Bhargava, S. Deshmukh, A. Modi, and R. Srivastava, “Ionogels for flexible conductive substrates and their application in biosensing,” *Int J Biol Macromol*, vol. 254, p. 127736, Jan. 2024, doi: 10.1016/J.IJBIOMAC.2023.127736.

[39] S. Wang *et al.*, “Trends in Flexible Sensing Technology in Smart Wearable Mechanisms–Materials–Applications,” *Nanomaterials*, vol. 15, no. 4, p. 298, 2025.

[40] J. Chen *et al.*, “Self-healing materials-based electronic skin: mechanism, development and applications,” *Gels*, vol. 8, no. 6, p. 356, 2022.

[41] “Extrinsic (left) and intrinsic self-healing (right) process. 14,15... | Download Scientific Diagram.” Accessed: May 12, 2025. [Online]. Available: https://www.researchgate.net/figure/Extrinsic-left-and-intrinsic-self-healing-right-process-14-15-left-Reproduced-with_fig1_350478404

[42] “Scanning Electron Microscope (SEM): Principle, Parts, Uses - Microbe Notes.” Accessed: Jun. 20, 2025. [Online]. Available: https://microbenotes.com/scanning-electron-microscope-sem/

[43] B. D. A. Levin *et al.*, “Nanomaterial datasets to advance tomography in scanning transmission electron microscopy,” *Sci Data*, vol. 3, p. 160041, Jun. 2016, doi: 10.1038/sdata.2016.41.

[44] F. J. Giessibl, “Advances in atomic force microscopy,” *Rev Mod Phys*, vol. 75, no. 3, pp. 949–983, Jul. 2003, doi: 10.1103/RevModPhys.75.949.

[45] “Self-Healing Materials: The Future Of Construction And Manufacturing.” Accessed: May 12, 2025. [Online]. Available: https://quantumzeitgeist.com/self-healing-materials-the-future-of-construction-and-manufacturing/

[46] G. Kordas and G. Kordas, “Self-Healing of Concrete through Ceramic Nanocontainers Loaded with Corrosion Inhibitors and Microorganisms,” *Advanced Ceramic Materials*, Sep. 2020, doi: 10.5772/INTECHOPEN.93514.

[47] M. Bellah, M. Nosonovsky, and P. Rohatgi, “Shape Memory Alloy Reinforced Self-Healing Metal Matrix Composites,” *Applied Sciences 2023, Vol. 13, Page 6884*, vol. 13, no. 12, p. 6884, Jun. 2023, doi: 10.3390/APP13126884.

[48] J. Meurer *et al.*, “In-depth characterization of self-healing polymers based on π–π interactions,” *Beilstein Journal of Organic Chemistry*, vol. 17, pp. 2496–2504, Jan. 2021, doi: 10.3762/BJOC.17.166.

[49] R. Dallaev, “Advances in Materials with Self-Healing Properties: A Brief Review,” May 01, 2024, *Multidisciplinary Digital Publishing Institute (MDPI)*. doi: 10.3390/ma17102464.

[50] H. W. Park, N. G. Jang, H. S. Seo, K. Kwon, and S. Shin, “Facile Synthesis of Self-Adhesion and Ion-Conducting 2-Acrylamido-2-Methylpropane Sulfonic Acid/Tannic Acid Hydrogels Using Electron Beam Irradiation,” *Polymers 2023, Vol. 15, Page 3836*, vol. 15, no. 18, p. 3836, Sep. 2023, doi: 10.3390/POLYM15183836.

[51] H. Liu *et al.*, “A functional chitosan-based hydrogel as a wound dressing and drug delivery system in the treatment of wound healing,” 2018, *Royal Society of Chemistry*. doi: 10.1039/c7ra13510f.

[52] F. Abasalizadeh *et al.*, “Alginate-based hydrogels as drug delivery vehicles in cancer treatment and their applications in wound dressing and 3D bioprinting,” Mar. 13, 2020, *BioMed Central Ltd*. doi: 10.1186/s13036-020-0227-7.

[53] K. Saravanakumar *et al.*, “Application of hyaluronic acid in tissue engineering, regenerative medicine, and nanomedicine: A review,” *Int J Biol Macromol*, vol. 222, pp. 2744–2760, Dec. 2022, doi: 10.1016/J.IJBIOMAC.2022.10.055.

[54] M. Vahdani *et al.*, “Bio-Disintegrable Elastic Polymers for Stretchable Piezoresistive Strain Sensors,” *Adv Sustain Syst*, p. 2300482, 2024.

[55] R. Yang, Z. Tu, X. Chen, and X. Wu, “Highly stretchable, robust, sensitive and wearable strain sensors based on mesh-structured conductive hydrogels,” *Chemical Engineering Journal*, vol. 480, Jan. 2024, doi: 10.1016/j.cej.2023.148228.

[56] P. Kateb, A. Fornaciari, C. Ahmadizadeh, A. Shokurov, F. Cicoira, and C. Menon, “High-Performance Textile-Based Capacitive Strain Sensors via Enhanced Vapor Phase Polymerization of Pyrrole and Their Application to Machine Learning-Assisted Hand Gesture Recognition,” *Advanced Intelligent Systems*, vol. 6, no. 11, p. 2400292, 2024.

[57] P. Shukla *et al.*, “Prototyping a wearable and stretchable graphene-on-PDMS sensor for strain detection on human body physiological and joint movements,” *Microchimica Acta*, vol. 191, no. 6, p. 301, 2024.

[58] W. Hong *et al.*, “Dual bionic-inspired stretchable strain sensor based on graphene/multi-walled carbon nanotubes/polymer composites for electronic skin,” *Compos Part A Appl Sci Manuf*, vol. 179, p. 108043, 2024.

[59] X. Bao, J. Meng, Z. Tan, C. Zhang, L. Li, and T. Liu, “Direct-ink-write 3D printing of highly-stretchable polyaniline gel with hierarchical conducting network for customized wearable strain sensors,” *Chemical Engineering Journal*, vol. 491, no. January, 2024, doi: 10.1016/j.cej.2024.151918.

[60] Z. Wu *et al.*, “A wearable ionic hydrogel strain sensor with double cross-linked network for human–machine interface,” *Adv Compos Hybrid Mater*, vol. 8, no. 1, Feb. 2025, doi: 10.1007/s42114-024-01083-2.

[61] H. Wu *et al.*, “Bioinspired Stretchable Strain Sensor with High Linearity and Superhydrophobicity for Underwater Applications,” *Adv Funct Mater*, Jan. 2024, doi: 10.1002/adfm.202413552.

[62] A. K. Padhan, D. Sharma, T. S. Thomas, A. P. Sinha, A. N. Mallick, and D. Mandal, “Rapid self-healing and superior toughness in ionically crosslinked polymer ionogels and strain sensing applications,” *J Mater Chem A Mater*, vol. 12, no. 16, pp. 9508–9517, 2024.

[63] D. Chen, H. Bai, H. Zhu, S. Zhang, W. Wang, and W. Dong, “Anti-freezing, tough, and stretchable ionic conductive hydrogel with multi-crosslinked double-network for a flexible strain sensor,” *Chemical Engineering Journal*, vol. 480, p. 148192, 2024.

[64] K. Wang, Y. Zhang, J. Hu, M. Li, and B. Wu, “Flexible Strain Sensor Based on a Dual Crosslinked Network of PAMgA/GL/PANI Antifreeze Conductive Hydrogel,” *Macromol Chem Phys*, Jan. 2024, doi: 10.1002/macp.202400341.

[65] T. Truong and J. Kim, “A Wearable Strain Sensor Utilizing Shape Memory Polymer/Carbon Nanotube Composites Measuring Respiration Movements,” *Polymers (Basel)*, vol. 16, no. 3, p. 373, 2024.

[66] H. Cheng, X. Zhang, T. Zhang, Y. Chen, D. Yu, and W. Wang, “Durable TPU/PDA/MXene Fiber-Based Strain Sensors with High Strain Range and Sensitivity,” *ChemistrySelect*, vol. 9, no. 31, p. e202402076, 2024.

[67] R. Wang *et al.*, “Fiber-Based Miniature Strain Sensor with Fast Response and Low Hysteresis,” *Adv Funct Mater*, Oct. 2024, doi: 10.1002/adfm.202403918.

[68] L. Guo *et al.*, “Integrated wearable collaborative strain sensor with simultaneous self-healing and superhydrophobic abilities for stable sensing monitoring,” *Appl Mater Today*, vol. 39, p. 102339, 2024.

[69] X. Dai *et al.*, “Self-powered sensors for flexible electronic skins capable of self-healing under multiple extreme environments,” *Nano Energy*, vol. 121, Mar. 2024, doi: 10.1016/j.nanoen.2023.109239.

[70] N. D. Sanandiya, A. R. Pai, S. Seyedin, F. Tang, S. Thomas, and F. Xie, “Chitosan-based electroconductive inks without chemical reaction for cost-effective and versatile 3D printing for electromagnetic interference (EMI) shielding and strain-sensing applications,” *Carbohydr Polym*, vol. 337, Aug. 2024, doi: 10.1016/j.carbpol.2024.122161.

[71] W. Zhong *et al.*, “Multi-Layer Polyurethane-Fiber-Prepared Entangled Strain Sensor with Tunable Sensitivity and Working Range for Human Motion Detection,” *Polymers (Basel)*, vol. 16, no. 8, Apr. 2024, doi: 10.3390/polym16081023.

[72] C. Zhang, W. Ouyang, L. Zhang, and D. Li, “A dual-mode fiber-shaped flexible capacitive strain sensor fabricated by direct ink writing technology for wearable and implantable health monitoring applications,” *Microsyst Nanoeng*, vol. 9, no. 1, Dec. 2023, doi: 10.1038/s41378-023-00634-9.

[73] M. N. Alam, V. Kumar, D.-J. Lee, and J. Choi, “Synergistically toughened silicone rubber nanocomposites using carbon nanotubes and molybdenum disulfide for stretchable strain sensors,” *Compos B Eng*, vol. 259, p. 110759, 2023.

[74] Y. Chen *et al.*, “Highly stretchable, adhesive and antibacterial double-network hydrogels toward flexible strain sensor,” *Polym Test*, vol. 124, p. 108087, 2023.

[75] T. Jamatia *et al.*, “Wearable and stretchable SEBS/CB polymer conductive strand as a piezoresistive strain sensor,” *Polymers (Basel)*, vol. 15, no. 7, p. 1618, 2023.

[76] “Sonication: Definition, Diagram, Principle, Working, Types, Uses.” Accessed: Mar. 27, 2025. [Online]. Available: https://testbook.com/physics/sonication

[77] “What is An Ultrasonic Bath - All The Information.” Accessed: Mar. 27, 2025. [Online]. Available: https://www.mrclab.com/what-is-an-ultrasonic-bath

[78] “Schematic representation of ultrasonicator equipment. Ultrasonication... | Download Scientific Diagram.” Accessed: Mar. 27, 2025. [Online]. Available: https://www.researchgate.net/figure/Schematic-representation-of-ultrasonicator-equipment-Ultrasonication-bath-left-and_fig4_344926851

[79] “Magnetic Stirrer: Definition, Principle, Features, Advantages, Applications.” Accessed: Mar. 25, 2025. [Online]. Available: https://scienceinfo.com/magnetic-stirrer-definition-principle-advantages/

[80] “Magnetic Stirrer: Working Principle, Types & Uses in Labs.” Accessed: Jun. 20, 2025. [Online]. Available: https://www.borosilscientific.com/magnetic-stirrer-operating-principle-and-applications/

[81] “Hotplate Magnetic Stirrer, Temp. 380°C, HPS-380-1 - Infitek.” Accessed: Jun. 20, 2025. [Online]. Available: https://infitek.com/products/hotplate-magnetic-stirrer-temp-380c-hps-380-1/#

[82] “Spin coating - Wikipedia.” Accessed: Mar. 25, 2025. [Online]. Available: https://en.wikipedia.org/wiki/Spin_coating

[83] “Spin Coater | Low Price, Vacuum-Free Systems | Ossila.” Accessed: Jun. 21, 2025. [Online]. Available: https://www.ossila.com/products/spin-coater

[84] J. Zhou *et al.*, “High-performance amorphous carbon/PDMS flexible strain sensors by introducing low interfacial mismatch,” *Diam Relat Mater*, vol. 139, p. 110272, 2023.

[85] F. Shi and F. Shi, “Introductory Chapter: Basic Theory of Magnetron Sputtering,” *Magnetron Sputtering [Working Title]*, Nov. 2018, doi: 10.5772/INTECHOPEN.80550.

[86] “UV curing - Wikipedia.” Accessed: Mar. 25, 2025. [Online]. Available: https://en.wikipedia.org/wiki/UV_curing

[87] “Scanning Electron Microscope (SEM): Principle, Parts, Uses - Microbe Notes.” Accessed: Mar. 26, 2025. [Online]. Available: https://microbenotes.com/scanning-electron-microscope-sem/

[88] S. Da Wu *et al.*, “Fabrication of Eco-Friendly Wearable Strain Sensor Arrays via Facile Contact Printing for Healthcare Applications,” *Small Methods*, vol. 7, no. 9, Sep. 2023, doi: 10.1002/SMTD.202300170.

[89] W. W. Kong, C. G. Zhou, K. Dai, L. C. Jia, D. X. Yan, and Z. M. Li, “Highly stretchable and durable fibrous strain sensor with growth ring-like spiral structure for wearable electronics,” *Compos B Eng*, vol. 225, Nov. 2021, doi: 10.1016/j.compositesb.2021.109275.

[90] Y. Zheng *et al.*, “A highly stretchable and stable strain sensor based on hybrid carbon nanofillers/polydimethylsiloxane conductive composites for large human motions monitoring,” *Compos Sci Technol*, vol. 156, pp. 276–286, Mar. 2018, doi: 10.1016/j.compscitech.2018.01.019.

[91] C. Tan *et al.*, “A high performance wearable strain sensor with advanced thermal management for motion monitoring,” *Nature Communications 2020 11:1*, vol. 11, no. 1, pp. 1–10, Jul. 2020, doi: 10.1038/s41467-020-17301-6.

[92] N. Afsarimanesh, A. Nag, S. Sarkar, G. S. Sabet, T. Han, and S. C. Mukhopadhyay, “A review on fabrication, characterization and implementation of wearable strain sensors,” Nov. 01, 2020, *Elsevier B.V.* doi: 10.1016/j.sna.2020.112355.

[93] R. Dong and J. Xie, “Stretchable strain sensor with controllable negative resistance sensitivity coefficient based on patterned carbon nanotubes/silicone rubber composites,” *Micromachines (Basel)*, vol. 12, no. 6, Jun. 2021, doi: 10.3390/MI12060716.

[94] D. Hardman, T. George Thuruthel, and F. Iida, “Self-healing ionic gelatin/glycerol hydrogels for strain sensing applications,” *NPG Asia Materials 2022 14:1*, vol. 14, no. 1, pp. 1–13, Feb. 2022, doi: 10.1038/s41427-022-00357-9.

[95] X. Huang, Y. Xue, S. Ren, and F. Wang, “Sensor-based wearable systems for monitoring human motion and posture: A review,” *Sensors*, vol. 23, no. 22, p. 9047, 2023.

[96] Y. Wang *et al.*, “High Linearity, Low Hysteresis Ti3C2Tx MXene/AgNW/Liquid Metal Self-Healing Strain Sensor Modulated by Dynamic Disulfide and Hydrogen Bonds,” *Adv Funct Mater*, vol. 33, no. 37, Sep. 2023, doi: 10.1002/adfm.202301587.

[97] R. Yang, S. Zhao, Z. Tu, H. Hu, X. Chen, and X. Wu, “Synthesis of Self-Adhesive, Self-Healing and Antifreeze Conductive Hydrogels for Flexible Strain sensors,” *Advanced Sensor Research*, vol. 3, no. 11, Nov. 2024, doi: 10.1002/adsr.202400063.

[98] G. Mirzaei, A. Mirzaei, and S. Javanshir, “Flexible mussel-inspired hydrogel for transparent wearable strain sensors: Investigation of mechanical, physical properties, self-healing, and electrical conductivity,” *J Appl Polym Sci*, vol. 141, no. 38, p. e55983, 2024.

[99] A. Khadka *et al.*, “Rapidly self-healing, highly conductive, stretchable, body-attachable hydrogel sensor for soft electronics,” *Composites Communications*, vol. 52, p. 102158, Dec. 2024, doi: 10.1016/J.COCO.2024.102158.

[100] Z. Li *et al.*, “Highly Stretchable, Self-Healable, and Conductive Gelatin Methacryloyl Hydrogel for Long-Lasting Wearable Tactile Sensors,” *Advanced Science*, May 2025, doi: 10.1002/advs.202502678.

[101] C. Cong *et al.*, “Self-powered strain sensing devices with wireless transmission: DIW-printed conductive hydrogel electrodes featuring stretchable and self-healing properties,” *J Colloid Interface Sci*, vol. 678, pp. 588–598, Jan. 2025, doi: 10.1016/J.JCIS.2024.08.262.